DISSERTATION

# ANTICANCER POTENTIAL OF NITRIC OXIDE-BASED THERAPEUTICS FOR PEDIATRIC AND ADULT CANCERS

Submitted by

Jenna Leigh Gordon

Department of Chemistry

In partial fulfillment of the requirements

For the Degree of Doctor of Philosophy

Colorado State University

Fort Collins, Colorado

Fall 2021

Doctoral Committee:

Advisor: Melissa Reynolds

Chuck Henry
Alan Kennan
Mark Brown

# ABSTRACT

## ANTICANCER POTENTIAL OF NITRIC OXIDE-BASED THERAPEUTICS FOR PEDIATRIC AND ADULT CANCERS

Based on 2015-2017 data, nearly 40% of men and women will be diagnosed with cancer at some point throughout their lives. As a worldwide pandemic, cancer presents a colossal challenge for researchers and clinicians to continually develop and implement new strategies to prevent, diagnose, and treat the many variations of this disease. Currently, treatment protocols are dominated by surgery, chemotherapy, and radiation therapy. Although valuable, these treatments are often ineffective and are limited to specific situations. Surgery is typically useful for early-stage cancer treatment while chemotherapy and radiation therapy are more common for late-stage treatment. Chemotherapy and radiation therapies are subject to drug resistance and all three produce patient side effects. Thus, a persistent need to develop drugs that are more effective, preferential (to neoplastic cells), and accessible remains. This work implements therapeutics that addresses those concerns while demonstrating efficacy within both pediatric and adult cancers.

An evaluation of the anticancer potential of nitric oxide (NO) releasing *S*-nitrosothiol based anticancer therapeutics is presented herein. In the determination of clinical translatability of a drug, it is essential to understand the desired outcome and potential sources of error prior to execution of analyses and the corresponding methodologies and measurements. Thus, an in-depth analysis of indicators for therapeutic efficacy using tumor-derived cell lines and a detailed investigation of the protocol development and potential interferences of three common cellular viability assays is presented prior to the *in vitro* work detailed in this study. Specifically, this study involves the

application of the NO releasing *S*-Nitrosothiol, *S*-Nitrosoglutathione (GSNO) in two variations to determine efficacy against pediatric neuroblastomas and adult breast cancers. Initially, two studies explore the application of GSNO in solution to multiple neuroblastoma cell lines of various origins to determine the potential of NO to act as an adjuvant therapeutic in the clinical management of the prevalent pediatric cancer neuroblastoma. These studies highlight the incredible impact of NO on clonogenic capacity as well as remarkable discriminatory characteristics between neoplastic and healthy cells. Further, the insight presented regarding the mechanism of action of NO on neuroblastomas expands the comprehension of NO-based anticancer therapeutics. Excitingly, when the same GSNO preparation is subsequently applied to more common adult breast cancers to determine if therapeutic efficacy is maintained, results display analogous consequences to those mentioned above. The final study in this dissertation will also explore another application of solution-phase GSNO to adult breast malignancies by combining it with a novel SMYD-3 inhibitor, termed Inhibitor-4 (by collaborators). Since Inhibitor-4 has been shown to similarly impact viability, clonogenic capacity, and apoptosis, this combination is expected to reveal a greater impact than each individual treatment. Overall, an analysis of the significance and feasibility of NO-based therapeutics, delivered via GSNO, is explored to determine their potential application in the clinical management of various cancers. Ultimately, this work expands the knowledge of the practicality, mechanism of action, and effectiveness of NO-based anticancer therapeutics in various cancers with a specific focus on its applicability in neuroblastomas, a malignancy where minimal focus has been placed on NO as a treatment option.

# ACKNOWLEDGEMENTS

I am humbled and honored by the support and guidance I have received throughout my doctoral program from both my family and friends, as well as faculty and staff. First, I would like to express my deepest gratitude to my husband, best friend, and number one supporter, Cody Gordon. He supported me always, even when I was up until 2 A.M. finishing a paper or nursing one of our babies, motivated me to reach for the best (my best) even when I was on the floor sobbing and certain I couldn't finish the project or breastfeed for an entire year while progressing in my program, listened to me intently even through my countless practice talks filled with words he barely understood or my candor about feeling equally isolated and empowered as a woman and mom in my program. Secondly, I would like to express equally sincere appreciation to my sweet children – my daughter, Preslee Nyx Gordon, traveled with me through this entire journey (from embryo to spunky preschooler), continuously lighting my path, both in spirit and in passion and my new baby girl, Alessi Grae Gordon, who inspired me to pursue happiness and fulfillment for myself and my growing family.

I would also like to thank my driven parents, Kim and Eric Short, for instilling in me the desire to persevere and reach my goals. Additionally, I am so thankful for my brother, Jace Short, who has been my bro, my bud, my dude since his day one. I am so fortunate to have so many other family members in my life cheering me on, including my sweet grandparents, Colleen, Kathy, and Jerry, aunts and uncles, and cousins too. Further, I'd like to honor my non-blood family, my friends, my mentors, my teachers - your support, guidance, and grace has encouraged me to continue in my pursuits.

I would like to express deep gratitude to my principal investigator, Professor Melissa Reynolds, who is divinely wise and seemingly tireless. Melissa instilled a desire to investigate with passion while maintaining objective, critical discernment. Despite inescapable struggles, she ardently encouraged, ensuring that the process was as important as the product. Without her steadfast guidance and support, this dissertation would not have been possible.

With great appreciation, I would like to recognize my out-of-area committee member, Professor Mark Brown, for the countless hours he spent editing papers, assessing my results, and providing expertise on cancer therapeutics. His knowledge and support were vital components in this dissertation.

Finally, sincere gratitude goes out to another key member in my overall success, Delphine Farmer. In the first two years of my doctoral program, she provided me with key support to progress as a graduate student and new mother.

Thank you all for your support, I will be forever grateful!

TABLE OF CONTENTS

CHAPTER 1

# INTRODUCTION

## 1.1 CANCER

**1.1.1 Definition and characteristics of cancer.** By definition, cancer is a group of diseases caused by uncontrollable division of abnormal cells in part of the body that can invade adjacent tissues or spread through the blood and lymph systems.[1] Cancer, technically known as neoplasia, originates through genetic mutations due to internal and external circumstances that cause tissue changes.[2] However, all tissue changes are not cancerous.[3,4] For example, hyperplasia is defined by faster proliferation of cells that still display normal characteristics.[3] Dysplasia involves faster proliferation of cells that display abnormal characteristics.[4] In each case, these cells may or may not become cancerous.[3,4] Distinctly, cancerous cells divide faster, look abnormal, and invade nearby tissues.[5] Additionally, cancer cells ignore body signals that indicate to cells to stop dividing or die.[5]

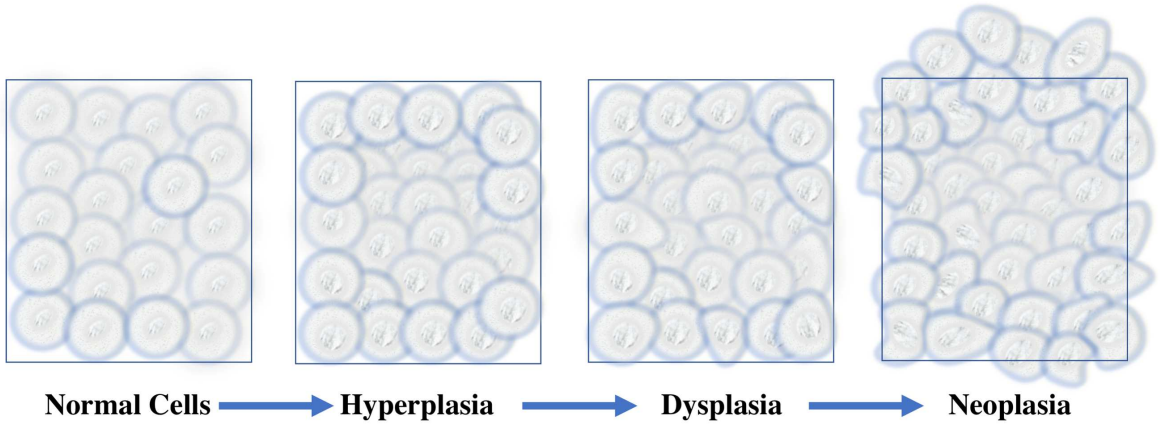


**Figure 1.1** Graphical representation of normal cells and possible tissue changes (hyperplasia/dysplasia) that may or may not develop into cancer (neoplasia).

One particularly challenging aspect of cancer is that it is not a single disease, but rather a term encompassing numerous diseases (also known as malignancies) that exist in various forms within the body. Malignancies can exist as solid tumors, liquid tumors, or a combination.[2] Tumors, or masses of cells, can be benign (non-cancerous) or malignant (cancerous).[6] Clinically, there are six primary categories of cancer that are used to classify malignant tumor types based on their histological characteristics: carcinomas, sarcomas, myelomas, leukemias, lymphomas, and mixed types.[7] Carcinomas, the most common type of cancer, begin in internal or external tissues that cover surfaces, such as skin or organ/gland surfaces.[7] Often, carcinomas form solid tumors, such as those of the prostate, breast, and lungs. Sarcomas originate in tissues that connect and support the body, such as those of the muscles, fat, bone, cartilage, nerves, tendons, joints, blood vessels, and lymph vessels, like osteosarcoma (bone) and liposarcoma (adipose tissue).[7] Myelomas develop in bone marrow plasma cells.[7] Leukemias are liquid cancers, or cancers of the blood, such as lymphatic, lymphocytic, and lymphoblastic leukemia.[7] Lymphomas are cancers that begin in the lymphatic system, the system of vessels, glands, nodes, and organs that fight against infection. These are subclassified into two types, Hodgkin lymphoma and non-Hodgkin lymphoma, despite their location or origination point.[7] Lastly, mixed types are cancers with components of multiple of the five aforementioned categories (ex: carcinosarcoma, adenosquamous carcinoma).[7] Despite vast efforts in cancer research, treatments, and technologies, cancer remains one of the most lethal diseases worldwide.

As malignancies proliferate, cancerous cells can travel to other parts of the body via the lymphatic system or bloodstream.[2] The transport of these cancerous cells can create additional tumors, a process known as metastasis.[2] Often, metastatic cancer spreads to the nearby lymph nodes throughout the body, but it can also travel to distant parts of the body such as the liver, lungs,

bones, or brain.[2] Even if metastasis occurs, cancers are classified according to the original tumor site. For example, if lung cancer metastasizes to the breast, it is termed metastatic lung cancer, not breast cancer.

Generally, there are three types of genes involved in the development and progression of cancer. These genes are termed cancer "drivers" and include proto-oncogenes, tumor suppressor genes, and DNA repair genes.[2] In a healthy body, proto-oncogenes are involved in normal cell growth and division.[2] When these genes are altered or become more active than usual, these turn into oncogenes (cancer causing genes) that allow cells to grow and divide uncontrollably.[2] Similarly, in a healthy body, tumor suppressor genes are involved in the regulation of cell growth and division.[2] When these become altered, they also allow uncontrollable division of cells. Finally, in a healthy body, DNA repair genes play a role in restoring damaged DNA.[2] Mutations in these genes tend to induce mutations in other genes and together these cells can become cancerous.[2,5]

**1.1.2 Prevalence and diagnosis of cancer.** As previously stated, there are numerous types of malignancies that exist in various forms within the human body. In fact, there are more than 100 clinically defined types of cancer attributing to more than 1,800,000 diagnoses and over 600,000 deaths per year in the United States.[8] The most common types of cancer include breast, lung and bronchus, prostate, colon and rectal, skin melanomas, bladder, non-Hodgkin lymphoma, kidney and renal, endometrial, leukemia, pancreatic, thyroid, and liver cancers. By gender, the most common include prostate, lung, and colorectal in men (~43% of total cases), and breast, lung, and colorectal in women (~50% of total cases).[8] Additionally, trachea, bronchus, and lung cancers collectively account for the fifth most common cause of death in the world and the fourth most common in western countries.[9] Lung cancer alone attributes to more than one million deaths per year and is the leading cause of worldwide cancer-related deaths.[9] Overall, the incidence of cancer

diagnosis has increased while the death rate has declined.[10] The increase in incidence may indicate augmented risk factors but can also be attributed to amplified and/or improved screening. The decrease in death rate implies some progress has been made in treatment and that many challenges remain.

Several factors impact the challenges associated with cancer diagnosis. In particular, the presentation of different cancers ranges vastly from individual to individual. Additionally, there are only a few regularly implemented screening tests that can indicate the presence of abnormal cells including Pap tests, colonoscopies, and mammography tests.[11] Generally, diagnosis relies on the presentation of unusual symptoms that are discussed with a medical provider. However, many of these symptoms are ambiguous and do not directly correspond to cancer or a specific malignancy. Nonetheless, when unusual symptoms are explored, a range of tests are usually completed to identify potential causes. In the majority of cancer cases, a biopsy is needed to make a definitive diagnosis. Biopsies require the removal of a small amount of tissue (or blood) that is examined further to determine its malignant potential.[12] If the sample does display the characteristics associated with a certain malignancy, further examination of the patient is required to determine if metastasis has occurred and if the patient's body or immune system is compromised in any way. After this examination is complete, treatment options are explored. Despite nearly a century of advances in cancer research, it remains one of the most lethal diseases worldwide.[13] In the United States alone, more than one-third of all people dealing with cancer do not survive five years post-diagnosis.[14]

**1.1.3 Treatment options: benefits and concerns.** Currently, the most common therapeutic options to treat cancer include surgery, chemotherapy, and radiation therapy. Surgery is commonly employed, in over 80% of cancer cases, to remove all or as much of a solid tumor as possible, with

the hope that the removal of the cancerous tissue will prevent further replication of cancerous cells and metastasis.[15] Sometimes surgery is still employed in metastatic cancer when multiple tumors are found in various locations. Various factors, such as the location, extent, and necessity for hospital stay and/or continued care influence the cost of surgical treatment.[16] Occasionally, surgery and observation are the only methods necessary to induce partial or complete (all indications of cancer are gone) remission, which can also be referred to as "no evidence of disease" (NED).[15]

Often, chemotherapy is coupled with surgery as a treatment protocol. Chemotherapy as an anticancer treatment option began in the in the early 1940s with the application of nitrogen mustard.[17] Since then, the discovery and application of chemotherapeutics have developed into a multi-billion dollar industry.[17] Today, there are more than 50 chemotherapy drugs of clinical relevance[18] that can be delivered in various fashions (i.e. intravenously and orally). Generally, cytotoxic chemotherapeutics target cells that grow and divide rapidly, including cancer cells, but also some normal cells, such as those that comprise skin, hair, intestinal, and bone marrow. Regularly, multiple treatment methods are necessary to fight cancer, including the application of multiple chemotherapeutic drugs. Several factors influence the generation of a treatment regimen with several agents: the anticancer capacity of each therapeutic agent against the specific neoplasm, the ability to target multiple cell cycle phases, and the capacity to impact diverse mechanisms of action.[18] The cost of chemotherapy treatment regimens is largely dependent on the type(s), dosage amount, length of treatment, and necessity for hospital stay and/or additional care.[19]

Another frequent option employed in cancer treatment is radiation therapy (also known as radiotherapy). Radiation therapy uses high doses of ionizing radiation (X-rays) to induce DNA damage, thereby killing cells and shrinking tumors.[20] This can be done in a targeted (external) or

non-targeted (internal) manner.[20] Generally, a single round of radiation treatment lasts days to weeks but cells continue to die to weeks to months after treatment.[20] Similar to chemotherapy, the cost of radiation therapy depends on the type, length of treatment, number of treatments, and the necessity for lengthened hospital stays and/or additional care.[21]

Through advancements in technology and medicine, alternative treatment options for cancer have been discovered and implemented, such as immunotherapies and targeted cancer therapies, as a result of the significant challenges associated with existing treatment options.[22,23] Expressly, the primary challenge with chemotherapy and radiation therapy is that they are not cancer cell specific, which leads to patient side effects that can be severe such as nausea, vomiting, hair loss, anemia, alopecia, fatigue, anorexia, and many more.[18,20] As a result, both chemotherapy and radiation therapy are restricted by dose-limiting toxicity (the maximum amount/level of drug or treatment that can be administered before side effects of that treatment become too severe).[18,20] Prominently, there exists a lifetime dose limit of radiation therapy, or a limit to the total amount of radiation a body (or area of the body) can safely receive over the course of a lifetime.[21] Furthermore, chemotherapeutic drugs present a further challenge in the development of drug resistance or multi-drug resistance (MDR).[24,25] Drug resistance can develop via numerous mechanisms, some of which include decreased drug uptake, increased drug efflux, activation of DNA repair mechanisms, and activation of detoxifying systems.[25] Due to the significant obstacles presented within these treatment options, researchers and clinicians continue to emphasize the development of alternative anticancer treatment options that are safe, effective, and attainable.

## 1.2 PEDIATRIC CANCER

**1.2.1 Prevalence.** Even though pediatric cancer is less common than adult cancer, it remains the most common cause of death by disease for children and adolescents in the United States.[26]

Fortuitously, while the incidence of childhood cancer continues to increase mortality rates continue to decrease.[27,28] The decrease in mortality rates can be highly correlated to better diagnostic procedures, multimodal therapies, and exceptionally dramatic increases in survival rates for a few types of pediatric cancer, including the most common, acute lymphocytic leukemia (ALL), as well as lymphomas and kidney cancer.[27–29] Currently, overall 5-year survival rates remain optimistic, about 80%.[27–29]

Although these rates appear promising, there are some critical components to consider in regard to pediatric cancer. First, children tend to have fewer genetic mutations than adults and pediatric cancers tend to form in quickly growing, developmental cell types.[28] Often, pediatric cancers originate in embryological developmental processes.[28] Childhood cancers tend to be more aggressive and progress more rapidly than adult cancers.[28,30] At the time of diagnosis, childhood cancers have usually metastasized (~60% of cases).[31] Strikingly, childhood cancer treatments are often identical to adult treatments[32] despite differences (sometimes drastic) in tumors of the same genotype.[28,33] Unsurprisingly, these treatments tend to be more detrimental to children than adults, both short-term and long-term. Since radiation and most chemotherapeutics tend to target rapidly developing cell types, and children are rapidly developing and growing, children are more susceptible to the effects of these treatments, especially in the brain, heart, and reproductive system.[28,34] As such, it is vital to monitor pediatric cancer patients and survivors for the development of long-term effects and relapse as well as focus on the development of alternative pediatric cancer therapeutics.

**1.2.2 Neuroblastoma.** Behind leukemia, the most common childhood cancers include brain and spinal cord tumors, neuroblastoma, Wilms tumor, and lymphoma.[28] Neuroblastoma, the most common extracranial solid tumor of childhood, is frequently diagnosed at late-stages and

categorized as high-risk, about 60% of cases.[35–37] The malignancy forms in embryological development of the sympathetic nervous system.[38] In normal developmental processes, neuroblasts, or immature nerve cells, mature into healthy nerve cells. However, in some instances, these neuroblasts mutate and multiply uncontrollably, inducing the formation of a solid tumor. Often, these tumors form in the adrenal glands of the kidneys.[35,37] A few specific oncogenes are associated with the likelihood of high-risk categorization and metastasis, including MYCN (v-myc avian myelocytomatosis viral oncogene neuroblastoma derived homologue), anaplastic lymphoma kinase (ALK), and paired-like homeobox 2b (PHOX2B) genes.[37]

Although neuroblastoma accounts for only about 8% of all pediatric cancer diagnoses,[36] it attributes to about 15% of all pediatric cancer deaths.[36] Long-term survival rates vary dramatically and are highly dependent on the stage of the disease at diagnosis: low, intermediate, or high risk.[35] Additional factors contribute to the long-term prognosis and treatment plan, including (but not limited to) patient age, MYCN gene amplification status, and chromosomal aberrations.[35] Low and intermediate risk tumors have favorable survival rates, >90%[39,40] and >80%[41] five-year survival rates, respectively. Unfortunately, over 60% of initial diagnoses are classified as high risk tumors with especially poor prognosis and only ~15% ten-year survival rates.[37] As a result, treatment options for neuroblastoma range substantively based on the classification and progression of the disease at diagnosis.

**1.2.3 Treatment Options.** The most common treatment options for neuroblastoma reflect those of various other cancers, with surgery, chemotherapy, and radiation covering the majority of neuroblastoma cases. Currently, both low and intermediate risk neuroblastomas, which represent about 25% and 15% of initial diagnoses, respectively, are treated in similar manners.[35] Low risk neuroblastoma is most often treated via surgery and observation.[39,40] Intermediate risk

neuroblastoma treatment often includes surgery, observation, and chemotherapy and radiation, if necessary.[41] High risk neuroblastoma, due to its aggressive nature, is often treated with the previously mentioned treatments and various permutations of additional treatments, such as immunotherapy, bone marrow transplants, cytotoxic agents, targeted agents, retinoids, angiogenesis inhibitors, tyrosine kinase inhibitors, and various other methods.[42,43] Despite the multitude of potential treatments, prognosis for high risk neuroblastoma remains abysmal, necessitating new, alternative therapeutic options.

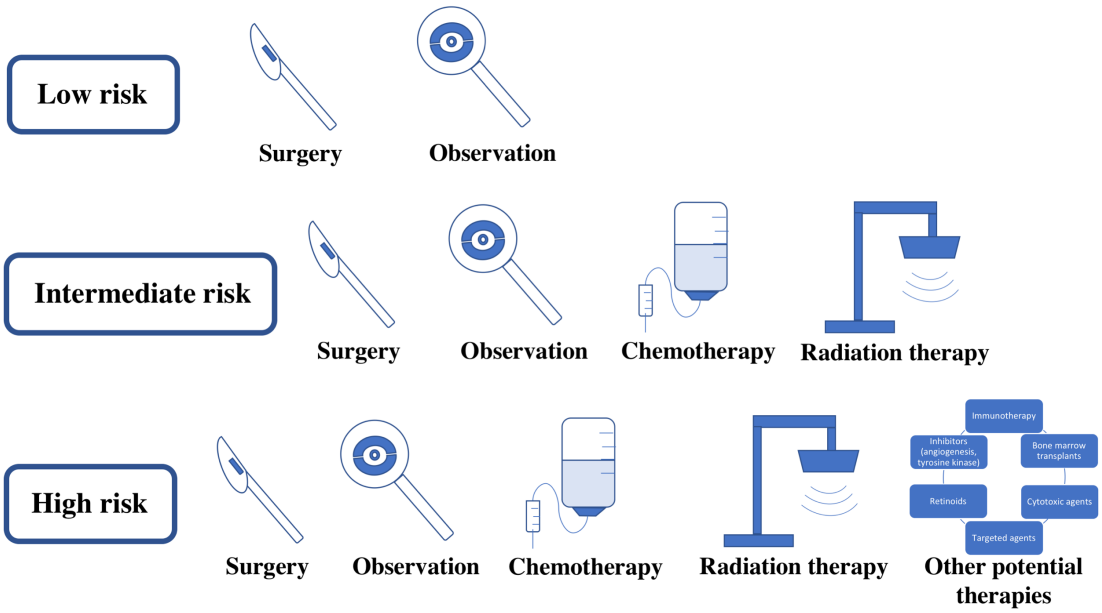


**Figure 1.2** Current approaches to treat neuroblastoma based on the level of risk at diagnosis: low, intermediate, and high. Low-risk neuroblastoma generally displays favorable outcomes with minimal treatment, intermediate-risk neuroblastoma largely exhibits promising outcomes with standard treatment, and high-risk neuroblastoma often presents ill-fated outcomes with aggressive treatment.

## 1.3 ALTERNATIVE APPROACHES TO CANCER THERAPY

**1.3.1 Targeted therapy as an anticancer therapeutic.** In cancer treatment, targeted therapy is a selective agent that targets a specific enzyme, growth factor receptor, or signal transducer to impact the growth, division, or life cycle of cancer cells.[23,44,45] Often, targeted therapeutics are small-molecule drugs or monoclonal antibodies. Small-molecule drugs are effective as anticancer

therapeutics due to their ability to cross the cellular membrane of cancer cells and target a specific element within that cell.[46] Conversely, monoclonal antibodies are proteins that are designed to attach to a section on the exterior of a cancer cell.[46] Once attached, cells are either "tagged" and the body's immune system can then identify and target them for destruction, halt growth, or expose them to toxins carried by the antibody.[46] Another distinct type of targeted therapy involves enzyme inhibitors, which also attach to the exterior membrane of cancer cells.[44] These inhibitors block the action of an enzyme that cancer cells need to grow or divide, in a reversible or irreversible manner. Reversible enzyme inhibitors can be detached upon washing with inhibitor free media whereas irreversible enzyme inhibitors have a negligible rate of dissociation after binding, despite washing. Therapeutic efficacy of these targeted methods varies extensively based on the target, malignancy, and a multitude of other factors.

Although targeted therapy can be very effective, there are also various limitations to this therapeutic approach. For example, targeted therapy can only be used if the relevant malignancy contains the target cellular components necessary for the therapeutic. Also, drugs can be difficult to develop for a specific target, cancer cells can develop resistance to targeted therapies, and some targeted therapies only take effect over a long time-scale (weeks to months). Physical side effects to targeted therapies (varying based on the type of therapy) can include dizziness, fatigue, nausea, rash, blood clotting, decreased wound healing, liver problems, and more.[44,46,47] Generally, these side effects are minimized through prescription medications that combat the presenting symptoms.

In neuroblastoma, a multitude of targeted therapeutics have been investigated, including ALK, Aurora A and B (AURKA/AURKB), MYCN and MYCN downstream pathway inhibitors, and many more.[47] As previously stated, neuroblastoma prognosis is largely influenced by MYCN, ALK, and PHOX2B oncogene expression.[37] Of these three oncogenes, MYCN is a difficult

primary target for therapeutics due to lack of suitable drug binding sites on its DNA binding domain.[47] As a result, various indirect pathways have been of interest to inhibit its expression. AURKA and AURKB kinases are integral components in the regulation of the cell cycle and MYCN function. Although expression of either or both of these kinases have been correlated to poor prognosis, they serve as enzyme targets to indirectly inhibit the function of MYCN and/or cell cycle progression.[47] Similarly, MYCN/MAX, BET, p53/MDM2, ornithine decarboxylase 1 (ODC1), and P13K/AKT/mTOR have all been identified and investigated as indirect targets of MYCN function.[47] Unlike MYCN, ALK is a highly promising direct target in neuroblastoma treatment.[37] ALK is a receptor tyrosine kinase that is mutated or amplified in about 14% of high-risk neuroblastoma cases and contains various suitable DNA binding sites.[47–49] The efficacy of ALK inhibitors on neuroblastoma is dependent upon the location of the mutation which impacts the ability of the inhibitor to bind.[47,50,51] Several ALK inhibitors including crizotinib, ceritinib, ensartinib, entrectinib, lorlatinib, and alectinib, have been and continue to be explored in neuroblastoma research.[47,52] Comparatively, PHOX2B as a target for neuroblastoma therapy has received less focus than MYCN or ALK. However, a recent study detailed the high throughput screening of various drugs directly targeting the overexpression of PHOX2B on various neuroblastoma cell lines. This study resulted in three of six selected compounds exhibiting favorable potential to decrease PHOX2B expression enough to influence neuroblastoma survival and progression.[53] Even though targeted therapeutics for these three oncogenes show promise, they are highly dependent on the type and location of the mutation and/or amplifications present. Therefore, it is imperative to continue searching for therapeutics that are more widely applicable but still highly efficacious.

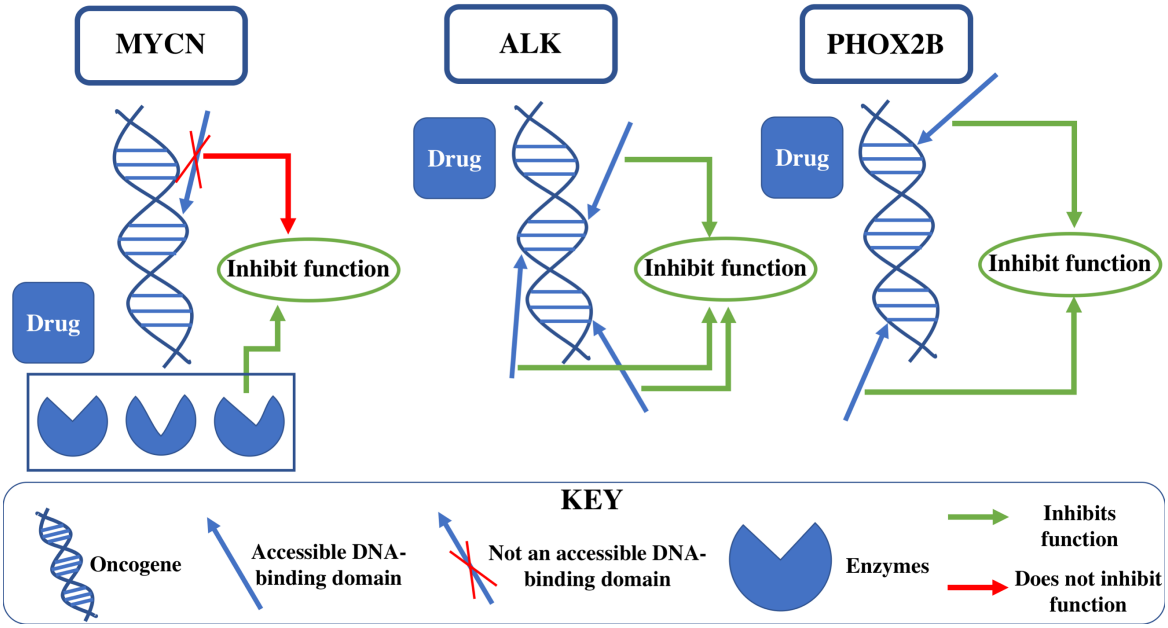


**Figure 1.3** Graphical representation of three categories of targeted anticancer therapeutics for neuroblastoma treatment. The three categories refer to the three major oncogenes that influence prognosis: MYCN, ALK, and PHOX2B. MYCN lacks suitable drug binding sites in the DNA-binding domain so enzymes are targeted to indirectly interfere with MYCN function or cell cycle progression. Alternatively, ALK and PHOX2B both contain at least two suitable DNA binding sites (ALK contains multiple) for direct inhibition of function and/or cell cycle progression. (**DNA-binding domains indicated in graphic are examples, not exact locations.)

In other malignancies, a multitude of targets have been identified and exploited. The SMYD proteins (a family of SET and MYND Domain containing lysine methyltransferases) are involved in a variety of normal cellular processes, but have also been linked to tumor development and progression.[54–56] In particular, SMYD3 overexpression lends to its tumor-promoting tendencies as it upregulates over 80 genes, including several oncogenes. These oncogenes increase proliferation and contribute to metastatic propensities.[57,58] In the majority of carcinomas, like those of the breast, lungs, colon, pancreas, and liver, SMYD3 has been identified as a valuable molecular target for regulating the uncontrolled proliferation and viability of malignant cells.[54,59,60] Based on these principles, SMYD3 inhibitors have been highly efficacious depending on the extent of overexpression of SMYD3 and its impact on downstream oncogenes and tumor-promoting

characteristics.[54,59] However, the use of SMYD3 inhibitors is limited to specific malignancies and often requires additional therapeutics to achieve complete knockdown, prompting further research.

**1.3.2 Nitric oxide and cancer.** Nitric oxide (NO), a small biological signaling molecule, innately influences various cellular functions. The specific biologic role that NO plays varies based on its production mechanism, location, concentration, release kinetics, and presence of NO scavenging agents. Biologically, the body produces NO via three forms of nitric oxide synthase (NOS), endothelial NOS (eNOS), neuronal NOS (nNOS), and inducible NOS (iNOS). NO produced by each form of NOS varies in concentration, longevity, and resultant impact on cell processes.[61] Expressly, eNOS and nNOS produce nanomolar concentrations of NO that is consumed on a time scale of seconds to hours and is involved in cell signaling.[61] Furthermore, micromolar concentrations of NO are generated by iNOS which is consumed in hours to days and is involved in cell growth and signaling.[61] Knowledge of these functions and the concentrations necessary to induce the desired impact can be exploited to implement NO as a therapeutic in a variety of circumstances.

Overall, some of the most notable functions of NO are its roles as a vasodilator, a neurotransmitter, inhibitor of platelet activation, proliferator of smooth muscle cells, and role as a cytotoxic agent.[62] Many of these functions are particularly advantageous in anticancer therapeutics: vasodilation can increase blood flow to malignancies and the surrounding areas, inhibition of platelet activation and cytotoxicity towards bacterial cells can reduce the potential for infections, and most importantly, cytotoxicity towards malignant cells at high, localized concentrations can reduce overall cancer cell counts.[63–68] Several other factors highlight NO as a prime candidate for anticancer therapeutics. For example, it is exceedingly unlikely that cancer cells will develop resistance to NO due to its extremely small size and highly reactive nature (due

to its existence as a free radical). NO is also lipophilic and tends to dissolve or combine with lipids or fats. This is important because fat is used by the body to create lymphatic vessels which is the primary route of cancer spread.[2] Despite the obvious benefits, there are some apparent limitations to the use of NO as an anticancer therapeutic. One limitation is the dual role of nitric oxide in cancer treatment, namely that low concentrations of NO have been observed to augment tumor cell proliferation.[69–74] Another is that NO has a very short half-life, on the millisecond time scale.[62] Other limitations include the lack of target specification and controlled release kinetics. Finally, unlike most biosignaling molecules that impact cells via binding interactions, NO effects cells via numerous reactions. The ultimate consequences of the NO-involved reactions are highly dependent on the concentration, location, release kinetics, and intracellular/extracellular composition of the surrounding biological area.[64,75–80,65–67,81–84]

Although the aforementioned limitations constrain the use of NO in cancer therapy, there are methods that can be used to address these concerns. One of the most common methods is the use of NO donor platforms. NO donor platforms generally impact the half-life, stability, and release kinetics of NO. Several types of NO donor platforms have been applied to achieve these goals such as liposomes, *S*-Nitrosothiols (RSNOs), and *N*-diazeniumdiolates.[63,78,80–82] Diazeniumdiolates contain two moles of NO per mole of donor compound, however they can be highly toxic to human and animal cells. Alternatively, RSNOs have one mole of NO per mole of donor compound and are endogenously produced in humans and animals.[79–81] Since the ultimate goal anticancer applications is selective neoplastic cell death with retained normal cell health, RSNOs were chosen for further exploration in this work. Purposely, the RSNO, *S*-Nitrosoglutathione (GSNO) was applied in this work due to its prolonged stability and NO-release profile at characteristic body temperature (~37°C) and pH (~7).

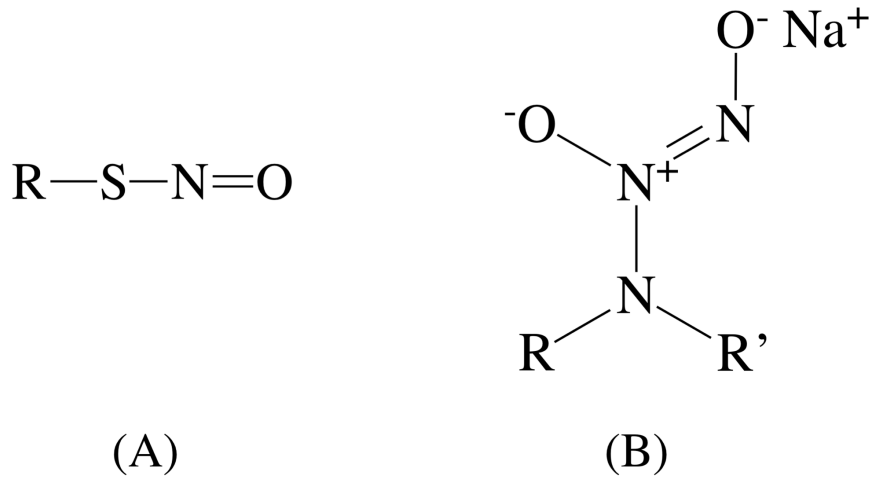


**Figure 1.4** General forms of two common NO donors applied in anticancer applications including (A) *S*-Nitrosothiols (RSNOs) and (B) *N*-diazeniumdiolates.

In neuroblastoma research, the use of NO donating agents has not been thoroughly explored. However, a few studies have shown the applicability of NO-based anticancer therapeutics in neuroblastomas. Namely, the peroxynitrite donor 3-morpholino-sydnonimine (SIN-1) has been shown to induce cell death in SH-SY5Y human neuroblastoma cells.[75] Additionally, the NO donor sodium nitroprusside (SNP) demonstrated NO-induced cell death in SH-SY5Y[85,86] and SH-EP1 human neuroblastoma cells[87]. This research, combined with the aforementioned NO-based anticancer research on other malignancies, led to the expanded exploration of NO-based anticancer therapeutics in pediatric neuroblastomas presented in this dissertation (Chapters 4 and 5).

Furthermore, to expand the knowledge regarding NO-based anticancer therapeutics and combinations, adult breast cancers were also implemented (in Chapter 6) to determine the difference (if any) in impact of NO on pediatric and adult cancers. This step was crucial to compare the efficacy of NO in pediatric and adult cancers, specifically because of the differences between

pediatric and adult cancers explained above. Ultimately, this work highlighted the potential of NO-based therapeutics in the treatment of pediatric and adult cancers and its consistent potential for specific neoplastic cell death.

## 1.4 DETERMINATION OF ANTICANCER THERAPEUTIC EFFICACY

Since the ability to accurately determine therapeutic efficacy remains a major concern in the development of new therapeutic options for cancer treatment, multiple phases are necessary to determine its clinical relevance, including drug discovery, *in vitro* testing, pre-clinical animal studies, and clinical trials.[88–90] Though the latter stages are essential to determine safety and efficacy, the initial stages are vital to determination of efficacy and practicality for application in patients (human and animal). In those initial stages of drug discovery and *in vitro* efficacy testing, the use of tumor-derived cell lines is crucial due to financial feasibility, translational relevance, and humane methodology.[91] Chapter 2 of this dissertation provides in-depth coverage of the different assay types, examples of specific assays that are included in each type, and the information that is obtained through application of these assays. In this work, *in vitro* assays from several categories were applied to get a clear picture of the overall impact and clinical potential of the therapeutics assessed.

In all of the studies comprising this dissertation, cell viability assays were performed. Three different cell viability assays, resazurin, MTT, and WST-8 were applied to determine the number of live cells remaining after treatment with the therapeutic of interest. Generally, a single cell viability is performed in anticancer therapeutic efficacy studies. One reason for this is that these assays often produce varying results.[92–94] In attempt to explain this, Chapter 3 of this dissertation explores the protocol development related to each of these three cellular viability assays. After this extensive protocol development, all three of these viability assays were performed in Chapter 4.

The results of these assays indicated that when performed appropriately, these assays do indeed yield similar results. With this information established, resazurin and MTT were both applied in Chapter 5 and Chapter 6.

After the cell viability assays were completed in each study, a variety of additional assays were completed to determine therapeutic efficacy. Specifically, an assortment of colony formation, cytotoxicity, RNA-sequence, and apoptosis assays were implemented. Colony formation assays were utilized in each study and corresponding chapters (Chapters 4-6) to highlight the notable impact of NO and NO + Inhibitor-4 on the proliferation capacity of malignancies. Cytotoxicity assays further illuminated the effect of NO and NO + Inhibitor-4 by exposing both live and dead cells after treatment in Chapters 5 and 6. RNA-sequence analysis provided exceedingly valuable information about the mechanism of action of NO on neuroblastomas in Chapter 5. Finally, apoptosis assays were performed to determine critical information about the nature of NO and NO + Inhibitor-4 induced cell death (necrosis versus early/late apoptosis).

Overall, each of the assays performed in the studies that comprise this dissertation led to a more complete picture of the precise role of NO and NO + SMYD-3 inhibitor, Inhibitor-4, on both pediatric neuroblastomas and adult breast cancers. Individually, the assay results show that the therapeutics investigated exhibit some anticancer potential. Together, the assay results definitively demonstrate that NO-based anticancer therapeutics are effective, particularly as an adjuvant therapeutic to traditional therapeutic options.

**1.5 DISSERTATION OUTLINE** – This dissertation encompasses assessments of relevant NO-based anticancer therapeutics and their impact on various clinically relevant cell lines, including pediatric neuroblastomas and adult breast cancers. Additionally, there is an evaluation

of the impact of a combination of SMYD-3 inhibitor, Inhibitor-4, and GSNO on adult breast cancers.

*Chapter 2.* A critical evaluation of pertinent cell-based methods for determination of anticancer therapeutic efficacy was included in Chapter 2. The breakdown of assay categories included in this section was a crucial addition to the overall field of anticancer therapeutic clinical relevance as well as this dissertation. Assay categories, their descriptions, and common examples of the cell-based methods that are generally applied in these categories were included. Specifically, cell viability and proliferation assays, colorimetric assays, binding assays, ATP production assays, colony formation assays, cytotoxicity assays, cell apoptosis assays, cell cycle arrest assays, and 3D cell culture systems are covered in this chapter. **Importantly, this section emphasizes the necessity to perform a variety of assays from multiple categories to determine anticancer therapeutic efficacy and potential clinical relevance.** In accordance to this chapter, various methods from the aforementioned categories were applied in the following chapters.

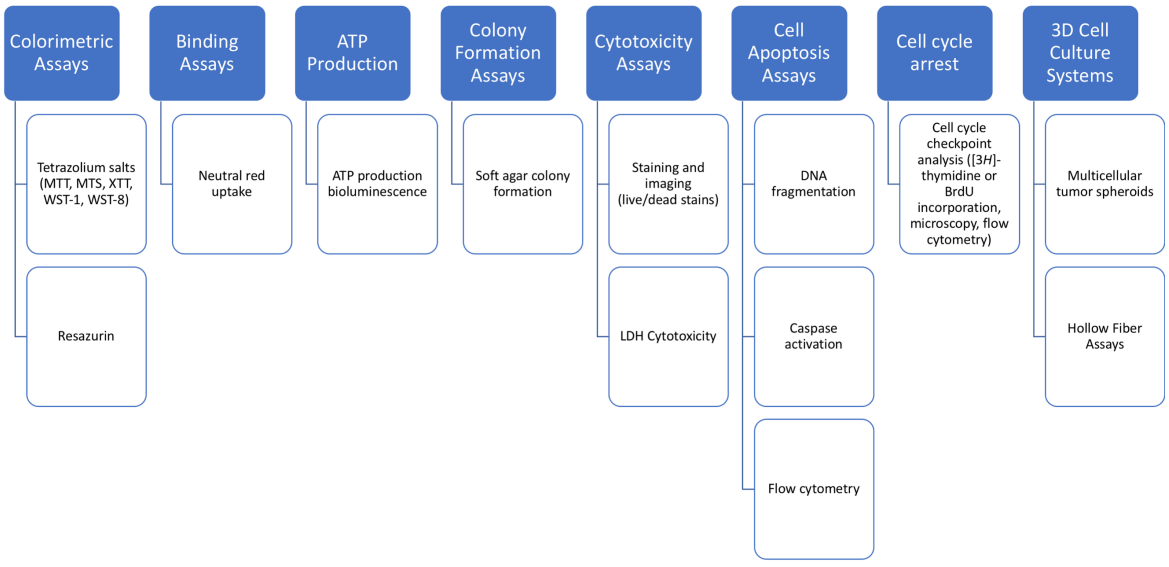


**Figure 1.5** Graphical representation of the pertinent cell-based methods for determination of anticancer therapeutic efficacy described in Chapter 2. The first four types of assays, colorimetric,

binding, ATP production, and colony formation assays are cell viability and proliferation assays. The next three types, cytotoxicity, cell apoptosis, and cell cycle arrest assays are cell death assays. All seven of these assay types are applied in monolayer cultures. The final assay type, 3D cell culture systems, are more extensive model systems that can encompass cell viability, proliferation, and death assays as well as account for additional impacts of a natural system.

*Chapter 3.* Chapter 3 of this dissertation elucidated the in-depth protocol development and the shortcomings of current assay protocols that were revealed by the initial cellular viability assay results. Some of the most important factors that were explored in this chapter include an examination of the deficiencies in general cellular viability assay protocols, such as the removal and/or avoidance of air bubbles and consideration of potential assay interferences. Also, the factors impacting assay sensitivity in the three cellular viability assays applied in this work, WST-8, resazurin, and MTT, were critically evaluated. **This chapter was an essential addition in this dissertation due to the extensive analytical analysis that was conducted to make this and future work applicable and relevant in the anticancer therapeutic field.**

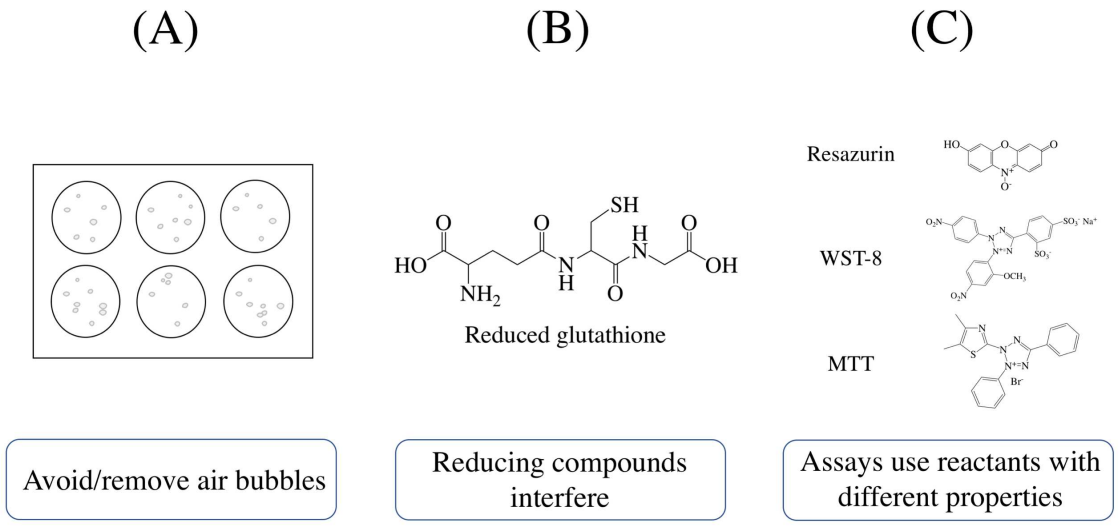


**Figure 1.6** Graphical representation of the cellular viability protocol development and assay shortcomings illuminated in Chapter 3. The three main findings highlighted in this chapter include the necessity to avoid/remove air bubbles, avoid/remove reducing compounds (due to the potential for interference), and account for differences in the properties of assay reactants.

*Chapter 4.* The fourth chapter of this dissertation highlighted the potential of NO as a treatment for pediatric neuroblastoma using murine neuro-2a (N2a) neuroblastoma cells as a principal cell line. In this work, N2a cells were exposed to the NO-releasing donor, 1 mM GSNO, and analyzed for cell viability (MTT, CTB, and WST-8) and colony formation capacity. Consistently, 24 h of exposure to GSNO resulted in ~20-25% of cells with arrested metabolic activity and 100% exhibiting no colony formation capacity. Additionally, an identical treatment on Adult Human Dermal Fibroblasts (HDFa) did not demonstrate a decrease in cellular viability. **This data collectively illustrates the potential of NO to act as an adjuvant therapeutic to traditional neuroblastoma treatment methods while simultaneously decreasing patient risk.**

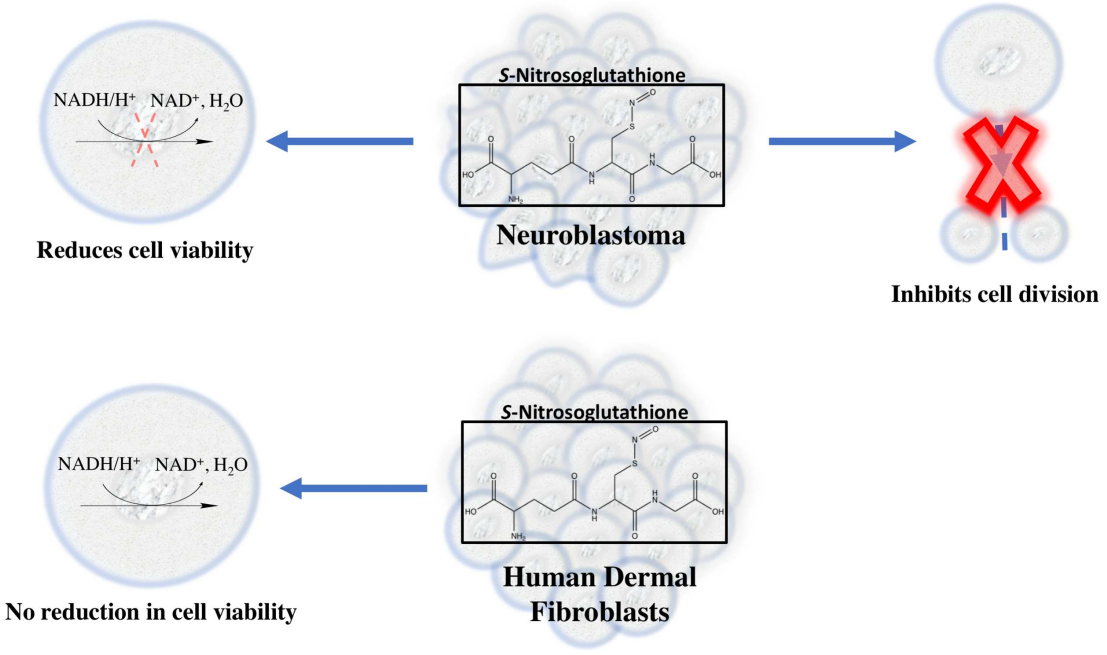


**Figure 1.7** Schematic of the conclusions collected in Chapter 4 wherein cell viability and clonogenic capacity were evaluated on N2a neuroblastoma cells exposed to 1 mM GSNO for 24 h. Similarly, cell viability was assessed on Adult Human Dermal Fibroblasts (HDFa) following an identical treatment.

*Chapter 5.* Chapter 5 expanded the exploration of NO-donor treatments for pediatric neuroblastoma on various cell lines. In this study, GSNO was applied as an anticancer NO-donor against SK-N-SH (murine), IMR-32 (human), and B104 (rat) cell lines and then probed for

anticancer potency and therapeutic mechanism of action. Consistently, 24 h of exposure to 1 mM GSNO resulted in ~13-29% of cells with arrested metabolic activity and ~79-94% of cells losing colony formation capability across the three cell lines of interest. Additionally, LIVE/DEAD cytotoxicity assays displayed a discernable qualitative decrease in the number of live cells and increase in number of dead cells after treatment. Finally, RNA-sequence analysis of B104 neuroblastoma cells exposed significant insight into the mechanism of action of NO against neuroblastomas which is a highly under-explored and ambiguous area of research. Prominently, these innovative results displayed significantly more differentially expressed genes in NO-treated samples than GSH-treated samples (functional control). Notably, the upregulated and downregulated transcripts in the NO-treated samples were linked to ATP depletion leading to apoptosis, oxidative stress, growth inhibition, and cell cycle arrest. **Prominently, this data represents the first study highlighting the mechanism of action of NO against pediatric neuroblastomas while simultaneously highlighting its potential as an adjuvant therapeutic to traditional methods of cancer treatment.**

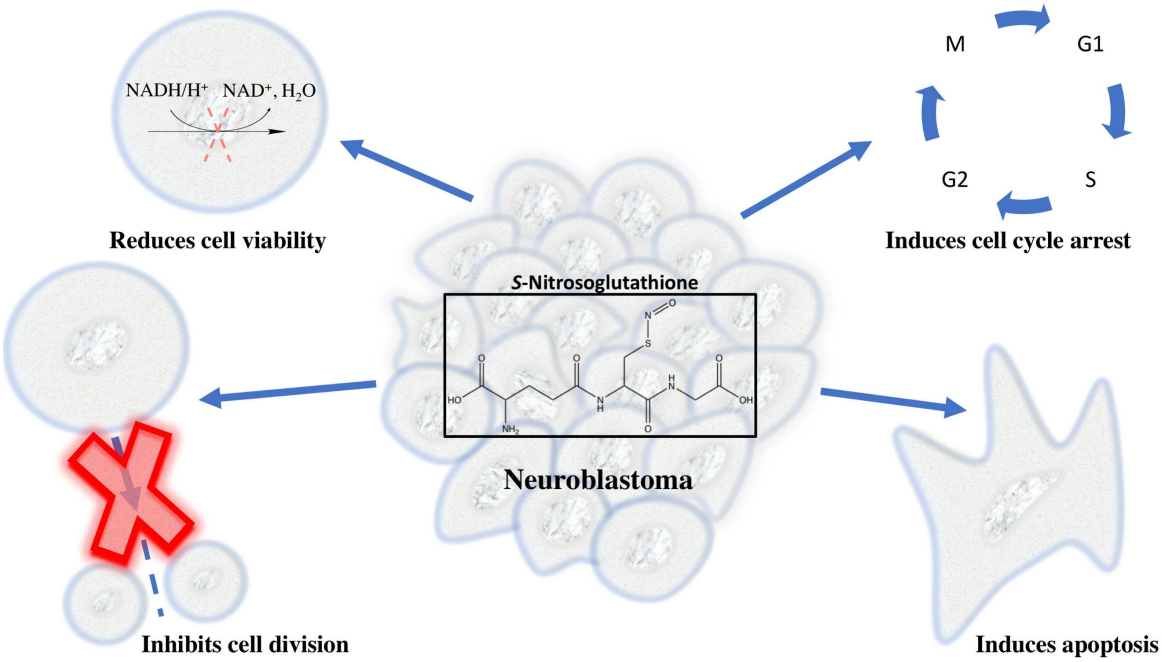

**Figure 1.8** Schematic of the conclusions observed in the investigation described in Chapter 5 wherein cell viability, clonogenic capacity (ability to complete the cellular division process), appearance of live and dead cells, and RNA-sequence analyses were applied on various neuroblastoma cell lines (SK-N-SH, B104, IMR-32) exposed to 1 mM GSNO for 24 h.

*Chapter 6.* Chapter 6 concludes this thesis with an investigation of the anticancer effect of NO, delivered by GSNO, on adult breast cancer cell lines, MCF7 and MDA-MB-231, and normal breast cell line, MCF10A. **Specifically, this study showed that NO moderatly reduced cell viability and greatly reduced colony formation capacity in adult breast cancer lines, MCF7 and MDA-MB-231.** Unfortunately, normal MCF10A breast cell viability was also reduced. These findings indicate potential for application of NO in breast cancers with some obvious limitations. As such, this study is currently being expanded to include an analysis of a combination treatment including NO, delivered by GSNO, and SMYD-3 inhibitor, Inhibitor-4, on MCF7 and MDA-MB-231 breast cancer cells as well as normal MCF10A breast cells. Alone, Inhibitor-4 has been shown to induce reduction of MCF7 and MDA-MB-231 cell viability and colony formation capacity as well as induction of apoptosis. Fortuitously, Inhibitor-4 does not impact normal MCF10A cell viability or apoptosis.[95] Ideally, the combination of the two therapeutics will be synergistic and much more effective than either individual treatment.

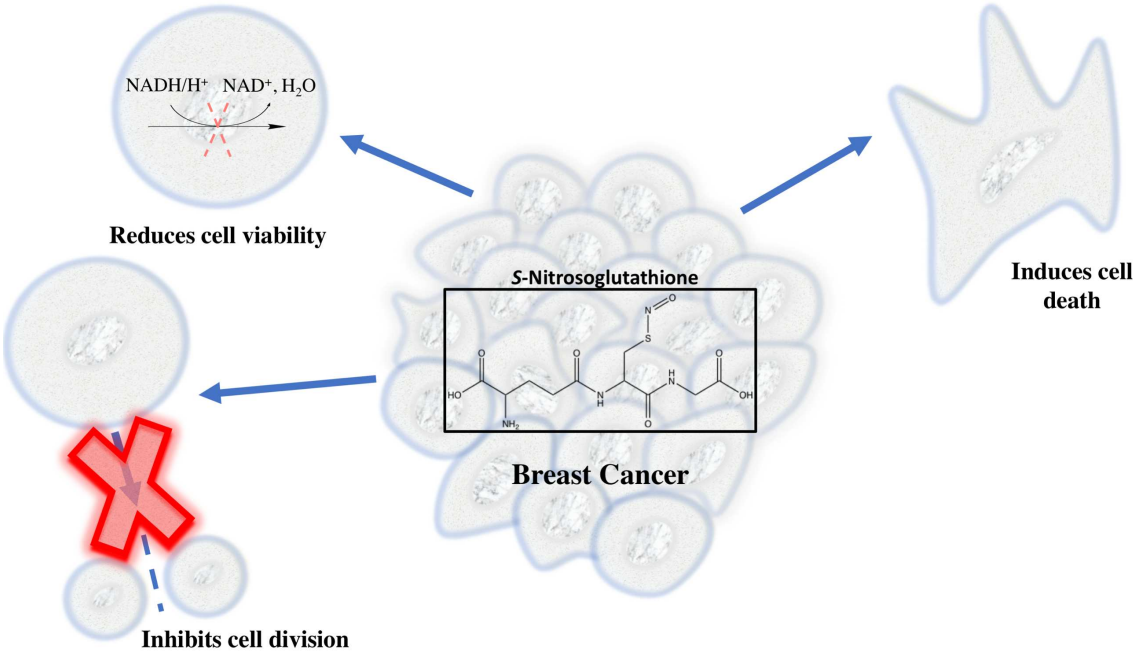


**Figure 1.9** Schematic of the conclusions gained in Chapter 6 wherein cell viability, colony formation capacity, and cytotoxicity were investigated after application of 1 mM GSNO on MCF7 and MDA-MB-231 breast cancer cells for 24 h. Normal MCF10A breast cells were identically treated and also experienced a decrease in cellular viability.

*Summarizing remarks.* This dissertation presents various studies that emphasize the potential of NO (delivered by GSNO) to act as an anticancer agent against pediatric neuroblastomas and adult breast cancers. Explicitly, application of NO, delivered via 1 mM GSNO, exhibited moderate reduction of cellular viability, extreme reduction of colony formation capacity, and mild to moderate increases in cell death in both pediatric neuroblastomas and adult breast cancers. NO (delivered by GSNO) did NOT reduce the viability of normal HDFa cells. However, NO did reduce viability of normal MCF10A breast cells. This data collectively illustrates the potential of NO to act as an adjuvant therapeutic to traditional and alternative anticancer therapeutic methods while simultaneously decreasing patient risk. In some experiments done by a collaborator, SMYD-3 inhibitor, Inhibitor-4, was applied to adult breast cancers and healthy breast tissue to assess its therapeutic impact. This treatment alone showed a similar response to that of the individual NO treatments, showing a statistically significant impact on cell viability, clonogenic capacity, and

cell apoptosis of the malignant cell lines (MCF7 and MDA-MB-231) while imparting no change on these qualities in the normal breast tissue line MCF10A.[95] Ultimately, a combination of both NO (delivered by GSNO) and SMYD-3 inhibitor, Inhibitor-4, will be applied to identical breast cell lines. Ideally, the combination of NO (delivered by GSNO) and SMYD-3 inhibitor, Inhibitor-4, will be more effective than either therapeutic individually. Overall, these findings significantly expanded the knowledge of NO-based anticancer therapeutics and open a gateway for the exciting anticancer potential of a novel combination of NO and SMYD-3 in various cancers.

# CHAPTER 1 – REFERENCES


1 National Cancer Institute, Definition of cancer- NCI Dictionary of Cancer Terms - National Cancer Institute, https://www.cancer.gov/publications/dictionaries/cancer-terms/def/cancer-cell-line.

2 M. E. Miller, in *Cancer*, 2018, pp. xii–xxii.

3 National Cancer Institute, Definition of hyperplasia, https://www.cancer.gov/publications/dictionaries/cancer-terms/def/metastasis.

4 National Cancer Institute, Definition of dysplasia - NCI Dictionary of Cancer Terms - National Cancer Institute, https://www.cancer.gov/publications/dictionaries/cancer-terms/def/metastasis.

5 National Cancer Institute, What Is Cancer?, https://www.cancer.gov/about-cancer/understanding/what-is-cancer.

6 G. M. Cooper and R. E. Hausman, *Cell A Mol. Approach*, 2007, 743.

7 G. P. Rédei, *Encycl. Genet. Genomics, Proteomics Informatics*, 2008, 262–262.

8 National Cancer Institute, Cancer Statistics, https://www.cancer.gov/about-cancer/understanding/statistics.

9 World Health Organisation, 2017, 1–3.

10 R. L. Siegel, K. D. Miller and A. Jemal, *CA. Cancer J. Clin.*, 2017, **67**, 7–30.

11 National Cancer Institute, Screening Tests.

12 National Cancer Institute, How Cancer Is Diagnosed.

13 R. H. Bradbury, *Cancer*, 2007, **1**, 1–17.

14 *Five-Year Relative Survival*, 2017.

15 R. Sullivan, O. I. Alatise, B. O. Anderson, R. Audisio, P. Autier, A. Aggarwal, C. Balch, M. F. Brennan, A. Dare, A. D'Cruz, A. M. M. Eggermont, K. Fleming, S. M. Gueye, L. Hagander, C. A. Herrera, H. Holmer, A. M. Ilbawi, A. Jarnheimer, J. fu Ji, T. P. Kingham, J. Liberman, A. J. M. Leather, J. G. Meara, S. Mukhopadhyay, S. S. Murthy, S. Omar, G. P. Parham, C. S. Pramesh, R. Riviello, D. Rodin, L. Santini, S. V. Shrikhande, M. Shrime, R. Thomas, A. T. Tsunoda, C. van de Velde, U. Veronesi, D. K. Vijaykumar, D. Watters, S. Wang, Y. L. Wu, M. Zeiton and A. Purushotham, *Lancet Oncol.*, 2015, **16**, 1193–1224.

16 National Cancer Institute, Surgery to Treat Cancer.

17 B. A. Chabner and T. G. Roberts, *Nat. Rev. Cancer*, 2005, **5**, 65–72.

18 R. Jones and J. Ocen, *Med. (United Kingdom)*, 2020, **48**, 97–102.

19 National Cancer Institute, Chemotherapy to Treat Cancer.

20 R. Baskar, K. A. Lee, R. Yeo and K. W. Yeoh, *Int. J. Med. Sci.*, 2012, **9**, 193–199.

21 National Cancer Institute, Radiation Therapy to Treat Cancer.

22 O. Tureci, T. Klamp, M. Koslowski and S. Kreiter, *Immunotherapy of Cancer*, Humana Press, 2006.

23 S. Mocellin, J. Shrager, R. Scolyer, S. Pasquali, D. Verdi, F. M. Marincola, M. Briarava, R. Gobbel, C. Rossi and D. Nitti, *PLoS One*, 2010, **5**, 1–11.

24 Y. Yuan, S. Xu, C.-J. Zhang and B. Liu, *Polym. Chem.*, 2016, **7**, 3530–3539.

25 U. Stein, W. Walther, P. Schlag and H. Gelderblom, *Regional Cancer Therapy*, Humana Press, 2007.

26 *Natl. Cancer Inst.*, 2017, 1–7.

27 A. Jemal, E. M. Ward, C. J. Johnson, K. A. Cronin, J. Ma, A. B. Ryerson, A. Mariotto, A. J. Lake, R. Wilson, R. L. Sherman, R. N. Anderson, S. J. Henley, B. A. Kohler, L.

Penberthy, E. J. Feuer and H. K. Weir, *J. Natl. Cancer Inst.*, 2017, **109**, 1–22.

28 T. Macdonald, *Can. Pharm. J.*, 2010, **143**, 176–183.

29 L. a. G. Ries, M. a. Smith, J. G. Gurney, M. Linet, T. Tamra, J. L. Young and G. R. Bunin, *Cancer incidence and survival among children and adolescents: United States SEER Program 1975-1995.*, 1999.

30 NCI, Cancer in Children and Adolescents, https://www.cancer.gov/types/childhood-cancers/child-adolescent-cancers-fact-sheet.

31 M. Hewitt, S. L. Weiner and J. V. Simone, *Childhood Cancer Survivorship: Improving Care and Quality of Life*, 2003.

32 National Cancer Institute, 2017.

33 M. F. G. Murphy, J. F. Bithell, C. A. Stiller, G. M. Kendall and K. A. O'Neill, *Maturitas*, 2013, **76**, 95–98.

34 Oncology Center of Excellence > Pediatric Oncology, http://jama.jamanetwork.com/article.aspx?doi=10.1001/jama.292.19.2403.

35 M. Hayat, *Neuroblastoma*, Springer, 2012.

36 D. H. Colon, Nadja C.; Chung, *Adv. Pediatr.*, 2012, **23**, 1–7.

37 J. Shohet and J. Foster, *Br. Med. J.*, 2017, **357**, j1863;1-8.

38 *Natl. Inst. Heal.*, 2011.

39 C. A. Perez, K. K. Matthay, J. B. Atkinson, R. C. Seeger, H. Shimada, G. M. Haase, D. O. Stram, R. B. Gerbing and J. N. Lukens, *J. Clin. Oncol.*, 2000, **18**, 18–26.

40 J. G. Nuchtem, W. B. London, C. E. Barnewolt, A. Naranjo and P. W. McGrady, *Ann. Surg.*, 2017, **256**, 573–580.

41 D. Pe, C. Le, C. Oscarlambret and H. Dieu, *Br. J. Cancer*, 2003, **89**, 1605–1609.

42 A. Garaventa, S. Parodi, B. De Bernardi, D. Dau, C. Manzitti, M. Conte, F. Casale, E. Viscardi, M. Bianchi, P. D. Angelo, G. Andrea, R. Luksch, C. Favre, A. Tamburini and R. Haupt, *Eur. J. Cancer*, 2009, **45**, 2835–2842.

43 F. Berthold, B. Hero, H. Breu, H. Christiansen, R. Erttmann, A. Gnekow, F. Herrmann, T. Klingebiel, F. Lampert, S. Miiller-weihrich and P. Weinel, *Ann. Oncol.*, 1996, **7**, 183–187.

44 A. M. Tsimberidou, *Cancer Chemother. Pharmacol.*, 2015, **76**, 1113–1132.

45 T. P. Kenakin, in *Pharmacology in Drug Discovery and Development*, 2017, pp. 131–156.

46 J. S. Ross, *Am. J. Cancer*, 2004, **3**, 205–214.

47 E. G. Greengard, *Children*, , DOI:10.3390/children5100142.

48 a Arora and E. M. Scholar, *J Pharmacol Exp Ther*, 2005, **315**, 971–979.

49 V. R. Holla, Y. Y. Elamin, A. M. Bailey, A. M. Johnson, B. C. Litzenburger, Y. B. Khotskaya, N. S. Sanchez, J. Zeng, M. A. Shufean, K. R. Shaw, J. Mendelsohn, G. B. Mills, F. Meric-Bernstam and G. R. Simon, *Mol. Case Stud.*, 2017, **3**, a001115.

50 S. C. Bresler, D. A. Weiser, P. J. Huwe, J. H. Park, K. Krytska, H. Ryles, M. Laudenslager, E. F. Rappaport, A. C. Wood, P. W. McGrady, M. D. Hogarty, W. B. London, R. Radhakrishnan, M. A. Lemmon and Y. P. Mossé, *Cancer Cell*, 2014, **26**, 682–694.

51 L. Chen, A. Humphreys, L. Turnbull, A. Bellini, G. Schleiermacher, H. Salwen, S. L. Cohn, N. Bown and D. A. Tweddle, *Oncotarget*, 2016, **7**, 87301–87311.

52 J. Lu, S. Guan, Y. Zhao, Y. Yu, S. E. Woodfield, H. Zhang, K. L. Yang, S. Bieerkehazhi, L. Qi, X. Li, J. Gu, X. Xu, J. Jin, J. A. Muscal, T. Yang, G.-T. Xu and J. Yang, *Cancer Lett.*, 2017, **400**, 61–68.

53 E. Di Zanni, G. Bianchi, R. Ravazzolo, L. Raffaghello, I. Ceccherini and T. Bachetti,

*Oncotarget*, 2017, **8**, 72133–72146.

54 R. Hamamoto, Y. Furukawa, M. Morita, Y. Iimura, F. P. Silva, M. Li, R. Yagyu and Y. Nakamura, *Nat. Cell Biol.*, 2004, **6**, 731–740.

55 M. A. Brown, K. Foreman, J. Harriss, C. Das, L. Zhu, M. Edwards, S. Shaaban and H. Tucker, *Oncotarget*, 2015, **6**, 4005–4019.

56 S. Komatsu, I. Imoto, H. Tsuda, K. I. Kozaki, T. Muramatsu, Y. Shimada, S. Aiko, Y. Yoshizumi, D. Ichikawa, E. Otsuji and J. Inazawa, *Carcinogenesis*, 2009, **30**, 1139–1146.

57 A. M. Cock-Rada, S. Medjkane, N. Janski, N. Yousfi, M. Perichon, M. Chaussepied, J. Chluba, G. Langsley and J. B. Weitzman, *Cancer Res.*, 2012, **72**, 810–820.

58 X. G. Luo, C. L. Zhang, W. W. Zhao, Z. P. Liu, L. Liu, A. Mu, S. Guo, N. Wang, H. Zhou and T. C. Zhang, *Cancer Lett.*, 2014, **344**, 129–137.

59 R. Hamamoto, F. P. Silva, M. Tsuge, T. Nishidate, T. Katagiri, Y. Nakamura and Y. Furukawa, *Cancer Sci.*, 2006, **97**, 113–118.

60 P. K. Mazur, N. Reynoird, P. Khatri, P. W. T. C. Jansen, A. W. Wilkinson, S. Liu, O. Barbash, G. S. Van Aller, M. Huddleston, D. Dhanak, P. J. Tummino, R. G. Kruger, B. A. Garcia, A. J. Butte, M. Vermeulen, J. Sage and O. Gozani, *Nature*, 2014, **510**, 283–287.

61 O. W. Griffith and D. Stueh, *Annu. Rev. Physiol.*, 1995, **57**, 707–736.

62 J. M. Fukuto, *Adv. Pharmacol.*, 1995, **34**, 1–15.

63 M. M. Reynolds, S. D. Witzeling, V. B. Damodaran, T. N. Medeiros, R. D. Knodle, M. A. Edwards, P. P. Lookian and M. A. Brown, *Biochem. Biophys. Res. Commun.*, 2013, **431**, 647–651.

64 S. Korde Choudhari, M. Chaudhary, S. Bagde, A. R. Gadbail and V. Joshi, *World J. Surg. Oncol.*, 2013, **11**, 1.

65 A. Nortcliffe, A. G. Ekstrom, J. R. Black, J. A. Ross, F. K. Habib, N. P. Botting and D. O'Hagan, *Bioorganic Med. Chem.*, 2014, **22**, 756–761.

66 S. Y. Lee, Y. Rim, D. D. McPherson, S. L. Huang and H. Kim, *Biomed. Mater. Eng.*, 2014, **24**, 61–67.

67 M. M. Reynolds, S. D. Witzeling, V. B. Damodaran, D. M. Jarigese, M. A. Edwards, R. D. Knodle, P. P. Lookian and M. A. Brown, *J. Vet. Sci. Med.*

68 H.-K. Jeon, S. Choi and N.-P. Jung, *Cell Biol. Toxicol.*, 2005, **21**, 115–25.

69 D. A. Wink, Y. Vodovotz, J. Laval, F. Laval, M. W. Dewhirst and J. B. Mitchell, *Carcinogenesis*, 1998, **19**, 711–721.

70 B. J. Oleson and J. A. Corbett, *Antioxidants Redox Signal.*, 2018, **29**, 1432–1445.

71 S. Pervin, R. Singh, S. Sen and G. Chaudhuri, *Nitric Oxide (NO) and Cancer*, 2010, 39–57.

72 J. Hickok and D. Thomas, *Curr. Pharm. Des.*, 2010, **16**, 381–391.

73 Z. Huang, J. Fu and Y. Zhang, *J. Med. Chem.*, 2017, **60**, 7617–7635.

74 W. Badn and P. Siesjo, *Curr Pharm Des*, 2010, **16**, 428–30.

75 K. Oh-hashi, W. Maruyama, H. Yi, T. Takahashi, M. Naoi and K. Isobe, *Biochem. Biophys. Res. Commun.*, 1999, **1999 Sep 2**, 504–509.

76 B.-C. Kim, Y.-S. Kim, J.-W. Lee, J.-H. Seo, E.-S. Ji, H. Lee, Y.-I. Park and C.-J. Kim, *Exp. Neurobiol.*, 2011, **20**, 100.

77 E. V. Stevens, A. W. Carpenter, J. H. Shin, J. Liu, C. J. Der and M. H. Schoenfisch, *Mol. Pharm.*, 2010, **7**, 775–785.

78 D. J. Suchyta and M. H. Schoenfisch, *RSC Adv.*, 2017, **7**, 53236–53246.

79 E. Kogias, N. Osterberg, B. Baumer, N. Psarras, C. Koentges, A. Papazoglou, J. E.

Saavedra, L. K. Keefer and A. Weyerbrock, *Int. J. Cancer*, 2012, **130**, 1184–1194.

80 V. J. Findlay, D. M. Townsend, J. E. Saavedra, G. S. Buzard, M. L. Citro, L. K. Keefer, X. Ji and K. D. Tew, *Mol. Pharmacol.*, 2004, **65**, 1070–1079.

81 Y. Hou, J. Wang, P. R. Andreana, G. Cantauria, S. Tarasia, L. Sharp, P. G. Braunschweiger and P. G. Wang, *Bioorganic Med. Chem. Lett.*, 1999, **9**, 2255–2258.

82 R. Dong, X. Wang, H. Wang, Z. Liu, J. Liu and J. E. Saavedra, *Biomed. Pharmacother.*, 2017, **88**, 367–373.

83 J. Fu, J. Han, T. Meng, J. Hu and J. Yin, *Chem. Commun.*, 2019, **55**, 12904–12907.

84 D. J. Suchyta and M. H. Schoenfisch, *Mol. Pharm.*, 2015, **12**, 3569–3574.

85 H. J. Lee, D. H. Lyu, U. Koo, K. W. Nam, S. S. Hong, K. O. Kim, K. H. Kim, D. Lee and W. Mar, *Arch. Pharm. Res.*, 2012, **35**, 163–170.

86 G. Tovilovic, N. Zogovic, L. Harhaji-Trajkovic, M. Misirkic-Marjanovic, K. Janjetovic, L. Vucicevic, S. Kostic-Rajacic, A. Schrattenholz, A. Isakovic, V. Soskic and V. Trajkovic, *ChemMedChem*, 2012, **7**, 495–508.

87 L. Wang, B. F. Cheng, H. J. Yang, M. Wang and Z. W. Feng, *Am. J. Transl. Res.*, 2015, **7**, 1541–1552.

88 J. A. Dimasi, L. Feldman, A. Seckler and A. Wilson, *Clin. Pharmacol. Ther.*, 2010, **87**, 272–277.

89 J. Scannell, A. Blanckley, H. Boldon and B. Warrington, *Nat. Rev. Drug Discov.*, 2012, **11**, 191–200.

90 A. Eastman, *Oncotarget*, 2016, **8**, 8854–8866.

91 E. Michelini, L. Cevenini, L. Mezzanotte, A. Coppa and A. Roda, *Anal. Bioanal. Chem.*, 2010, **398**, 227–238.

92 M. J. Stoddart, K. S. Louis, A. C. Siegel, L. Kupcsik and E. M. Czekanska, *Chapters 1-5: Mammalian Cell Viability*, Humana Press, 2011, vol. 740.

93 T. Riss, R. Moravec, A. Niles and S. Duellman, in *Assay Guidance Manual [Internet]*, 2013, pp. 1–55.

94 K. Prabst, H. Engelhardt, S. Ringgeler, H. Hubner, G. Ates, T. Vanhaeke, V. Rogiers, R. Rodrigues, L. L.-Y. Chan, K. J. McCulley, S. L. Kessel, D. P. Ivanov, A. M. Grabowska, M. C. Garnett, N. Suganuma, N. I. Molefe and N. Inoue, *Chapters 1-4, 8: Cell Viability Assays*, Humana Press, 2017, vol. 1601.

95 I. M. Alshiraihi, D. K. Jarrell, Z. Arhouma, K. N. Hassell, J. Montgomery, A. Padilla, H. M. Ibrahim, D. C. Crans, T. A. Kato and M. A. Brown, *Int. J. Mol. Sci.*, 2020, **21**, 1–15.

# CHAPTER 2

# CELL-BASED METHODS FOR DETERMINATION OF ANTICANCER THERAPEUTIC EFFICACY

## 2.1 BACKGROUND

The genesis of this chapter emerged following the conclusion of the literature seminar developed by Jenna L. Gordon for the Doctor of Philosophy requirement at Colorado State University. While researching for this seminar, it became clear that there are numerous methods applied in the determination of therapeutic efficacy but that there is no standard method or specific guidelines in this field. The lack of definitive methodology highlighted the obvious necessity to create a comprehensive review of all of the methods used for determining anticancer therapeutic efficacy as well as the motive for applying them (manuscript reformed below). The full manuscript was prepared in collaboration with a colleague from the School of Biomedical Sciences at Colorado State University, Mark A. Brown. Draft preparation was completed by Jenna L. Gordon and Mark A. Brown. Melissa M. Reynolds acted as the advisor on this work and was involved in draft revision. This chapter encompasses the compilation of the pertinent assay types, examples of those assays, and motivations for application in the development of therapeutics intended for the clinical management of cancer. This manuscript was originally published in 2018 and has been adapted with permission. [1] 

[1] Gordon, J.L.; Brown, M.A.; Reynolds, M.M. Cell-Based Methods for Determination of Efficacy for Candidate Therapeutics in the Clinical Management of Cancer. *Diseases* **2018**, 6(4), 85. doi:10.3390/diseases6040085

## 2.2 INTRODUCTION

Despite advances in technology and medicine, cancer remains one of the most lethal diseases in the world.[1] Lung cancer alone, the leading cause of worldwide cancer-related deaths, causes more than one million deaths per year.[2,3] Even after nearly a century of research on cancer treatments, more than one-third of all cancer patients in developed nations fail to survive five years post-diagnosis.[4] As the incidence of cancer continues to increase[5], attention must be placed on refining existing techniques and developing new methods to diagnose, prevent, and treat cancer patients. Although the best opportunity for achieving complete remission is early detection[6], many types of cancer do not manifest evident symptoms in the earliest stages[7]. As a result, it is important to develop and administer the most effective treatments possible for cancer patients at all stages.

The development of therapeutics for the clinical management of cancer is traditionally defined in several distinct phases, including discovery, *in vitro* testing, pre-clinical animal studies, and clinical trials (see Figure 1). While the focus of the latter phases is to assess both safety and efficacy, most studies in the early phases of drug development focus on establishing efficacy alone. Tumor-derived cell lines have been the mainstay for anti-cancer drug discovery, and the assessment of *in vitro*, efficacy since the 1950s.[8] However, issues related to cross-contamination of cell lines and lack of translational relevance plagued early cell-based studies.[9] It was not until the establishment of the National Cancer Institute 60 (NCI-60) panel of human tumor-derived cell lines that cell-based efficacy studies became both economically feasible and translationally relevant. Shortly thereafter, the Japanese Foundation for Cancer Research established a similar panel of tumor-derived cell lines.[9] Both panels have been used extensively and have yielded thousands of candidate therapeutics. More recently, the Center for Molecular Therapeutics 1000 (CMT1000) platform of tumor-derived cell lines has been developed and validated to capture the

greatest possible breadth of heterogeneity across cancer types.[10] This more comprehensive representation of human cancers has been more effective in predicting variation in clinical responses to treatment and it has ultimately paved the way for more efficient stratification of cancer patients according to the most suitable treatments.

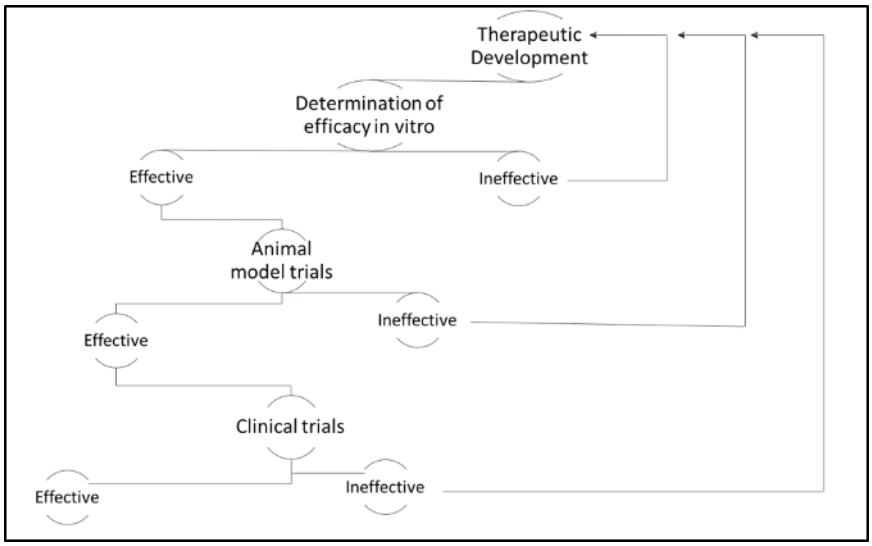


**Figure 2.1** Diagram of therapeutic application post-therapeutic development. Therapeutics that are determined efficacious *in vitro* are applied in animal model trials. Therapeutics that are determined efficacious in animal model trials are applied in clinical trials. At any point, if the therapeutic is determined to be ineffective, researchers must return to the therapeutic development stage.

Once the sensitivity of certain tumor types has been established for a candidate anti-cancer therapeutic, researchers are able to scale back the breadth of cell types in order to focus their efficacy studies on the select cell lines, for which the drug exhibited the greatest potential. A range of indicators is commonly assessed at this point to gauge therapeutic efficacy including the impact of the drug on cell viability, cell proliferation, colony formation, cytotoxicity, cytostasis, induction of apoptosis, and cell cycle arrest.[11-18] To observe these impacts, a battery of *in vitro* assays may be employed, such as monoculture proliferation assays, 3D tumor spheroid models, drug-drug and drug-radiation combinatorial analysis, and invasion and migration assays. Cell-based studies can

also serve as a platform for evaluating mechanism of action, impacts on invasion and migration, tumor hypoxia, cell-cell interactions, and cell-matrix interactions.

In the determination of therapeutic efficacy, it is important to ascertain the appropriate method(s) to employ. This decision includes thorough evaluation of any pertinent analytical, clinical, and general considerations. Explicitly, important analytical considerations include detection sensitivity, data reproducibility, the ability to multiplex, reagent stability, and the number of cells present in a sample. Some of the clinical considerations are the cell line(s) of interest and the mode of action of the relevant anticancer pharmaceutical(s) (e.g., chemicals, antibodies, CAR-T cells). Additionally, some general considerations critical to assay selection include time, cost, ease of use, and instrument availability.[19] The section below provides an overview of common cell-based assays, which can be used to observe indicators of therapeutic efficacy.

## 2.3 CELL-BASED ASSAYS FOR DETERMINATION OF THERAPEUTIC EFFICACY

**2.3.1 Cell Viability and Proliferation Assays.** Cellular viability and proliferation assays are ubiquitously used to assess the effect of candidate anti-cancer therapeutics, including cytostatic and cytotoxic agents.[12-16] Cellular viability represents the number of healthy cells present in a population.[20] Cellular proliferation represents the ability of healthy cells to divide and create progeny.[21] Therefore, cell viability assays and cell proliferation assays are used to quantify the number of healthy cells in a population and/or the rate of growth of a population of cells.[22] This is accomplished by measuring markers of cell activity, such as metabolic activity, the number of cells present or divisions occurring within the population, ATP production, or DNA synthesis.[21] Often, these parameters are measured via colorimetric, binding, or staining assays. However, it can be difficult to distinguish between cytotoxicity and cytostasis using these methods alone, which can lead to ambiguous cell survival results.[23] Distinguishing these impacts is often accomplished using

the adenine triphosphate-based tumor chemosensitivity assay (ATP-TCA)[24], or laser scanning cytometry[25]. Cytostatic agents are often employed as adjuvant therapeutics in tandem with a cytotoxic agent, such as a chemotherapeutic, to circumvent issues related to resistance and dose-limiting toxicity.[13,16,26,27]

**2.3.2 Colorimetric Assays.** Metabolic activity is a common indicator of cell health. Thus, cell-based colorimetric assays are often employed in the determination of cellular metabolic activity. For example, tetrazolium salts and resazurin are reduced through mitochondrial dehydrogenase activity by viable cells.[23] As cells die or stop proliferating, there is a measurable change in the reduction of resazurin and tetrazolium salts.[28-30] The corresponding change in turnover rate can be analyzed via colorimetric and/or fluorescent detection.[23] Some of the most common tetrazolium salts used in cell-based metabolic studies are MTT (3-(4,5-dimethylthiazol-2-yl)-2,5-diphenyltetrazolium bromide), MTS (3-(4,5-dimethylthiazol-2-yl)-5-(3-carboxymethoxyphenyl)-2-(4-sulfophenyl)-2H-tetrazolium), XTT (2,3-bis-(2-methoxy-4-nitro-5-sulfophenyl)-2H-tetrazolium-5-carboxanilide), WST-1, and WST-8 (2-(2-methoxy-4-nitrophenyl)-3-(4-nitrophenyl)-5-(2,4-disulfophenyl)-2H-tetrazolium, monosodium salt).[23,31] Due to the vast number of colorimetric assays, the advantages and disadvantages vary between individual analyses. Thus, the individual strengths and limitations of each assay are highlighted in Table 1. In general, colorimetric assays are easy to use, permit retrieval of high-throughput data, and provide a cost-effective approach to determination of therapeutic efficacy. However, colorimetric assays often do not provide the ability to multiplex or obtain real-time measurements. Further, sufficient sensitivity may not be obtained when working with smaller samples of cells (<1000).[23]

**Table 2.1** Comparison of the advantages and disadvantages of determining cell viability and/or proliferation using various colorimetric assays. Advantages are indicated via check marks (√). Disadvantages are indicated through an x (χ). Multiple check marks (√) indicate the degree of advantage of one assay in comparison to others.[22,23,30-33]

| Assay | Real-Time Measurements | Sensitivity | Multiplexing | Water-Soluble | Additional Intermediates Not Required | Ease-of-Use | Cost |
|---|---|---|---|---|---|---|---|
| MTT | χ | √ | χ | χ | √ | √ | √ |
| MTS | χ | √ | χ | √ | χ | √√ | √ |
| XTT | χ | √ | χ | √ | χ | √√ | √ |
| WST-1 | χ | √ | χ | √ | χ | √√ | √ |
| WST-8 | √ | √√ | √ | √ | √ (Already incorporated) | √√√ | √ |
| Resazurin | √ | √√ | √ | √ | √ | √√ | √√ |

Analysis of colorimetric assays generate absorbance values, which are an indirect measurement of cell viability. Treated samples are expressed as a percentage of 100% viable cells (absorbance of untreated sample—absorbance of cell media).[23] Colorimetric assay results can produce a viability of zero, which does not necessarily indicate that every cell is dead, but instead indicates that there is no detectable change in absorbance between the cell media itself and the sample.

### 2.3.3 Binding Assays

*Neutral Red Uptake.* The neutral red (3-amino-7-dimethylamino-2-methylphenazine hydrochloride) assay is another assay, commonly used to determine cell viability.[34-39] Similar to tetrazolium salts and resazurin, the neutral red (NR) assay is a colorimetric assay that allows

quantitative determination of healthy cells through spectrophotometric detection.[40] Unlike the previously mentioned colorimetric assays, the NR assay depends on the ability of healthy cells to uptake NR within the lysosomes subsequent to exposure to a toxic substance.[23] NR is a weakly cationic dye that changes from an orange-red to deep red after forming bonds with anionic sites within the lysosomal matrix.[41] After exposure to a toxic substance, cell viability is expressed as a concentration dependent reduction of the NR uptake into the cell. This is possible because toxic substances alter the integrity of the cell, leading to a reduced uptake of NR. Although the NR assay is both rapid and sensitive, it does not definitively distinguish between cytotoxicity and cytostasis.[23]

**2.3.4 ATP Production.** Another technique to analyze cellular viability in cell-based anti-cancer studies is the quantitation of ATP production.[42-45] The ATP production bioluminescence assay is based on the ability of luciferase to convert luciferin into oxyluciferin in an ATP-dependent reaction that generates light. Thus, the level of ATP correlates with the amount of light emission.[23] Cell viability can then be correlated to an increase in the overall amount of ATP produced in a population of exponentially growing cells.[45,46] This assay is particularly useful because it is sensitive enough to reproducibly detect the ATP production from a single mammalian cell.[47] An additional benefit is the large dynamic range of this assay, as concentration of ATP and cellular viability are directly proportional for cell numbers between one and one-hundred million cells.[23] However, as with other such assays, the ATP production assay does not allow for multiplexing and cannot distinguish between cytotoxicity and cytostasis. Additionally, accurate quantitation of ATP requires medium, long-term exposure to a toxic drug *in vitro* (48–72 h).[23]

**2.3.5 Colony Formation Assays.** Soft agar colony formation assays are often valuable in cancer research[13,15,16,48,49] because they allow for direct evaluation of tumor progression *in vitro* in a

cellular environment that mimics *in vivo* conditions.[48] Colony formation assays operate on the principal that healthy cells require contact with the extracellular matrix present in the body to grow and divide. Conversely, transformed or malignant cells are able to grow and divide without regard to the surrounding environment.[17] As a result, transformed cells form colonies within the semi-solid agar matrix. When counted as colony forming units (CFUs), the number of colonies formed provides a quantitative assessment of the malignant potential of individual cell lines. Subsequent to exposure of a colony-forming cell line to an anti-tumor therapeutic on agar, a decrease in colony-formation with respect to increasing therapeutic concentration is indicative of therapeutic efficacy.[50]

**2.3.6 Cytotoxicity Assays.**

*Staining and Imaging.* Cytotoxicity assays are used to assess both live and dead cells after treatment with a therapeutic.[23] Staining techniques are often used in cytotoxicity assays to quickly visualize the presence of live and dead cells through fluorescence microscopy.[14,51-53] Propidium iodide is a fluorescent, membrane impermeable stain that binds to DNA of dead cells by intercalating between bases with little or no sequence preference.[54] Since propidium iodide has a molecular weight of only 668.4 Da, it can bind to dead cells with minimal disruption to the cell membrane.[51] Live cells with intact cell membranes will exclude the dye and exhibit little to no fluorescence.[55] The application of a live cell counter stain (membrane permeable DNA stain) facilitates the assessment of both live and dead cells simultaneously.[56] Advantages of propidium iodide staining include the ability to multiplex cell samples, rapid analysis, and ease of use. Conversely, this method does not reveal the mechanism of cell death[23] and data reproducibility relies on the control of variations in exposure time and camera/software settings[56].

*LDH Cytotoxicity Assay.* Another commonly used cytotoxicity assay is the lactate dehydrogenase (LDH) release assay, which allows for the rapid and sensitive short-term (1 h post cell death) detection of cytotoxicity in various cell types.[23] The LDH assay resembles colorimetric cell viability assays in light of the mechanistic and detection similarities. When a cell loses membrane integrity, it releases LDH, which is then used as a catalyst to promote a two-step reaction. The first step is the oxidation-reduction reaction between NAD+ and lactate. This is followed by the reduction of a tetrazolium salt (INT) to a colored formazan. The colored formazan product can be detected colorimetrically through the absorbance maximum at 490–520 nm. In order to accurately determine cytotoxicity using this assay, it is important to account for the inherent LDH activity that occurs within the cell culture medium. Additionally, if the candidate therapeutic induces cell death intracellularly and without the loss of plasma membrane integrity, the LDH assay will not detect the occurrence of cell death.[23] One potential benefit of the LDH cytotoxicity assay is the potential to distinguish between cell death and growth inhibition with a modified LDH-based cytotoxicity assay.[57]

**2.3.7 Cell Apoptosis Assays.** Apoptosis is a reliable indicator of cancer therapeutic efficacy and can be evaluated based on a variety of biochemical and morphological indicators.[58] The most common methods for observing apoptosis in cancer cells are described below.

*DNA Fragmentation.* DNA fragmentation assays have been a mainstay for observing apoptosis.[36,57-61] As cells undergo apoptosis, nuclear DNA fragmentation occurs, providing a detectable parameter for the observation of late stage apoptosis. Traditionally, DNA fragmentation has been observed via laddering on agarose gels through assays, such as conventional agarose gel electrophoresis (CAGE) and pulsed-field gel electrophoresis (PFGE). Specifically, CAGE allows for the detection of low-molecular-weight fragments and can be refined to include radioactive end

labeling, permitting the detection of small quantities of fragmented DNA. Alternatively, PFGE allows for the detection of high-molecular-weight DNA fragments.[62] However, results obtained through these assays can be ambiguous, because homogenate preparation and necrotic cells can also produce DNA fragments. Although these methods are simple to perform, large cell samples (at least 1 million cells) are necessary to achieve reliable results.[23]

In attempt to increase DNA fragmentation assay utility, the Single Cell Gel Electrophoresis (Comet) assay has been developed.[24] In 1984, the first microelectrophoretic method for visualization of DNA damages in individual mammalian cells was introduced by Ostling and Johansen.[63] Six years later, the Ostling and Johansen method was refined to enhance single-cell sensitivity and simultaneously coined the Comet assay.[64] Advantageously, the Comet assay requires relatively few cells (~1000 cells) and allows for distinction of heterogeneity within a sample population.[23,65] Nevertheless, relatively small sample populations can be detrimental when large variation exists within that population. Further, the Comet assay does not provide any information about the size of the DNA fragments produced.[65] Additionally, the assay can be adapted from its original basic conditions to allow for measurement of cells at lower pH (termed "neutral" assay).[23,65]

Subsequent to the development of the Comet assay, terminal deoxynucleotidyl transferase dUTP nick end labeling (TUNEL) was developed for the visualization of nuclei containing DNA fragments.[66,67] Specifically, TUNEL allows for detection of DNA fragments in situ through labeling of the free 3′-hydroxyl termini on DNA fragments. However, in its early-nineties form, the TUNEL assay was considered nonspecific, prohibiting consistent distinction between DNA fragments produced by apoptotic or necrotic cells.[54] Since then, the sensitivity and selectivity of the TUNEL assay have been optimized to further ensure accurate distinction between apoptosis

and necrosis.[68] Advantageously, TUNEL can also be combined with Annexin V to comprise a more robust assay that is capable of distinguishing apoptosis and necrosis. Since Annexin V binding is reported to occur prior to DNA fragmentation, it is capable of detecting necrotic or early apoptotic cells that exhibit a negative response from TUNEL.[69]

*Caspase Activation.* Since caspase activation is a hallmark of cell apoptosis[23], numerous assays have been developed to detect activation of apoptosis-related caspases. One of the most common of these employs the Western blot to measure caspase activation.[11-16,27,70,71] However, Western blotting is only semi-quantitative, does not allow for multiplexing[72], and does not demonstrate the type of cell undergoing apoptosis[23]. Alternatively, numerous commercial kits exist to monitor apoptosis-related caspases, including the Caspase-Glo 3/7 Assay[73], caspase 3 colorimetric assay kit[52], and CellEvent caspase-3/7 Green Detection Reagent[74]. The use of assay kits can be advantageous when a limited number of analyses are planned. Additionally, assay kits allow for analysis of individual caspases signaling various apoptotic processes. However, more extensive studies economically compel in-house preparation of assay components.[75]

*Flow Cytometry.* Flow cytometry presents a reliable multi-parameter detection technique for observation of cell apoptosis.[76] In flow cytometry, it is possible to measure the size and complexity of cells, as well as fluorescence. For example, a treated sample of cells can be stained with a live and/or dead cell stain and fluorescing antibodies against markers of apoptosis. Often, stains, such as PI, 7-aminoactinomycin (7AAD), 4′,6-diamidino-2-phenylindole (DAPI), or Annexin V, are applied singularly or in combination [62]. Additionally, fluorescent dyes (fluorochromes) are commonly linked to mono- or polyclonal antibodies. The application of antibodies in flow cytometry is beneficial for the detection of different apoptotic pathways.[77] For example, Anti-caspase 3 allows for the detection of caspase 3 dependent apoptosis. Similarly, numerous

antibodies exist for the detection of different apoptotic pathways, including other members of the caspase family, PARP, and BRdU.[78]

After an incubation period, the sample is introduced into the flow cytometer in conjunction with a sheath fluid that is flowing at a different rate than the sample suspension. The varying flow rates between the two fluids allows for hydrodynamic focusing of the sample suspension, which directs the sample cells to pass through the laser light source in a single file line.[77] As the cells pass through the laser light source, they exhibit forward and side scattered light, and potentially fluorescence. Forward scattered light corresponds to the size of the cell with more forward scatter corresponding to a larger cell. Similarly, side scattered light corresponds to the complexity of the cell, with more side scatter corresponding to a more complex cell. Finally, fluorescence at a specific wavelength is observed from live or dead cells, depending on the type of cell stain and/or antibodies used. Flow cytometry provides researchers with the specific mechanism of cell death, highly reproducible data, due to the possibility of single cell analysis, and the ability to rapidly multiplex cell samples.[79]

**2.3.8 Cell Cycle Arrest Assays.** Cell cycle arrest assays operate on the foundation of cellular regulation through cell cycle checkpoints. Cancer therapeutics can be designed to target specific cell cycle checkpoints in neoplastic cells in order to induce cell death. The phase at which a therapeutic causes neoplastic cell arrest *in vitro* can indicate its potential efficacy *in vivo*. Although there are various methods through, which cell cycle checkpoints can be analyzed, such as [3H]-thymidine incorporation, BrdU incorporation, and microscopy, cell cycle arrest assays are often analyzed using flow cytometry.[80]

Flow cytometry permits single-cell quantification of stained DNA to indicate the percentage of cells existing in each cell cycle phase. Through fluorescence detection, flow cytometric data is

provided in the form of a histogram, indicating the percentage of cells in the $G_0$ and $G_1$ phase (2N DNA content), the S phase (between 2N and 4N DNA content), and the G2/M phase (4N DNA content).[81] Apoptotic cells can further be distinguished between the cells in various phases, because the DNA content (and fluorescence intensity) are less than that in the G0/G1 phase. Multiparameter analysis of cell cycle phase is also possible using flow cytometry, through the analysis of RNA content and DNA susceptibility to denaturation under various environmental parameters.[80]

**2.3.9 3D Cell Culture Systems.** The methods identified above were originally developed using monolayer cultures. Such systems lack the rich heterogeneity of tumor micro-environments and the corresponding analyses are limited to cell autonomous outcomes that fail to account for impacts on tumor-stromal interaction, angiogenesis and other such factors of a natural system. With greater emphasis on the importance of tumor three-dimensionality (3D) and their corresponding microenvironments with regard to therapeutic efficacy, the advanced stages of the *in vitro* testing phase often includes 3D cell culture systems to more closely model physiological conditions.[82-84] 3D cultures have the added utility of observing characteristics, such as variations in polarity, invasive potential, and matrix independent survival. However, substratum rigidity is an additional concern as it has been shown to be involved in regulation of cell processes.[85]

*Multicellular Tumor Spheroids.* Among 3D culture systems, the multicellular tumor spheroids (MTCS) system is one of the best characterized.[86,87] The MTCS system facilitates high fidelity simulation of tumor micro-environments and *in vivo* growth conditions with regard to pathophysiology and observed responsiveness to therapeutics.[86-88] It has been widely employed to evaluate a range of impacts associated with candidate therapeutics, including cell-cell interactions, cell-matrix interactions, chemical gradients, metabolic gradients, and resistance.[89]

*Hollow Fiber Assays.* The hollow fiber assay is a technological innovation built upon prior techniques for microencapsulation and subsequent cultivation of cells.[90-92] The hollow fiber assay involves a 1–2 day, *in vitro* culture incorporating a panel of tumor cell lines contained in biocompatible hollow fibers and the subsequent subcutaneous implantation of the fibers in mice. Mice are treated with the candidate therapeutic for a period of several days and the fibers are subsequently removed to facilitate cell viability assays. Thus, this method can assess therapeutic efficacy along with the ability of a drug to reach its target *in vivo*, and it can provide preliminary data related to the safety of the therapeutic. The hollow fiber assay is further advantageous for its savings on time and required quantity of therapeutic, relative to traditional *in vivo* assays. It also allows for the *in vivo* examination of therapeutic efficacy related to tumor-derived cell lines that would not otherwise grow in an animal model. Given the strong correlation between efficacy in hollow fiber assays and efficacy observed with human xenografts, the hollow fiber system also serves as an effective way to screen potential therapeutics prior to costly xenograft experiments.[90]

**2.3.10 Cell-Based Systems for Evaluating Combinatorial Efficacy.** Development of combinatorial treatments has been historically slow and often involved trial-and-error in clinical settings. However, advancements in cell-based systems has, more recently, facilitated the use of cell-based screening platforms to evaluate combinatorial efficacy in high-throughput systems. For example, one such experiment evaluated 600 commercially-approved therapeutics in a combinatorial analysis of almost 100,000 groupings for combinatorial efficacy in human, lung tumor-derived cells.[93] Studies of this kind have the potential to uncover synergism among therapeutic applications that may prevent the development of resistance common to single-drug approaches.

## 2.4 CONCLUSIONS

Tumor-derived cell lines largely preserve the genomic signature of the primary tumors, from which they were sourced[94,95] and data obtained using such cell lines is highly predictive of subsequent clinical outcomes.[10,96] Therefore, in attempt to improve the efficacy of anti-cancer drugs entering clinical trials, it is essential to determine the efficacy of each drug *in vitro* as accurately as possible. This process begins with proper assay understanding, selection, and execution. Cell viability assays are useful for indirect determination of the number of live cells present after treatment with a therapeutic. Colony formation assays directly illuminate the ability of a therapeutic to inhibit tumor proliferation. Cytotoxicity assays present a direct method for the visualization of live and dead cells after treatment with a therapeutic. Cell apoptosis assays allow for direct quantification of the number of apoptotic cells after treatment with a therapeutic. Lastly, cell cycle arrest assays allow for indirect quantification of the number of apoptotic cells that deceased at specific phases within the cell cycle. Although each assay presented encompasses various strengths and limitations, no single method proves therapeutic efficacy. It is important to strategize and employ multiple methods in order to ensure accurate and reliable results.

The importance of cell-based studies for evaluating therapeutic efficacy is underscored by the growing number of commercially approved drugs and biologics for the clinical management of cancer. However, there are major limitations to analyses of monocultured cell lines. Such cell lines often lack the rich heterogeneity of tumor micro-environments and the corresponding analyses are limited to cell autonomous outcomes that fail to account for impacts on tumor-stromal interaction, angiogenesis and other such factors of a natural system. While 3D cell culture platforms have been employed to respond to such limitations of monocultures, they do so at the expense of greater time

and cost. Despite these limitations, cell-based methods remain essential in the early stages of anti-cancer drug development.

# CHAPTER 2 – REFERENCES


1 Bradbury, R.H. Overview. *Cancer* **2007**, *1*, 1–17.

2 World Health Organisation Global Health Observatory (GHO) Data: Top 10 Causes of Death, 2017; pp. 1–3. Available online: http://www.who.int/gho/mortality_burden_disease/causes_death/top_10/en/ (accessed on 18 December 2017).

3 Joudeh, J.; Allen, J.; Das, A.; Prabhu, V. *Impact of Genetic Targets on Cancer Therapy*; El-Deiry, W.S., Ed.; Springer: New York, NY, USA, 2013; ISBN 9781461461753.

4 NCI SEER data. Five-Year Relative Survival. Avalaible online: https://seer.cancer.gov/seerstat/WebHelp/Relative_Survival.htm (accessed on 12 December 2017).

5 Siegel, R.L.; Miller, K.D.; Jemal, A. Cancer statistics, 2017. *CA Cancer J. Clin.* **2017**, *67*, 7–30, doi:10.3322/caac.21387.

6 Mocellin, S.; Shrager, J.; Scolyer, R.; Pasquali, S.; Verdi, D.; Marincola, F.M.; Briarava, M.; Gobbel, R.; Rossi, C.; Nitti, D. Targeted Therapy Database (TTD): A Model to Match Patient's Molecular Profile with Current Knowledge on Cancer Biology. *PLoS ONE* **2010**, *5*, 1–11, doi:10.1371/journal.pone.0011965.

7 American Cancer Society. Signs and Symptoms of Cancer. Avalaible online: https://www.cancer.org/cancer/cancer-basics/signs-and-symptoms-of-cancer.html (accessed on 5 January 2018).

8 Goodspeed, A.; Heiser, L.M.; Gray, J.W.; Costello, J.C. Tumor-Derived Cell Lines as Molecular Models of Cancer Pharmacogenomics. *Mol. Cancer Res.* **2016**, *14*, 3–13, doi:10.1158/1541-7786.MCR-15-0189.

9 Gillet, J.-P.; Varma, S.; Gottesman, M.M. The Clinical Relevance of Cancer Cell Lines. *JNCI J. Natl. Cancer Inst.* **2013**, *105*, 452–458, doi:10.1093/jnci/djt007.

10 Sharma, S.V.; Haber, D.A.; Settleman, J. Cell line-based platforms to evaluate the therapeutic efficacy of candidate anticancer agents. *Nat. Rev. Cancer* **2010**, *10*, 241–253, doi:10.1038/nrc2820.

11 Tanimoto, A.; Yamada, T.; Nanjo, S.; Takeuchi, S. Receptor ligand-triggered resistance to alectinib and its circumvention by Hsp90 inhibition in EML4-ALK lung cancer cells. *Oncotarget* **2014**, *5*, 4920–4928, doi:10.18632/oncotarget.2055.

12 Miyawaki, M.; Yasuda, H.; Tani, T.; Hamamoto, J.; Arai, D.; Ishioka, K.; Ohgino, K.; Nukaga, S.; Hirano, T.; Kawada, I.; et al. Overcoming EGFR Bypass Signal-Induced Acquired Resistance to ALK Tyrosine Kinase Inhibitors in ALK-Translocated Lung Cancer. *Mol. Cancer Res.* **2017**, *15*, 106–114, doi:10.1158/1541-7786.MCR-16-0211.

13 Wang, Y.; Wang, L.; Guan, S.; Cao, W.; Wang, H.; Chen, Z.; Zhao, Y.; Yu, Y.; Zhang, H.; Pang, J.C.; et al. Novel ALK inhibitor AZD3463 inhibits neuroblastoma growth by overcoming crizotinib resistance and inducing apoptosis. *Sci. Rep.* **2016**, *6*, 1–10, doi:10.1038/srep19423.

14 Wang, L.; Cheng, B.F.; Yang, H.J.; Wang, M.; Feng, Z.W. NF-κB protects human neuroblastoma cells from nitric oxide-induced apoptosis through upregulating biglycan. *Am. J. Transl. Res.* **2015**, *7*, 1541–1552.

15 Xu, F.; Li, H.; Sun, Y. Inhibition of Axl improves the targeted therapy against ALK-mutated neuroblastoma. *Biochem. Biophys. Res. Commun.* **2014**, *454*, 566–571, doi:10.1016/j.bbrc.2014.10.126.

16 Lu, J.; Guan, S.; Zhao, Y.; Yu, Y.; Woodfield, S.E.; Zhang, H.; Yang, K.L.; Bieerkehazhi, S.; Qi, L.; Li, X.; et al. The second-generation ALK inhibitor alectinib effectively induces apoptosis in human neuroblastoma cells and inhibits tumor growth in a TH-MYCN transgenic neuroblastoma mouse model. *Cancer Lett.* **2017**, *400*, 61–68, doi:10.1016/j.canlet.2017.04.022.

17 Borowicz, S.; Van Scoyk, M.; Avasarala, S.; Karuppusamy Rathinam, M.K.; Tauler, J.; Bikkavilli, R.K.; Winn, R.A. The Soft Agar Colony Formation Assay. *J. Vis. Exp.* **2014**, *92*, 1–6, doi:10.3791/51998.

18 McGowan, E.M.; Alling, N.; Jackson, E.A.; Yagoub, D.; Haass, N.K.; Allen, J.D.; Martinello-Wilks, R. Evaluation of cell cycle arrest in estrogen responsive MCF-7 breast cancer cells: Pitfalls of the MTS assay. *PLoS ONE* **2011**, *6*, 1–8, doi:10.1371/journal.pone.0020623.

19 Author. Chapter 4: Cell viability. In *Promega Protocols and Applications Guide*; Promega: Madison, WI, USA, 2011; Revision 3/11, pp. 1–23. Avalaible online: www.promega.com (accessed on 22 January 2018).

20 Stoddart, M.J.; Louis, K.S.; Siegel, A.C.; Kupcsik, L.; Czekanska, E.M. *Chapters 1-5: Mammalian Cell Viability*; Stoddart, M.J., Ed.; Humana Press: Totowa, NJ, USA, 2011; Volume 740, pp. 1–27; ISBN 978-1-61779-107-9.

21 Yang, N.; Ray, S.D.; Krafts, K. Cell Proliferation. *Encycl. Toxicol.* **2014**, *1*, 761–765, doi:10.1016/B978-0-12-386454-3.00274-8.

22 Prabst, K.; Engelhardt, H.; Ringgeler, S.; Hubner, H.; Ates, G.; Vanhaeke, T.; Rogiers, V.; Rodrigues, R.; Chan, L.L.-Y.; McCulley, K.J.; et al. *Chapters 1-4, 8: Cell Viability Assays*; Gilbert, D., Friedrich, O., Eds.; Humana Press: Totowa, NJ, USA, 2017; Volume 1601, pp. 1–43, 89–97; ISBN 978-1-4939-6959-3.

23 van Meerlo, J.; Kaspers, G.J.L.; Cloos, J.; Glaysher, S.; Cree, I.A.; Hartley, J.M.; Spanswick, V.J.; Hartley, J.A. *Chapters 20-22, 25: Cancer Cell Culture Methods and Protocols*, 2nd ed.; Cree, I.A., Ed.; Humana Press: Totowa, NJ, USA, 2013; Volume 731, pp. 237–259, 309–321; ISBN 978-1-84973-379-3.

24 Blumenthal, R.D. *Chapter 1: Chemosensitivity*; Blumenthal, R.D., Ed.; Humana Press: Totowa, NJ, USA, 2005; Volume 1, pp. 3–21; ISBN 9780874216561.

25 Pozarowski, P.; Huang, X.; Gong, R.W.; Priebe, W.; Darzynkiewicz, Z. Simple, semiautomatic assay of cytostatic and cytotoxic effects of antitumor drugs by laser scanning cytometry: Effects of the bis-intercalator WP631 on growth and cell cycle of T-24 cells. *Cytometry* **2004**, *57A*, 113–119, doi:10.1002/cyto.a.10121.

26 Kunze, D.; Wuttig, D.; Füssel, S.; Meye, A.; Wirth, M.P. Sirna-Mediated Inhibition of Antiapoptotic Genes in Human Bladder Cancer Cells. *Eur. Urol. Suppl.* **2006**, *5*, 800, doi:10.1016/S1569-9056(06)61306-7.

27 Bhola, N.E.; Balko, J.M.; Duggar, T.C.; Kuba, M.G.; Sanchez, V.; Sanders, V.; Sanders, M.; Stanford, J.; Cook, R.S.; Arteaga, C.L. TGF-β Inhibition enhances chemotherapy action against triple-negative breast cancer. *J. Clin. Investig.* **2013**, *123*, 1348–1358, doi:10.1172/JCI65416DS1.

28 Pagliacci, M.C.; Spinozzi, F.; Migliorati, G.; Fumi, G.; Smacchia, M.; Grignani, F.; Riccardi, C.; Nicoletti, I. Genistein Inhibits Tumour Cell Growth in vitro but Enhances

Mitochondrial Reduction of Tetrazolium Salts : A Further Pitfall in the Use of the MTT Assay for Evaluating Cell Growth and Survival. *Eur. J. Cancer* **1993**, *3030A*, 1573–1577.

29 Mosmann, T. Rapid Colorimetric Assay for Cellular Growth and Survival: Application to Proliferation and Cytotoxicity Assays. *J. Immunol. Methods* **1983**, *65*, 55–63, doi:10.1016/0022-1759(83)90303-4.

30 Brady, A.J.; Kearney, P.; Tunney, M.M. Comparative evaluation of 2,3-bis [2-methyloxy-4-nitro-5-sulfophenyl]-2*H*-tetrazolium-5-carboxanilide (XTT) and 2-(2-methoxy-4-nitrophenyl)-3-(4-nitrophenyl)-5-(2, 4-disulfophenyl)-2*H*-tetrazolium, monosodium salt (WST-8) rapid colorimetric assays for antim. *J. Microbiol. Methods* **2007**, *71*, 305–311, doi:10.1016/j.mimet.2007.09.014.

31 Uzunoglu, S.; Karaca, B.; Atmaca, H.; Kisim, A.; Sezgin, C.; Karabulut, B.; Uslu, R. Comparison of XTT and Alamar blue assays in the assessment of the viability of various human cancer cell lines by AT-101 (-/-gossypol). *Toxicol. Mech. Methods* **2010**, *20*, 482–486, doi:10.3109/15376516.2010.508080.

32 Riss, T.; Moravec, R.; Niles, A.; Duellman, S. Cell Viability Assays. In *Assay Guidance Manual*; Springer: Berlin, Germany, 2013; pp. 1–55; ISBN 978-1-4939-6959-3.

33 Author. *Cell Counting Kit-8 Technical Manual*; Dojindo Molecules Technology Inc.: Rockville, MD, USA, 2009; volume 8, pp. 1–7. Avalaible online: www.dojindo.com (accessed on 12 February 2018).

34 Griffiths, G.D.; Lindsay, C.D.; Upshall, D.G. Examination of the toxicity of several protein toxins of plant origin using bovine pulmonary endothelial cells. *Toxicology* **1994**, *90*, 11–27.

35 Fotakis, G.; Timbrell, J.A. In vitro cytotoxicity assays: Comparison of LDH, neutral red, MTT and protein assay in hepatoma cell lines following exposure to cadmium chloride. *Toxicol. Lett.* **2006**, *160*, 171–177, doi:10.1016/j.toxlet.2005.07.001.

36 Perez, M.G.; Fourcade, L.; Mateescu, M.A.; Paquin, J. Neutral Red versus MTT assay of cell viability in the presence of copper compounds. *Anal. Biochem.* **2017**, *535*, 43–46, doi:10.1016/j.ab.2017.07.027.

37 Mothana, R.A.A.; Kriegisch, S.; Harms, M.; Wende, K.; Lindequist, U. Assessment of selected Yemeni medicinal plants for their in vitro antimicrobial, anticancer, and antioxidant activities. *Pharm. Biol.* **2011**, *49*, 200–210, doi:10.3109/13880209.2010.512295.

38 Ramasamy, S.; Wahab, N.; Zainal Abidin, N.; Manickam, S.; Zakaria, Z. Growth inhibition of human gynecologic and colon cancer cells by Phyllanthus watsonii through apoptosis induction. *PLoS ONE* **2012**, *7*, doi:10.1371/journal.pone.0034793.

39 Borenfreund, E.; Puerner, J.A.; York, N. A Simple Quantitative Procedure Using Monolayer Cultures for Cytotoxicity Assays (HTD/NR-90). *J. Tissue Cult. Methods* **1984**, *9*, 7–9.

40 Chiba, K.; Kawakami, K.; Tohyama, K. Simultaneous Evaluation of Cell Viability by Neutral Red , MTT and Crystal Violet Staining Assays of the Same Cells. *Toxicol. Vitr.* **1998**, *12*, 251–258.

41 Nemes, Z.; Dietz, R.; Luth, J.B. The Pharmacological Relevance of Vital Staining with Neutral Red. *Experientia* **1979**, *35*, 1475–1476.

42 Soo, J.S.S.; Ng, C.H.; Tan, S.H.; Malik, R.A.; Teh, Y.C.; Tan, B.S.; Ho, G.F.; See, M.H.; Taib, N.A.M.; Yip, C.H.; et al. Metformin synergizes 5-fluorouracil, epirubicin, and

cyclophosphamide (FEC) combination therapy through impairing intracellular ATP production and DNA repair in breast cancer stem cells. *Apoptosis* **2015**, *20*, 1373–1387, doi:10.1007/s10495-015-1158-5.

43 Zhuang, Y.; Chan, D.K.; Miskimins, W. Preventing feedback activation of glycolytic ATP production enhances metformin cytotoxicity in breast cancer cells when oxidative phosphorylation is inhibited. *Cancer Metab.* **2014**, *2*, 89, doi:10.1186/2049-3002-2-S1-P89.

44 Distelmaier, F.; Valsecchi, F.; Liemburg-Apers, D.C.; Lebiedzinska, M.; Rodenburg, R.J.; Heil, S.; Keijer, J.; Fransen, J.; Imamura, H.; Danhauser, K.; et al. Mitochondrial dysfunction in primary human fibroblasts triggers an adaptive cell survival program that requires AMPK-α. *Biochim. Biophys. Acta-Mol. Basis Dis.* **2015**, *1852*, 529–540, doi:10.1016/j.bbadis.2014.12.012.

45 Radhakrishnan, P.; Ruh, N.; Harnoss, J.M.; Kiss, J.; Mollenhauer, M.; Scherr, A.L.; Platzer, L.K.; Schmidt, T.; Podar, K.; Opferman, J.T.; et al. Prolyl hydroxylase 3 attenuates MCL-1-mediated ATP production to suppress the metastatic potential of colorectal cancer cells. *Cancer Res.* **2016**, *76*, 2219–2230, doi:10.1158/0008-5472.CAN-15-1474.

46 *ATP Determination Kit ( A22066 )*.; Invitrogen Molecular Probes Inc.: Eugene, OR, USA, 2005; pp. 1–3. Avalaible online: http://www.thermofisher.com/order/catalog/product/A22066?CID=AFLBC-A22066 (accessed on 26 February 2018).

47 Paciello, L.; Falco, F.C.; Parascandola, P. Determination of yeast cell viability: Viable count vs ATP-based bioluminescence assay. *J. Biotechnol.* **2010**, *150*, 386–387, doi:10.1016/j.jbiotec.2010.09.487.

48 Wannlund, J.C. Analytical applications of firefly luciferase. *TrAC Trends Anal. Chem.* **1983**, *2*, 7–9, doi:10.1016/0165-9936(83)87066-6.

49 Saotome, K.; Morita, H.; Umeda, M. Cytotoxicity test with simplified crystal violet staining method using microtitre plates and its application to injection drugs. *Toxicol. Vitr.* **1989**, *3*, 317–321, doi:10.1016/0887-2333(89)90039-8.

50 Horibata, S.; Vo, T.V.; Subramanian, V.; Thompson, P.R.; Coonrod, S.A. Utilization of the Soft Agar Colony Formation Assay to Identify Inhibitors of Tumorigenicity in Breast Cancer Cells. *J. Vis. Exp.* **2015**, 1–7, doi:10.3791/52727.

51 Liao, T.T.; Jia, R.W.; Shi, Y.L.; Jia, J.W.; Wang, L.; Chua, H. Propidium iodide staining method for testing the cytotoxicity of 2,4,6-trichlorophenol and perfluorooctane sulfonate at low concentrations with Vero cells. *J. Environ. Sci. Heal.-Part A Toxic/Hazardous Subst. Environ. Eng.* **2011**, *46*, 1769–1775, doi:10.1080/10934529.2011.624016.

52 Cincin, Z.B.; Unlu, M.; Kiran, B.; Bireller, E.S.; Cakmakoglu, B. Apoptotic Effects of Quercitrin on DLD-1 Colon Cancer Cell Line. *Pathol. Oncol. Res.* **2015**, *21*, 333–338, doi:10.1007/s12253-014-9825-3.

53 De Nicola, M.; Gattia, D.M.; Bellucci, S.; De Bellis, G.; Micciulla, F.; Pastore, R.; Tiberia, A.; Cerella, C.; D'Alessio, M.; Antisari, M.V.; et al. Effect of different carbon nanotubes on cell viability and proliferation. *J. Phys. Condens. Matter* **2007**, *19*, doi:10.1088/0953-8984/19/39/395013.

54 Loo, D.T.; Darzynkiewicz, Z.; Zhao, H. *Chapter 1 & 8: DNA Damage Detection In Situ, Ex Vivo, and In Vivo*; Humana Press: Totowa, NJ, USA, 2011; Volume 682; ISBN 978-1-60327-408-1.

55 Matsuzaki, T.; Takeshi, S.; Fujikura, K.; Takata, K. Nuclear Staining for Laser Confocal Microscopy. *Acta Histochem. Cytochem.* **1997**, *30*, 309–314.

56 Boyd, V.; Cholewa, O.; Papas, K. Limitations in the use of fluorescein diacetate/propidium iodide (FDA/PI) and cell permeable nucleic acid stains for viability measurements of isolated islets of Langerhans. *Curr. Trends Biotechnol. Pharm.* **2008**, *2*, 66–84.

57 Smith, S.M.; Wunder, M.B.; Norris, D.A.; Shellman, Y.G. A simple protocol for using a LDH-Based cytotoxicity assay to assess the effects of death and growth inhibition at the same time. *PLoS ONE* **2011**, *6*, doi:10.1371/journal.pone.0026908.

58 Kumar, S.; Dorstyn, L.; Wlodkowic, D.; Skommer, J.; Darzynkiewicz, Z.; Tait, S.W.G.; Bouchier-Hayes, L.; Oberst, A.; Connell, S.; Green, D. *Chapters 1-3: Apoptosis Methods and Protocols*, 2nd ed; Erhardt, P., Toth, A., Eds.; Humana Press: Totowa, NJ, USA, 2009; Volume 559, pp. 3–33; ISBN 978-1-60327-016-8.

59 Ribeiro, T.M.; Bertolla, R.P.; Spaine, D.M.; Fraietta, R.; Ortiz, V.; Cedenho, A.P. Sperm nuclear apoptotic DNA fragmentation in men with testicular cancer. *Fertil. Steril.* **2008**, *90*, 1782–1786, doi:10.1016/j.fertnstert.2007.08.012.

60 Nath, M.; Vats, M.; Roy, P. Tri- and diorganotin(IV) complexes of biologically important orotic acid: Synthesis, spectroscopic studies, in vitro anti-cancer, DNA fragmentation, enzyme assays and in vivo anti-inflammatory activities. *Eur. J. Med. Chem.* **2013**, *59*, 310–321, doi:10.1016/j.ejmech.2012.11.023.

61 Ragheb, A.; Mahfouz, R.; Ghoneim, I.; Sharma, R.; Agarwal, A.; Sabanegh, E. Pretreatment Sperm DNA Fragmentation Index (DFI) in Cancer Patients and Its Relationship To Postcryopreservation Motile Sperm Concentration (PCMSC) and Sperm Motility (PCSM). *J. Urol.* **2010**, *183*, e750, doi:10.1016/j.juro.2010.02.1899.

62 Matassov, D.; Kagan, T.; Leblanc, J.; Sikorska, M.; Zakeri, Z.; Kumar, S.; Williams, O. *Chapters 1-3: Apoptosis Methods and Protocols*; Brady, H., Ed.; Humana Press: Totowa, NJ, USA, 2004; volume 282; ISBN 1617794899.

63 Ostling, O.; Johansen, K.L. Microelectrophoretic study of radiation-induced DNA damages in individual mammalian cells. *Biochem. Biophys. Res. Commun.* **1984**, 291–298.

64 Olive, P.L.; Banáth, J.P.; Durand, R.E.; Banath, J.P. Heterogeneity in Radiation-Induced DNA Damage and Repair in Tumor and Normal Cells Measured Using the "Comet" Assay. *Radiat. Res.* **1990**, *122*, 86, doi:10.2307/3577587.

65 Olive, P.L.; Banáth, J.P. The comet assay: A method to measure DNA damage in individual cells. *Nat. Protoc.* **2006**, *1*, 23–29, doi:10.1038/nprot.2006.5.

66 Gorczyca, W.; Gong, J.; Darzynkiewicz, Z. Detection of DNA strand breaks in individual apoptic cells by the in situ terminal deoxynucleotidyltransferse and nick translation assays. *Cancer Res.* **1993**, *53*, 1945–1951.

67 Gavrieli, Y.; Sherman, Y.; Ben-Sasson, S.A. Identification of programmed cell death in situ via specific labeling of nuclear DNA fragmentation. *J. Cell Biol.* **1992**, *119*, 493–501, doi:10.1083/jcb.119.3.493.

68 Negoescu, A.; Lorimier, P.; Labat-Moleur, F.; Drouet, C.; Robert, C.; Guillermet, C.; Brambilla, C.; Brambilla, E. In Situ Apoptotic Cell Labeling by the TUNEL Method:

Improvement and Evaluation on Cell Preparations. *J. Histochem. Cytochem.* **1996**, *4*, 959–968, doi:10.1016/S0008-6363(99)00396-X.

69 O'Brien, I.E.W.; Ferguson, I.B.; Holdaway, K.M. Annexin-V and TUNEL Use in Monitoring the Progression of Apoptosis in Plants. *Cytometry* **1997**, *29*, 28–33.

70 Jeong, M.; Paek, A.R.; Seung, J.; Youp, C.; Chae, K.; Hyang, J.; Hyun, S.; Jin, H. Regulation of cancer cell death by a novel compound, C604, in a c-Myc-overexpressing cellular environment. *Eur. J. Pharmacol.* **2015**, *769*, 257–265, doi:10.1016/j.ejphar.2015.11.027.

71 Katsumi, Y.; Iehara, T.; Miyachi, M.; Yagyu, S.; Tsubai-shimizu, S.; Kikuchi, K.; Tamura, S.; Kuwahara, Y.; Tsuchiya, K.; Kuroda, H.; et al. Sensitivity of malignant rhabdoid tumor cell lines to PD 0332991 is inversely correlated with p16 expression. *Biochem. Biophys. Res. Commun.* **2011**, *413*, 62–68, doi:10.1016/j.bbrc.2011.08.047.

72 Mahmood, T.; Yang, P.C. Western Blot: Technique, Theory, and Trouble Shooting. *N. Am. J. Med. Sci.* **2012**, *4*, 429–434, doi:10.4103/1947-2714.100998.

73 Bozkurt, E.; Atmaca, H.; Kisim, A.; Uzunoglu, S. Effects of Thymus serpyllum Extract on Cell Proliferation, Apoptosis and Epigenetic Events in Human Breast Cancer Cells. *Nutr. Cancer* **2012**, *64*, 1245–1250, doi:10.1080/01635581.2012.719658.

74 Tanaka, S.; Sakaguchi, M.; Yoneyama, H.; Usami, Y.; Harusawa, S. Biochemical and Biophysical Research Communications Histamine H 3 receptor antagonist OUP-186 attenuates the proliferation of cultured human breast cancer cell lines. *Biochem. Biophys. Res. Commun.* **2016**, *480*, 479–485, doi:10.1016/j.bbrc.2016.10.077.

75 McStay, G.P.; Green, D.R. Measuring apoptosis: Caspase inhibitors and activity assays. *Cold Spring Harb. Protoc.* **2014**, *2014*, 799–806, doi:10.1101/pdb.top070359.

76 Gupta, V.; Zhang, Q.-J.; Liu, Y.-Y. *Chapter 11: Drug Design and Discovery*; Satyanarayanajois, S.D., Ed.; Humana Press: Totowa, NJ, USA, 2011; volume 716, pp. 179–193; ISBN 978-1-61779-011-9.

77 Gottliner, C.; Mechtold, B.; Radbruch, A. *Chapter 1: Flow Cytometry and Cell Sorting*, 2nd ed.; Radbruch, A., Ed.; Springer: Berlin, Germany, 2000; pp. 1–26; ISBN 9783642084928.

78 Sigma Aldrich. Antibodies for Apoptosis. Avalaible online: https://www.sigmaaldrich.com/life-science/cell-biology/antibodies/antibody-products.html?TablePage=13832047 (accessed on 10 September 2018).

79 Wlodkowic, D.; Skommer, J.; Darzynkiewicz, Z. Flow cytometry-based apoptosi detection. *Methods Mol. Biol.* **2009**, *559*, 1–14, doi:10.1007/978-1-60327-017-5.

80 Dai, Y.; Grant, S. Methods to Study Cancer Therapeutic Drugs That Target Cell Cycle Checkpoints. In *Cell Cycle Checkpoints*; Springer: Berlin, Germany, 2011; Volume 782, pp. 257–304 ISBN 978-1-61779-272-4.

81 Mayhew, C.; Bosco, E.; Solomon, D.; Knudsen, E.; Angus, S.; Berndt, N. *Checkpoint Controls and Cancer*, 2nd ed.; Schonthal, A.H., Ed.; Humana Press: Totowa, NJ, USA, 2004; Volume 280, pp. 301–311; ISBN 1-59259-788-2.

82 Huang, B.W.; Gao, J.Q. Application of 3D cultured multicellular spheroid tumor models in tumor-targeted drug delivery system research. *J. Control. Release* **2018**, *270*, 246–259, doi:10.1016/j.jconrel.2017.12.005.

83 Griffith, L.G.; Swartz, M.A. Capturing complex 3D tissue physiology in vitro. *Nat. Rev. Mol. Cell Biol.* **2006**, *7*, 211.

84 Yamada, K.M.; Cukierman, E. Modeling Tissue Morphogenesis and Cancer in 3D. *Cell* **2007**, *130*, 601–610, doi:10.1016/j.cell.2007.08.006.

85 Cozzolino, A.M.; Noce, V.; Battistelli, C.; Marchetti, A.; Grassi, G.; Cicchini, C.; Tripodi, M.; Amicone, L. Modulating the Substrate Stiffness to Manipulate Differentiation of Resident Liver Stem Cells and to Improve the Differentiation State of Hepatocytes. *Stem Cells Int.* **2016**, *2016*, 1–12, doi:10.1155/2016/5481493.

86 Lee, G.Y.; Kenny, P.A.; Lee, E.H.; Bissell, M.J. Three-dimensional culture models of normal and malignant breast epithelial cells. *Nat. Methods* **2007**, *4*, 359.

87 Qiao, H.; Tang, T. Engineering 3D approaches to model the dynamic microenvironments of cancer bone metastasis. *Bone Res.* **2018**, *6*, doi:10.1038/s41413-018-0008-9.

88 Loessner, D.; Holzapfel, B.M.; Clements, J.A. Engineered microenvironments provide new insights into ovarian and prostate cancer progression and drug responses. *Adv. Drug Deliv. Rev.* **2014**, *79*, 193–213, doi:10.1016/j.addr.2014.06.001.

89 Mehta, G.; Hsiao, A.Y.; Ingram, M.; Luker, G.D.; Takayama, S. Opportunities and challenges for use of tumor spheroids as models to test drug delivery and efficacy. *J. Control. Release* **2012**, *164*, 192–204, doi:10.1016/j.jconrel.2012.04.045.

90 Suggitt, M.; Cooper, P.A.; Shnyder, S.D.; Bibby, M.C. The hollow fibre model - Facilitating anti-cancer pre-clinical pharmacodynamics and improving animal welfare. *Int. J. Oncol.* **2006**, *29*, 1493–1499, doi:10.3892/ijo.29.6.1493.

91 Decker, S.; Hollingshead, M.; Bonomi, C.A.; Carter, J.P.; Sausville, E.A. The hollow fibre model in cancer drug screening: The NCI experience. *Eur. J. Cancer* **2004**, *40*, 821–826, doi:10.1016/j.ejca.2003.11.029.

92 Hall, L.; Krauthauser, C.; Wexler, R.; Hollingshead, M.; Slee, A.; Kerr, J. The hollow fiber assay: continued characterization with novel approaches. *Anticancer Res.* **2000**, *20*, 903–911.

93 Lehár, J.; Krueger, A.S.; Avery, W.; Heilbut, A.M.; Johansen, L.M.; Price, E.R.; Rickles, R.J.; Short, G.F.; Staunton, J.E.; Jin, X.; et al. Synergistic drug combinations tend to improve therapeutically relevant selectivity. *Nat. Biotechnol.* **2009**, *27*, 659–666, doi:10.1038/nbt.1549.

94 Neve, R.M.; Chin, K.; Fridlyand, J.; Yeh, J.; Baehner, F.L.; Fevr, T.; Clark, L.; Bayani, N.; Coppe, J.P.; Tong, F.; et al. A collection of breast cancer cell lines for the study of functionally distinct cancer subtypes. *Cancer Cell* **2006**, *10*, 515–527, doi:10.1016/j.ccr.2006.10.008.

95 Sos, M.L.; Michel, K.; Zander, T.; Weiss, J.; Frommolt, P.; Peifer, M.; Li, D.; Ullrich, R.; Koker, M.; Fischer, F.; et al. Predicting drug susceptibility of non-small cell lung cancers based on genetic lesions. *J. Clin. Invest.* **2009**, *119*, 1727–1740, doi:10.1172/JCI37127DS1.

96 McDermott, U.; Sharma, S.V.; Dowell, L.; Greninger, P.; Montagut, C.; Lamb, J.; Archibald, H.; Raudales, R.; Tam, A.; Lee, D.; et al. Identification of genotype-correlated sensitivity to selective kinase inhibitors by using high-throughput tumor cell line profiling. *Proc. Natl. Acad. Sci. USA* **2007**, *104*, 19936–19941, doi:10.1073/pnas.0707498104.

# CHAPTER 3

# CELLULAR VIABILITY ASSAY PROTOCOL DEVELOPMENT AND SHORTCOMINGS OF CURRENT ASSAY PROTOCOLS

## 3.1 BACKGROUND

This chapter was written as a follow-up to the review published in the previous chapter. After gaining an understanding of the various *in vitro* analyses used to evaluate candidate anticancer therapeutics, it immediately became clear that the vast number of assays and various applications of those assays presented both practical and analytical challenges. Practically, the challenge emerged in lack of consistency which results in difficult/inaccurate comparisons of the therapeutic impact of one drug to another. Analytically, the challenge emerged in assessments of the impact of a single therapeutic. In attempt to investigate this concept further, three cellular viability assays were performed on treated and untreated neuroblastoma cells in order to compare and contrast the results obtained from each assay. In principle (based on the common understanding that "all cell viability assays are equal and relevant"), it was expected that each assay should provide similar results. In practice, extensive assay development was required to achieve this goal. This chapter details the process of protocol development that was implemented throughout the remaining work, shortcomings of current cellular viability assay protocols, and the context of this work in the field of anticancer therapeutic development. This work was exclusively completed by Jenna L. Gordon. Prof. Melissa M. Reynolds acted as the advisor on this project.

## 3.2 INTRODUCTION

In the early stages of anti-cancer drug development, cell-based analyses on human tumor derived cell lines remains essential.[1,2] Often, initial efficacy analysis is done through the use of cellular viability assays which provide information about the number of metabolically active cells present in a population.[3] Metabolic activity, a common indicator for cell health, can be indirectly measured through a variety of colorimetric assays.[4] These assays allow for straight-forward, high-throughput, cost-effective evaluation of anticancer efficacy in the primary stages of therapeutic development.[5–11] In general, these assays are known to operate similarly and are used interchangeably in cell-based analyses.[12–16] As such, it is typical for researchers to obtain results from a single cell viability assay before continuing with analysis of therapeutic efficacy.[12–16] While this does make practical sense, it presents a challenge in the field at large. As more assays are developed and used in various ways, it becomes more difficult to compare the effect of one therapeutic versus another – without an experimental comparison.

The vast number of cellular viability assays that exist for *in vitro* cell-based work rely on similar fundamental characteristics between living cells and assay reactants. For example, MTT (3-(4,5-dimethylthiazol-2-yl)-2,5-diphenyltetrazolium bromide), WST-8 (2-(2-methoxy-4-nitrophenyl)-3-(4-nitrophenyl)-5-(2,4-disulfophenyl)-2H -tetrazolium, monosodium salt), and CTB (7-hydroxy-3H-phenoxazin-3-one-10-oxide) are all reduced by a viable cell to produce formazans or resorufin, respectively (**Figure 1**). The assay products can then be detected via spectroscopy to determine a percentage of live cells in a treated sample versus an untreated sample.[6] Since each of these assays, along with various others, are consistently being used in current research, it is vital to have the ability to compare these assay results and overall efficacy between candidate therapeutics.

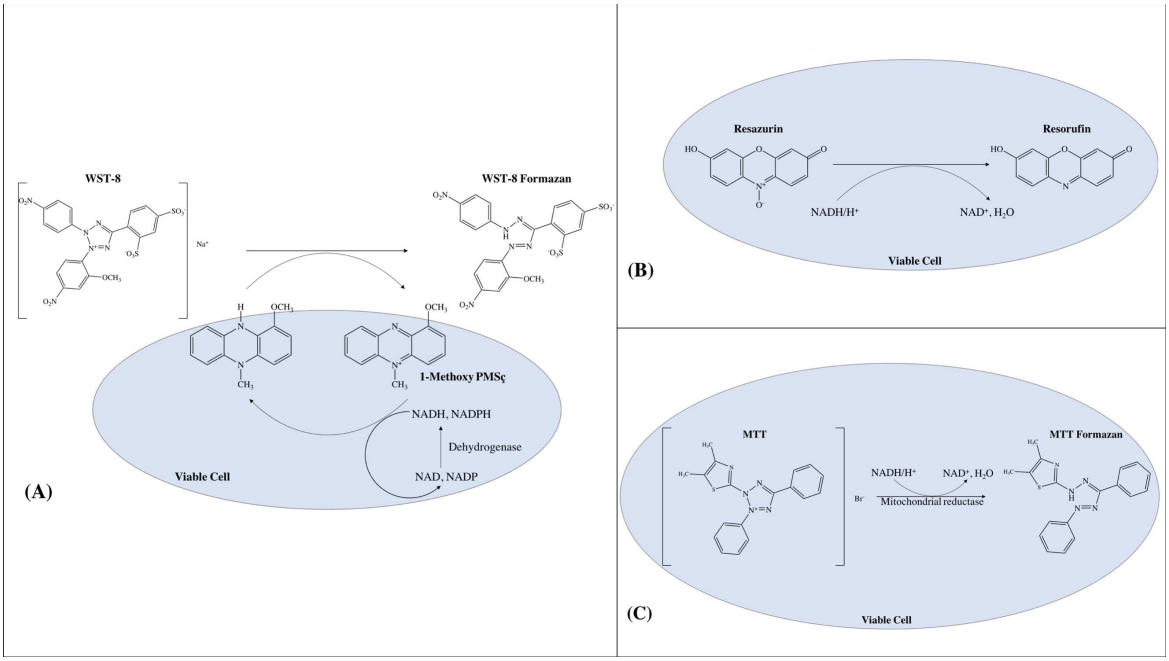


**Figure 3.1** Graphical representation of the reduction of three cell viability reactants, (A) WST-8 (later referred to as CCVK-1), (B) CTB, and (C) MTT to colored products that are measured via absorbance or fluorescence. It is important to note that the reactants are all different as well as the reaction mechanism.

However, it remains unclear if these assays can actually be directly compared. Based on their similarities, most colorimetric assays operate on very similar, pre-developed assay procedures. Unfortunately, these procedures do not account for the unique properties of these compounds, different interactions between assay reactants and metabolically active cells, and potential interferences.[17–19] Consequently, it was essential to develop and refine each individual assay procedure to determine if it is possible to achieve comparable results between assays and if so, how to achieve them.

In this work, three cell viability assays were employed to evaluate the effect of nitric oxide (NO), delivered by GSNO, on N2a neuroblastoma cells. Based on the similar fundamental properties of each assay, it was initially expected that similar viability results would be achieved in each case. Unfortunately, the data obtained from these experiments (following pre-developed

assay protocols*) did not support that hypothesis; the data was unreliable and inaccurate. This discovery led to troubleshooting and refining of each assay procedure to determine if comparable results were achievable and if so, what considerations and/or procedural steps were critical to attain them. Ultimately, the protocol development described herein was foundational and applied in every subsequent chapter of this dissertation. It is also important to note that these protocol refinements largely impact the field as a whole. Specifically, direct comparison of cellular viability assay results, regardless of which assay was applied, against other therapeutics would be extremely valuable in determining the clinical applicability of candidate anticancer therapeutics.

## 3.3 MATERIALS AND METHODS

### 3.3.1 *S*-Nitrosoglutathione (GSNO) synthesis.

*Materials*. Reduced glutathione (High purity) was purchased from VWR International (Radnor, PA, USA). Hydrochloric acid (HCl) and EPA vials were purchased from Thermo Fisher Scientific (Waltham, MA, USA). Sodium nitrite (99.999%, $NaNO_2$) was obtained through Alfa Aesar (Ward Hill, MA, USA) and acetone (≥99.5%) was purchased through Sigma Aldrich (St. Louis, MO, USA).

*Synthesis*. GSNO was synthesized through a previously developed synthesis. Briefly, the synthesis of GSNO required the addition of sodium nitrite to a solution of glutathione in Millipore water and 2 M hydrochloric acid. This mixture was continuously stirred in an ice bath for 40 minutes. The resulting solution was treated with acetone and then stirred continuously in an ice bath for an additional 10 minutes. The final red solution was filtered with gravity filtration for 10 minutes and then vacuum filtration for 3.5 hours to isolate the GSNO precipitate. The red filtrate solution was discarded and the dried solid pink powder (GSNO) was kept and analyzed by UV-Vis spectrophotometry at 336 nm to ensure >95% purity.

### 3.3.2 Cell Culture – N2a neuroblastoma cells.

*Materials*. Murine N2a neuroblastoma cells were acquired from Dr. Seonil Kim at Colorado State University. All cells were cultured and maintained with Dulbecco's Modified Eagle's Medium (DMEM) w/ L-glutamine purchased from Fisher Scientific (Hampton, NH, USA), supplemented with 10% EquaFETAL obtained through Atlas Biologicals (Fort Collins, CO, USA) and 1% Penicillin-Streptomycin Solution purchased from Fisher Scientific (Hampton, NH, USA).

*Method.* Complete cell media was used to culture and maintain all cells. Complete media consisted of 10% total volume bovine serum and 1% total volume penicillin-streptomycin to DMEM media. Initially, stock cultures were prepared by quickly thawing 1 mL (~$10^6$ cells) in 37°C water bath for 1-2 min. Immediately after thawing, the cells were transferred to 9 mL of pre-warmed, complete media in a 15 mL centrifuge tube. Cells were centrifuged at 2000 RPM, 4C, for 5 min. The supernatant was then discarded and the cell pellet was resuspended in complete media. This solution was transferred to a sterile T-25 $cm^2$ flask. The flasks were housed in a 37°C, 5% $CO_2$ incubator. Cells were appropriately provided fresh medium every 24-72 hours. Additionally, the cells were counted and split at appropriate intervals determined through both microscopic and macroscopic observation.

### 3.3.3 Cell Assays.

*Materials*. CellTiter-Blue Cell Viability Assay (CTB-Resazurin) and 3-(4,5-Dimethylthiazol-2-yl)-2,5-diphyltetrazolium bromide (MTT) were purchased from VWR International (Radnor, PA, USA). Colorimetric Cell Viability Kit I – WST-8 (2-(2-methoxy-4-nitrophenyl)-3-(4-nitrophenyl)-5-(2,4-disulfophenyl)-2H-tetrazolium, monosodium salt) (WST-8) was purchased from PromoCell (Heidelberg, Germany).

*Method*. Cells were plated in 96-well plates in 100 μL increments (containing between 100,000-200,000 cells per mL (~1,000-2,000 cells/well)). After 24 hours, the media was removed and replaced with 100 μL of one of these three solutions: complete media (Positive control – PC), 1 mM GSNO (Sample – S), or GSH (Functional control – GSH). After an additional 24 hours, the media was removed again and replaced with 100 μL of fresh complete media before analysis (this step is essential to avoid therapeutic assay interference – Section 3.3.2). Plates were analyzed using a Biotek Synergy 2 Multi-Detection Microplate Reader. An average and standard deviation of the untreated PC cells was calculated and compared to the absorbance value of each measured sample. An average of these values was calculated for each sample set.

*CTB assay*. For the CTB assay, cells were plated between 100,00 cells/well and 200,000 cells/well. Then, 20 μL of warm stock CTB solution was added to each well. The well plate was incubated in a static incubator at 37°C for 3.5 hours (protocol indicates 1-4 hours). Absorbance was measured at 570 nm and 600 nm using a microplate reader.

*WST-8 assay*. For the WST-8 (CCVK-I) assay, cells were plated at 100,000 cells/well and 200,000 cells/well. Immediately following the steps stated above, 10 μL of warm WST-8 solution was added to each well containing cells. The 96-well plate was incubated in a static incubator at 37°C for 3.5 hours (protocol indicates 1-4 hours). Absorbance was measured at 450 nm using a microplate reader.

*MTT assay*. For the MTT assay, cells were plated at 100,000 cells/well and 200,000 cells/well. Following the steps stated above, 10 μL of warm MTT solution was added to each well containing cells. The 96-well plate was incubated in a static incubator at 37°C for 3.5 hours (protocol indicates 1-4 hours). After the incubation period, 75 μL of media was removed from each well. Then 50 μL

DMSO was added to each well. The plate was incubated at 37°C for an additional 10 minutes. Absorbance was measured at 540 nm using a microplate reader.

## 3.4 DEFICIENCIES IN GENERAL CELLULAR VIABILITY ASSAY PROTOCOLS

**3.4.1 Introduction.** As previously stated, three cell viability assays were used to assess therapeutic impact on N2a neuroblastoma cells. In each case, the general assay protocol provided with the solution and/or kit was followed.[17–19] Unfortunately, the data obtained from these experiments provided unreliable and inaccurate data. In order to improve the overall utility of these assays and the ability to compare them, a few inadequacies of these protocols must be addressed. Namely, there are two important considerations that are valid for cellular viability assays that operate based on metabolic activity of cells, 1) air bubbles must be avoided and/ or removed and 2) reducing compounds interfere with cell viability assays. Further, to compare these assays, two additional considerations must be contemplated, 1) molecular weight of the measured analyte and 2) molar absorptivity of the measured analyte. Herein, these considerations are explored and analyzed.

**3.4.2 Air bubbles must be avoided and/or removed.** Each of these assay protocols, as well as many other general assay protocols, lack a statement regarding the presence of air bubbles in the assay well-plate analyzed by spectrophotometric detection.[17–19] However, initial analyses revealed that air bubbles significantly affected absorbance measurements in this work (**Figure 2**). When air bubbles were present in solution, the path length for the incident light beam was significantly increased. As a result, the absorbance value of the responsible well was significantly higher than expected. In some circumstances, one air bubble in one well could be considered statistical outliers that can be reliably removed from the data set. However, if there were multiple air bubbles or air bubbles in multiple wells, statistical testing would not suffice. To avoid this issue, it was essential to avoid air bubbles throughout the assay process. If air bubbles did persist despite mitigation

tactics, it was important to carefully remove (without changing the volume of the well) them before measuring absorbance.

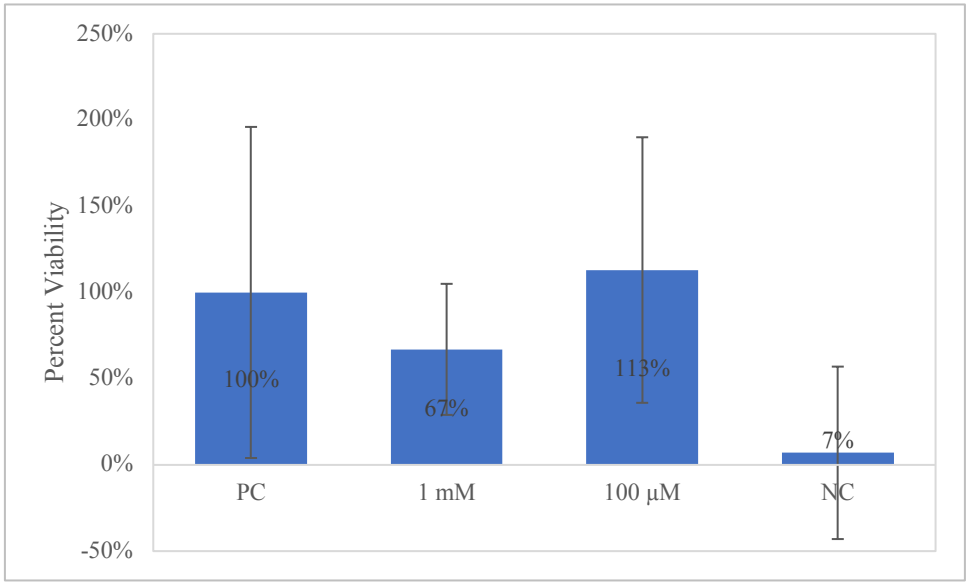


**Figure 3.2** Percent cellular viability of N2a neuroblastoma cells treated with 1 mM GSNO for 24 h. This data set was evaluated using the WST-8 assay. The results display extreme variability due to the **presence of air bubbles**. Each data point represents the average of n≥9 samples and the standard deviation.

**3.4.3 Reducing compounds interfere with cell viability assays.** Cellular viability assays are used to assess a range of therapeutics and their effects on cellular growth and proliferation. However, most general assay procedures fail to account for potential therapeutic interferences.[17–19] The assay procedures used in this work indicate immediate addition of the assay solution following therapeutic exposure. However, some therapeutics, like reducing compounds, can actually interfere with the cellular viability assays.[20] For example, a therapeutic with high reduction potential can induce conversion of CTB and other tetrazolium salts.[20] This artificially inflated conversion leads to false positives, or the appearance that more cells remain metabolically active after therapeutic exposure than there are in reality. This became an obvious source of interference in initial experiments in this work.

In this investigation, *S*-Nitrosoglutathione (GSNO) (**Figure 3 (A)**) was used as a NO-donor to assess the effect of NO on neuroblastoma. To ensure that NO was the active therapeutic, control studies were performed using reduced glutathione (GSH) (**Figure 3 (B)**). If NO was the only active therapeutic, then it would be expected that cells treated with GSH should exhibit similar metabolic activity as the untreated control cells. However, when the assay was performed in the presence of GSH, a marked increase in cellular viability was observed (**Figure 4**). Although this was an initial concern, when GSH was removed and replaced with complete media prior to completing the assay, the measured cellular viability of the GSH control was comparable to the positive, untreated control cells (**Figure 5**). To avoid any potential interferences in this work, all media (regardless of contents) was aspirated and replaced before performing viability assays.

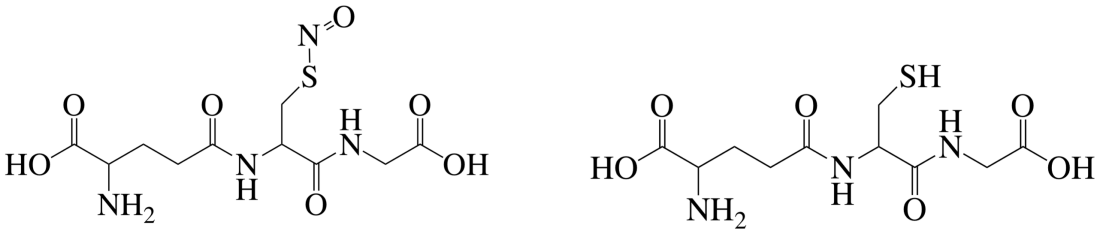


(A) (B)

**Figure 3.3** Structure of *S*-Nitrosoglutathione (GSNO) (A) and reduced glutathione (GSH) (B).

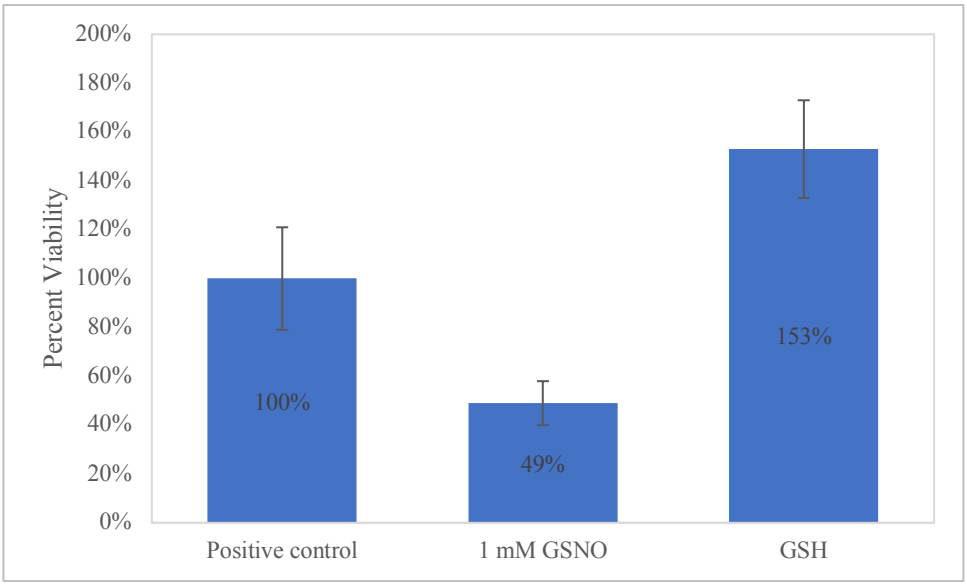


**Figure 3.4** Percent cellular viability of N2a neuroblastoma cells treated with 1 mM GSNO for 24 h assessed using the CTB assay. In this assay, air bubbles were avoided. Media containing therapeutics **were not removed** before the assay was performed. Each data point represents the average of n≥9 samples and the standard deviation.

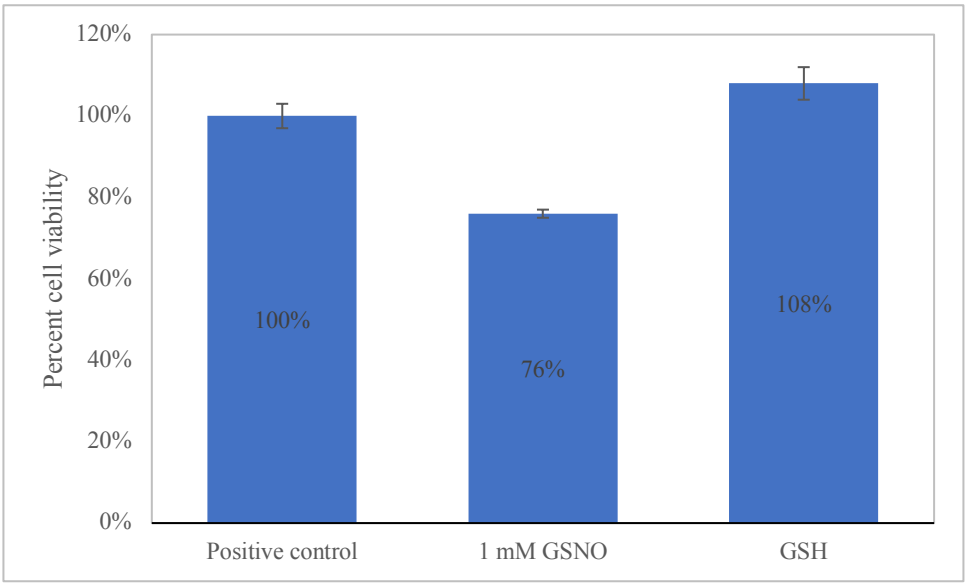


**Figure 3.5** Percent cellular viability of N2a neuroblastoma cells treated with 1 mM GSNO for 24 h assessed using the CTB assay. Air bubbles were avoided and all media and therapeutic content **was removed** and replaced with complete media before the assay was performed. Each data point represents the average of n≥9 samples and the standard deviation.

**3.4.4 Variations in molecular size, shape, and properties of assays.** Although cellular viability assays operate based on similar principles, each individual reactant interacts with cells and their components differently. This is a result of varying sizes, constituents, and properties. Of the three viability assays explored in this work (MTT, CTB, WST-8), two (MTT and WST-8) are tetrazolium salts while CTB is a blue dye. As a result of their structural differences, they have distinctive absorbance properties. As such, the three assays require different starting cellular counts to induce absorbance measurements within the linear range of the microplate reader (linear range: 0-2 absorbance units). Ultimately, the variations of molecular size, shape, and properties of the three viability assays applied in this work induced alterations in the approach and application of each assay.

WST-8 is an orange water-soluble tetrazolium salt that has a molecular weight of 600.47 g/mol. Due to the bulky molecular size, WST-8 is not membrane permeable and requires the presence of an intermediate electron acceptor.[21] The intermediate electron acceptor, 1-methoxy-5-methylphenaziniumm methyl sulfate (1-Methoxy PMS), is membrane permeable, which allows electron transfer from viable cells first to 1-Methoxy PMS and then to WST-8 in the cell media.[21] This reaction produces a yellow, water-soluble formazan that can be analyzed via absorbance and/or fluorescence spectrophotometry at 450 nm.[21] The absorbance value can then be directly correlated to the number of live cells present in the sample. In comparison to other tetrazolium salt-based viability assays such as MTT, XTT (2,3-bis-(2-methoxy-4-nitro-5-sulfophenyl)-2H-tetrazolium-5-carboxanilide), MTS (3-(4,5-dimethylthiazol-2-yl)-5-(3-carboxymethoxyphenyl)-2-(4-sulfophenyl)-2H-tetrazolium), and WST-1 (4-(3-(4-iodophenyl)-2-(4-nitrophenyl)-2H-5-tetrazolio)-1,3-benzene sulfonate), WST-8 is more analytically sensitive.[22] Several pre-mixed assay kits have been developed to incorporate both WST-8 and 1-Methoxy PMS to eliminate

additional steps. These kits have been termed Cell Counting Kit-8 (CCK-8) and Colorimetric Cell Viability Kit 1 (CCVK-I).[11,17] In this research, CCVK-I was selected to assess therapeutic effect on neuroblastoma cells. CCVK-I provided a single, ready-to use solution that provides cell viability data without additional solvents. Furthermore, in comparison to traditional viability assays, this assay kit did not require time consuming steps such as harvesting, washing, or solubilization. In the assay protocol, it was stated that accurate sensitivity could be achieved for adherent cells between 1,000-25,000 cells/well.[17] When cells were plated at higher initial seeding densities, closer to the top of the assay sensitivity range, the solutions became oversaturated at the top of the absorbance linear range (A~1.6-2.0) and the absorbance data was highly variable (**Figure 6**). As demonstrated in **Figure 7**, accurate results for CCVK-I on N2a neuroblastoma cells were achieved with an initial seeding density of 10,000 cells/well when the absorbance values were close to the middle of the absorbance linear range (A~1.0).

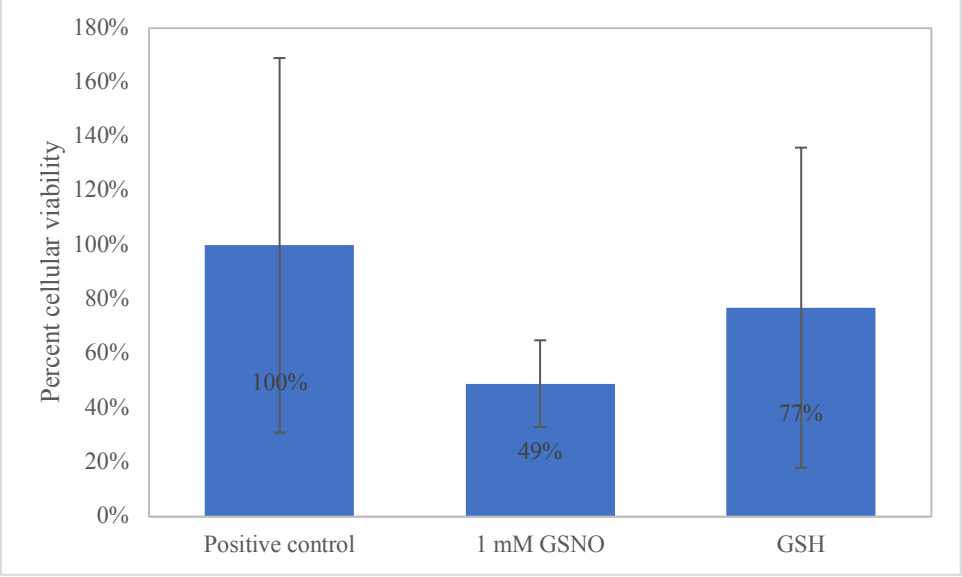


**Figure 3.6** Percent cellular viability of N2a neuroblastoma cells treated with 1 mM GSNO for 24 h assessed using the WST-8 assay. In this assay, air bubbles were avoided and all media and therapeutic content was removed and replaced with complete media before the assay was performed. Cells were plated at **20,000 cells/well**. Each data point represents the average of n≥9 samples and the standard deviation.

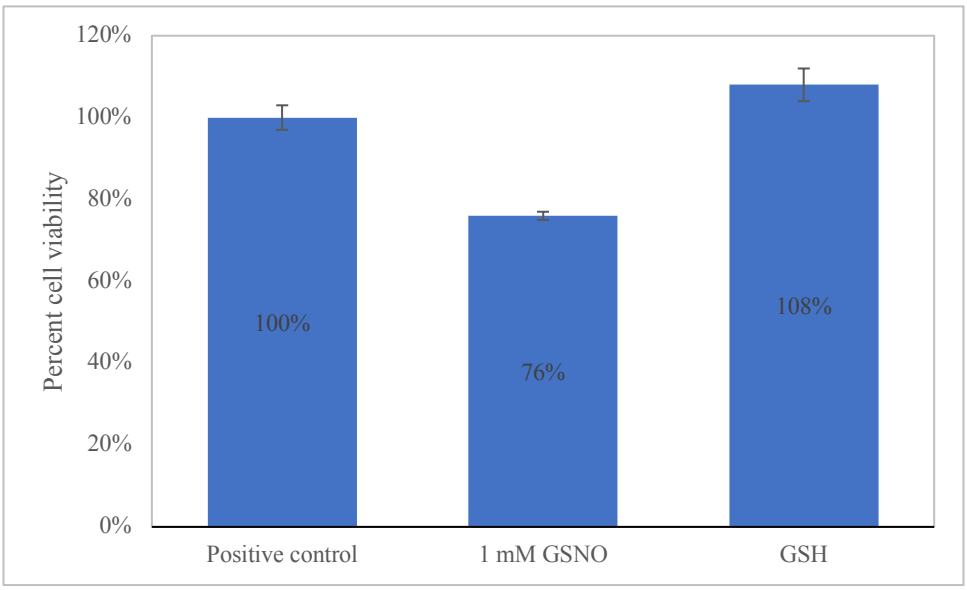


**Figure 3.7** Percent cellular viability of N2a neuroblastoma cells treated with 1 mM GSNO for 24 h assessed with the WST-8 assay. In this assay, air bubbles were avoided and all media and therapeutic content was removed and replaced with complete media before the assay was performed. Cells were plated at **10,000 cells/well**. Each data point represents the average of n≥9 samples and the standard deviation.

The CTB assay contains a starting reactant called resazurin, a small molecular weight blue dye (229.191 g/mol) that is membrane permeable. Resazurin is reduced by viable cells containing NAD(P)H oxidoreductase enzymes to a purple, water-soluble dye, resorufin. Resorufin can be directly analyzed via absorbance and/or fluorescence spectrophotometry. One important distinction between this assay and the other assays applied in this work, is the absorbance and/or fluorescence must be measured at two wavelength values, 570 nm and 600 nm, because the maximum wavelengths for resazurin (605 nm) and resorufin (573 nm) are so close.[19] As a result, analysis of this data is more elaborate and the number of live cells after treatment with a therapeutic is represented by the difference between the average absorbance values at each maximum wavelength multiplied by the molar extinction coefficient of the opposite wavelength value. Similar to WST-8, this assay did not require time consuming steps such as harvesting, washing, or solubilization. Additionally, like WST-8, it is more analytically sensitive than many tetrazolium

salt-based cell viability assays, like MTT, MTS, XTT, and WST-1.[23] According to the protocol guide for the CTB assay, the linear range of fluorescence /absorbance and cell density is dependent on the type of cell under investigation.[19] When initial analyses were performed with cell densities of 10,000 cells/well in a 96-well plate format (as done with the previous WST-8 assays) the results obtained were unreliable and exhibited large error margins (**Figure 8).** These results were concerning due to the large error margins and erratic absorbance values (A~1.1-2.2). Based on these concerns, the cell density was increased to 20,000 cells/well, resulting in small standard deviations (≤10%), results resonant with those of the previous assay, and consistent absorbance values within the linear range (A~1.3-1.6) (**Figure 9)**.

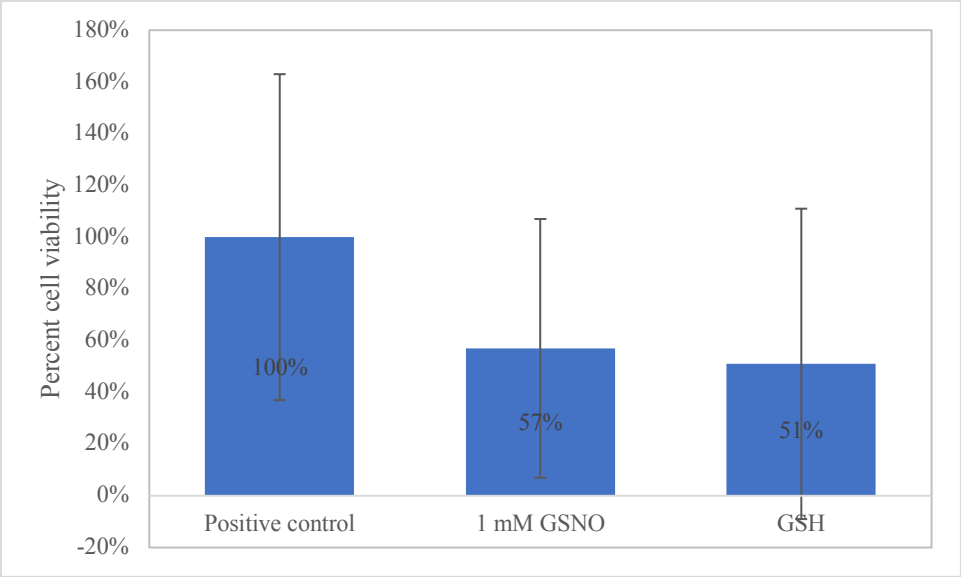

**Figure 3.8** Percent cellular viability of N2a neuroblastoma cells treated with 1 mM GSNO for 24 h analyzed with the CTB assay. Air bubbles were avoided and all media and drug content were removed and replaced with fresh media prior to performing the assay. The cells in this assay were plated at **10,000 cells/well**. Each data point represents the average of n≥9 and the standard deviation.

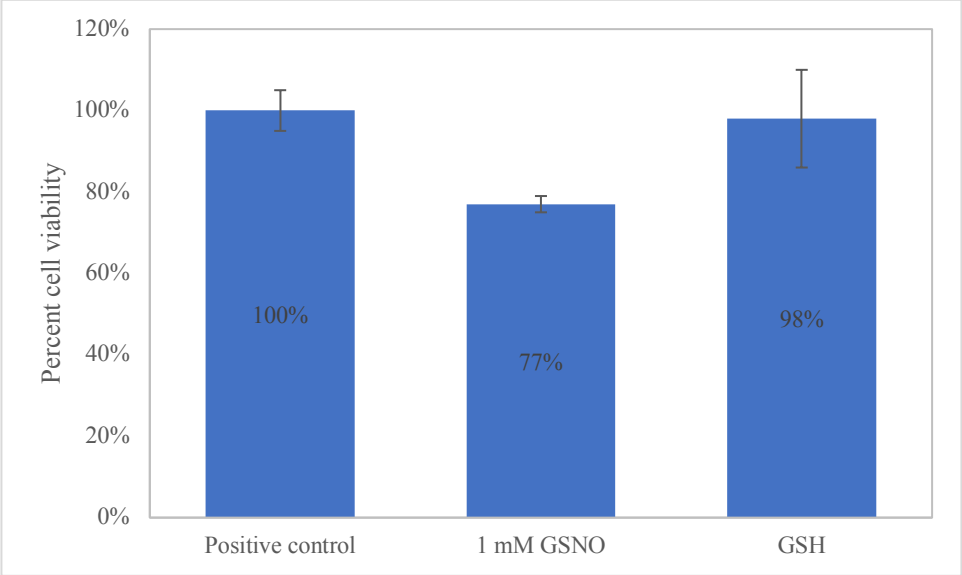


**Figure 3.9** Percent cellular viability of N2a neuroblastoma cells treated with 1 mM GSNO for 24 h, assessed with the CTB assay. Air bubbles were avoided and all media and therapeutics were removed and replaced with fresh media prior to performing this assay. In this assay, cells were plated at **20,000 cells/well**. Each data point represents an average of n≥9 and the standard deviation. Each data point represents the average of n≥9 and the standard deviation.

The final assay applied in the analysis of N2a neuroblastoma cell viability in this research was MTT. MTT is a yellow, water-soluble tetrazolium salt with a molecular weight of 414.3 g/mol. Due to its small molecular size, MTT is membrane permeable and coverts to a water-insoluble purple formazan in the presence of viable cells containing NAD(P)H oxidoreductase enzymes. This formazan salt must be solubilized using dimethyl sulfoxide (DMSO) prior to analysis via absorbance and/or fluorescence spectrophotometry at 540 nm.[18] The aforementioned step requires an additional solubilization step and incubation period of 10 min, making it more time-consuming than WST-8 and CTB. Further, MTT was less analytically sensitive than the two aforementioned

assays.[22,23] The average absorbance values acquired can be directly correlated to the number of live cells present in a sample.

According to the assay protocol guide for MTT, accurate sensitivity can be achieved when cells are plated between 250 – 100,000 cells/well.[18] Based on this information and the data from the previous two assays, N2a neuroblastoma cells were initially plated at 20,000 cells/well for analysis using the MTT assay. The resultant absorbance values were within the absorbance linear range (A~0.4-0.6) and the standard deviations were small (≤10%) (**Figure 10**). Promisingly, the observed data corresponded to that of the previous two assays. As such, the protocol for this assay on N2a cells was developed based on this initial cell density of 20,000 cells/well.

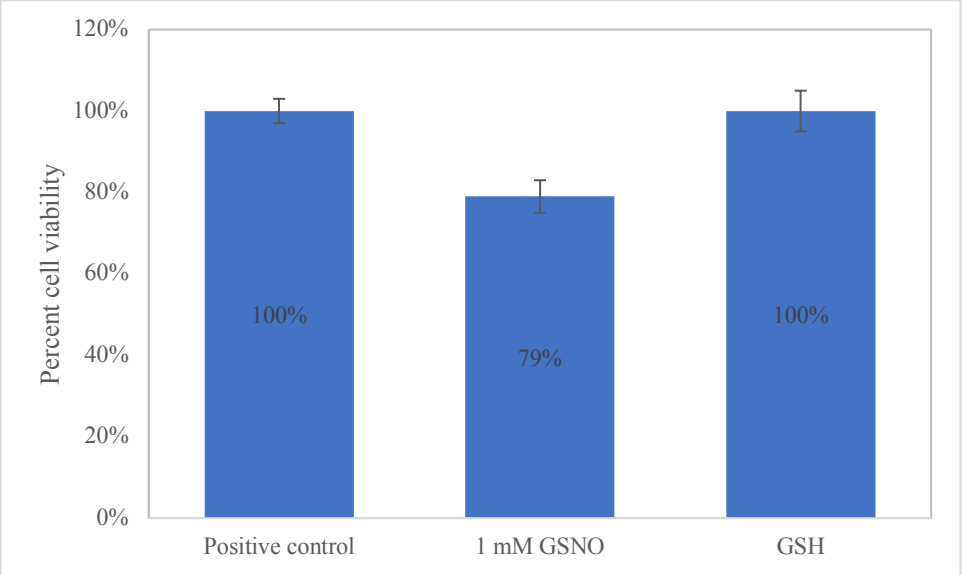


**Figure 3.10** Percent cellular viability of N2a neuroblastoma cells treated with 1 mM GSNO for 24 h, assessed with the MTT assay. Air bubbles were avoided and all therapeutic/control content was removed and replaced with fresh media prior to addition of the assay. In this experiment, cells were plated at **20,000 cells/well**.

## 3.5 CONCLUSIONS

In the preliminary stages of anticancer therapeutic development, it is essential to determine therapeutic efficacy using human tumor derived cell lines. Often, researchers use cellular viability assays to quickly analyze therapeutic efficacy in initial stages of development. These assays are invaluable, however the brief protocols associated with these assays are incomplete and over-generalized. As a result, it is important to discern possible sources of interferences and to develop individualized assay protocols. In this chapter, protocol development tactics and differences between each of the three assays (WST-8, CTB, and MTT) were analyzed and explored in attempt to create individualized variations of the standard assay protocols. Ultimately, this work revealed some extremely important pieces to consider, like the avoidance and/or removal of air bubbles, the avoidance and/or removal of reducing compounds before analysis, and considerations of the differences in size, shape, and properties of the assay reactants. These analyses resulted in the development of individualized assay protocols for each of the three viability assays that were applied in all of the following chapters.

# CHAPTER 3 – REFERENCES


1 J. Gordon, M. Brown and M. Reynolds, *Diseases*, 2018, **6**, 85.

2 A. Goodspeed, L. M. Heiser, J. W. Gray and J. C. Costello, *Mol. Cancer Res.*, 2016, **14**, 3–13.

3 Promega, in *Protocols and Applications Guide*, 2011, vol. 3/11, pp. 1–23.

4 M. J. Stoddart, K. S. Louis, A. C. Siegel, L. Kupcsik and E. M. Czekanska, *Chapters 1-5: Mammalian Cell Viability*, Humana Press, 2011, vol. 740.

5 K. Prabst, H. Engelhardt, S. Ringgeler, H. Hubner, G. Ates, T. Vanhaeke, V. Rogiers, R. Rodrigues, L. L.-Y. Chan, K. J. McCulley, S. L. Kessel, D. P. Ivanov, A. M. Grabowska, M. C. Garnett, N. Suganuma, N. I. Molefe and N. Inoue, *Chapters 1-4, 8: Cell Viability Assays*, Humana Press, 2017, vol. 1601.

6 J. van Meerlo, G. J. L. Kaspers, J. Cloos, S. Glaysher, I. A. Cree, J. M. Hartley, V. J. Spanswick and J. A. Hartley, *Chapters 20-22, 25: Cancer Cell Culture Methods and Protocols*, Humana Press, 2nd edn., 2013, vol. 731.

7 T. Mosmann, *J. Immunol. Methods*, 1983, **65**, 55–63.

8 A. J. Brady, P. Kearney and M. M. Tunney, *J. Microbiol. Methods*, 2007, **71**, 305–311.

9 S. Uzunoglu, B. Karaca, H. Atmaca, A. Kisim, C. Sezgin, B. Karabulut and R. Uslu, *Toxicol. Mech. Methods*, 2010, **20**, 482–486.

10 T. Riss, R. Moravec, A. Niles and S. Duellman, in *Assay Guidance Manual [Internet]*, 2013, pp. 1–55.

11 *Dojindo Mol. Technol.*, 2009, **8**, 1–7.

12 M. Miyawaki, H. Yasuda, T. Tani, J. Hamamoto, D. Arai, K. Ishioka, K. Ohgino, S.

Nukaga, T. Hirano, I. Kawada, K. Naoki, Y. Hayashi, T. Betsuyaku and K. Soejima, *Mol. Cancer Res.*, 2017, **15**, 106–114.

13 Y. Wang, L. Wang, S. Guan, W. Cao, H. Wang, Z. Chen, Y. Zhao, Y. Yu, H. Zhang, J. C. Pang, S. L. Huang, Y. Akiyama, Y. Yang, W. Sun, X. Xu, Y. Shi, H. Zhang, E. S. Kim, J. A. Muscal, F. Lu and J. Yang, *Sci. Rep.*, 2016, **6**, 1–10.

14 L. Wang, B. F. Cheng, H. J. Yang, M. Wang and Z. W. Feng, *Am. J. Transl. Res.*, 2015, **7**, 1541–1552.

15 F. Xu, H. Li and Y. Sun, *Biochem. Biophys. Res. Commun.*, 2014, **454**, 566–571.

16 J. Lu, S. Guan, Y. Zhao, Y. Yu, S. E. Woodfield, H. Zhang, K. L. Yang, S. Bieerkehazhi, L. Qi, X. Li, J. Gu, X. Xu, J. Jin, J. A. Muscal, T. Yang, G.-T. Xu and J. Yang, *Cancer Lett.*, 2017, **400**, 61–68.

17 PromoKine, 2014, 1–3.

18 OZBiosciences, 1–6.

19 Promega Cooperation, *Tech. Bull.*, 2016, 1–16.

20 B. H. Neufeld, J. B. Tapia, A. Lutzke and M. M. Reynolds, , DOI:10.1021/acs.analchem.8b01043.

21 M. Ishiyama, Y. Miyazono, K. Sasamoto, Y. Ohkura and K. Ueno, *Talanta*, 1997, **44**, 1299–1305.

22 H. Tahara, S. Matsuda, Y. Yamamoto, H. Yoshizawa, M. Fujita, Y. Katsuoka and T. Kasahara, *J. Pharmacol. Toxicol. Methods*, 2017, **88**, 92–99.

23 S. Ansar Ahmed, R. M. Gogal and J. E. Walsh, *J. Immunol. Methods*, 1994, **170**, 211–224.

CHAPTER 4

# NITRIC OXIDE AS A POTENTIAL ADJUVANT THERAPEUTIC FOR NEUROBLASTOMA: EFFECTS OF NO ON MURINE N2A CELLS

## 4.1 BACKGROUND

This chapter originated following studies done by Melissa Reynolds and collaborators from the Brown lab in the School of Biomedical Sciences at Colorado State University on the ability of nitric oxide (NO) to halt proliferation of tumor cells of diverse origins.[1,2] After reviewing these studies and numerous others, the potential of NO as an adjuvant therapeutic in the clinical management of cancer was apparent. To build on this concept, this work implements NO, delivered by *S*-Nitrosoglutathione (GSNO), as an anticancer therapeutic on pediatric neuroblastomas was conceived. This chapter details the first attempt to evaluate the impact of NO (delivered via GSNO) on murine N2a neuroblastoma cells. In this investigation, multiple methods from Chapter 2 (Cell-Based Methods for Determination of Anticancer Therapeutic Efficacy) were implemented to determine the impact of NO as an anticancer agent. Additional studies were done on healthy Adult Human Dermal Fibroblasts (HDFa) to establish the potential of NO to discriminate between neoplastic and healthy cells. All experiments, the corresponding analyses for this work, and draft preparation were performed by Jenna L Gordon. Melissa M Reynolds and Mark A Brown acted as advisors and contributed to draft revision. The paper was originally published in the MDPI journal Veterinary Sciences () and has been modified with permission.[2] Copyright 2020.

[2] Gordon, J.L.; Reynolds, M.M.; Brown, M.A. Nitric Oxide as a Potential Adjuvant Therapeutic for Neuroblastoma: Effects of NO on Murine N2a Cells. *Vet Sci* **2020**, 7(2), 51. doi: 10.3390/vetsci7020051

## 4.2 INTRODUCTION

Organismal development involves a host of regulatory mechanisms for directing highly conserved patterns in gene expression.[3-5] One such pathway involves epigenetic modifications, via posttranslational modifications, leading to synchronization in genetic patterns of expression.[3-5] These patterns of synchronization ultimately guide developmental pathways during embryogenesis. Although aberrations in posttranslational modifications are often associated with developmental diseases including tumorigenesis[6-10], posttranslational events can also be manipulated and/or targeted for positive clinical applications[11].

Although neuroblastoma, the most common extracranial solid tumor in children, accounts for only 8% of all pediatric cancer diagnoses, it is the cause of 15% of all pediatric cancer mortalities.[12] Tumors form in the sympathetic nervous system, largely originating in the adrenal glands.[13] Long-term disease prognosis is variable, dependent on a myriad of factors including but not limited to the stage of the disease, age of the patient, presence/absence of MYCN gene amplification, and chromosomal aberrations.[14] Treatment options for neuroblastoma reflect those of other malignant tumors and vary depending upon the stage of the disease as well as relevant risk factors. Due to the multitude and intricacy of disease progression and response to treatment, the International Neuroblastoma Staging System (INSS) was developed to classify the extent of the disease and impact the treatment approach.[14]

Three distinct stages comprise the INSS: low, intermediate, and high risk. Each risk group is comprised of definitions containing the stage(s), patient age, presence/absence of the MYCN gene, histology, and DNA ploidy. Currently, low risk tumors represent ≤25% of initial diagnoses, intermediate risk represent about ~15% of initial diagnoses, and high-risk tumors are the most commonly diagnosed, at ≥60%.[13] In patients with low risk disease, surgery and observation are the

central therapeutic options that contribute to >90% survival.[16-17] Patients with intermediate risk disease typically receive a variety of sequential treatments including chemotherapy, surgery, and radiation therapy, if necessary. Survival rates in this group drop some but remain favorable at >80%.[18-19] High-risk treatment protocols commence in an identical manner and additional treatments are frequently required, such as immunotherapy and bone marrow transplant. Despite the advances in treatments for low and intermediate risk disease, patients with high risk disease continue to face particularly poor prognosis, with ~40% five-year overall survival rates.[20,21] Overall relapse rates are additionally overwhelming, at >60%.[14] In a similar fashion, treatments for recurrent low-risk and intermediate-risk disease are largely effective. However, recurrent high-risk neuroblastoma remains a significant challenge.

Due to the aggressive and unpredictable nature of high-risk and recurrent neuroblastoma, recent work has focused on the development of new therapeutic techniques.[14] The multitude of new therapies include cytotoxic agents, targeted agents, immunotherapy, retinoids, angiogenesis inhibitors, tyrosine kinase inhibitors, as well as other approaches.[14] One approach that has been of little focus in pediatric neuroblastoma research is the use of nitric oxide (NO) as an anticancer agent.[22,23] Numerous studies have shown that NO effectively induces tumor-specific cytotoxicity and pharmaceutical applications of *S*-Nitrosylation have exhibited great potential for use as adjuvant therapeutics in the clinical management of cancer.[24-33] The body's physiological NO production is facilitated through three forms of the enzyme NO synthase (NOS), neuronal NOS (nNOS or NOS1), inducible NOS (iNOS or NOS2), and endothelial NOS (eNOS or NOS3). The routes that produce NO change under varying conditions (i.e., pH and temperature), require the use of different forms of NO synthase (NOS), and differ in production rates and expression patterns.[31] The variances in timing, longevity, and intensity of NO release by these different

pathways ultimately determines the resultant biological consequences. Current research indicates that specific, localized concentrations of NO are required to regulate platelet aggregation while bursts of elevated concentrations of NO induce cytotoxicity.[31] Based on normal physiological processes, it is understood that surges of concentrated NO induce cytotoxicity. Furthermore, NO-releasing compounds such as *S*-Nitrosothiols, which are naturally occurring components in the body, provide prolonged, regulated release of NO. As such, *S*-Nitrosoglutathione (GSNO) was applied as the NO donor in this work.

Herein, the utility of NO as a potential adjuvant therapeutic for murine N2a neuroblastoma cells was identified. The effect of NO, delivered by GSNO, on N2a cells was assessed by exposing 1 mM GSNO to N2a cells for 24 h in the absence of light at 37 °C in a 5% $CO_2$ incubator. Initially, therapeutic efficacy was assessed through three cell viability assays: resazurin, WST-8, and MTT. Each of these assays showed a modest 21–24% reduction in cell viability after therapeutic exposure. Colony formation assays further established the impact of NO on N2a cells, highlighting complete lack of colony formation capacity after the 24 h treatment period. Subsequently, a final cell viability assay was performed to determine the effect of 1 mM GSNO on non-carcinogenic HDFa cells. The results from this assay show that HDFa cells were not affected. Ultimately, the amount of NO available to N2a cells was explored by measuring the NO-release profile of 1 mM GSNO in PBS (0.54 ± 0.04 μmol NO in 24 h) and monitoring of the GSNO $\lambda_{max}$ in 1 mM GSNO in complete DMEM at 336 nm (decreased GSNO peak over 24 h corresponding to decrease in available NO). Overall, NO impact on murine N2a cells is unexceptional as a stand-alone treatment. However, this level of impact coupled with the observed minimized impact on healthy cells suggests exciting potential of NO as an adjuvant, offering the prospect of reducing detrimental patient side effects.

## 4.3 MATERIALS AND METHODS

### 4.3.1 *S*-Nitrosoglutathione Synthesis

*Materials.* Reduced glutathione (GSH; High purity) was purchased from VWR International (Radnor, PA, USA). Hydrochloric acid (HCl) and EPA vials were purchased from Thermo Fisher Scientific (Waltham, MA, USA). Sodium nitrite (99.999%, $NaNO_2$) was obtained through Alfa Aesar (Ward Hill, MA, USA) and acetone (≥99.5%) was purchased through Sigma Aldrich (St. Louis, MO, USA).

*Synthesis of S-Nitrosoglutathione (GSNO).* *S*-Nitrosoglutathione (GSNO) was synthesized through a previously developed synthesis. Briefly, GSNO was synthesized through the addition of $NaNO_2$ to a solution of GSH in Millipore water and 2 M HCl. The GSNO mixture was reacted with constant stirring in an ice bath. After 40 min, the solution was treated with acetone and allowed to continue reacting with constant stirring in an ice bath. After 10 min, the resultant red solution was filtered, first with gravity filtration for 10 min and then vacuum filtration for 3.5 h to isolate the GSNO precipitate. The GSNO precipitate was washed successively with ice-water and acetone. The red filtrate solution was discarded and the filtered solid pink powder (GSNO) was kept and analyzed by UV-Vis spectrophotometry at 336 nm to ensure >95% purity.

### 4.3.2 Cell Culture—N2a

*Materials.* Murine neuroblastoma N2a cells were acquired from Dr. Seonil Kim at Colorado State University. Cells were maintained with Dulbecco's Modified Eagle's Medium (DMEM) w/ L-glutamine purchased from Fisher Scientific (Hampton, NH, USA), supplemented with 10% EquaFETAL 100% U.S. Origin Bovine Serum obtained through Atlas Biologicals (Fort Collins, CO, USA) and 1% Penicillin-Streptomycin Solution purchased from Fisher Scientific (Hampton, NH, USA).

*Method.* Complete cell medias were prepared by adding 10% total volume fetal bovine serum and 1% total volume penicillin-streptomycin to DMEM media (complete DMEM). Initial stock cultures were prepared by quickly thawing 1 mL ($10^6$ cells) in 37 °C water bath for 1–2 min. Once thawed, cells were added to 9 mL of pre-warmed, complete media in a 15 mL centrifuge tube. After centrifugation at 2000 RPM, 4 °C, 5 min, the supernatant was discarded, and the cell pellet was resuspended in 5 mL complete media and transferred to a sterile T-25 $cm^2$ flask. The flasks were placed in a 37 °C, 5% $CO_2$ incubator. Cells were appropriately provided 10 mL fresh medium every 24–72 h. Cells were additionally counted and split at appropriate intervals determined through both microscopic and macroscopic observation.

### 4.3.3 Cell Culture—HDF

*Materials.* Adult human dermal fibroblasts (HDFa; lot # 80616174) were maintained with fibroblast basal medium (FBM) supplemented with fibroblast growth kit—low serum and penicillin-streptomycin-amphotericin B, all purchased from American Type Culture Collection (Manassas, VA, USA). Trypsin/EDTA Solution for Primary Cells and Trypsin Neutralizing Solution were also purchased from American Type Culture Collection (Manassas, VA, USA).

*Method.*Complete cell medias were prepared by adding the indicated volume of each supplement within the fibroblast growth kit – low serum. Initial stock cultures were prepared by quickly thawing 1 mL ($7.1 \times 10^5$ cells) in 37 °C water bath for 1–2 min. Once thawed, cells were added to 9 mL of pre-warmed, complete media in a T-25 $cm^2$ flask. The flasks were placed in a 37 °C, 5% $CO_2$ incubator. Cells were appropriately provided 10 mL fresh medium every 24–72 h. Cells were additionally counted and split at appropriate intervals determined through both microscopic and macroscopic observation.

### 4.3.4 *In vitro* Cell Viability Assays

*Materials.* Colorimetric Cell Viability Kit I – WST-8 (2-(2-methoxy-4-nitrophenyl)-3-(4-nitrophenyl)-5-(2,4-disulfophenyl)-2H-tetrazolium, monosodium salt) (WST-8) was purchased from PromoCell (Heidelberg, Germany). Trypan Blue Solution was purchased from Sigma-Aldrich (St. Louis, MO, USA). CellTiter-Blue Cell Viability Assay (Resazurin) and 3-(4,5-Dimethylthiazol-2-yl)-2,5-diphyltetrazolium bromide (MTT) were purchased from VWR International (Radnor, PA, USA).

*Method.* Cells were plated in 100 μL increments (containing between 100,000-200,000 cells per mL (~1,000–2,000 cells/well) in 96-well plates. After 24 h, the media was aspirated and replaced with either 100 μL of media (Positive control—PC; ≥7 samples), 100 μL of 1 mM GSNO (Sample—S; ≥7 samples), or 100 μL of 1 mM GSH (Functional control—GSH; ≥7 samples). After an additional 24 h, the media was aspirated and replaced with 100 μL of fresh complete media before performing the appropriate cell viability assay. All absorbance measurements were collecting using a BioTek Synergy 2 Multi-Detection Microplate Reader. An average and standard deviation of the untreated PC cells was calculated and compared to the absorbance value of each measured sample. Analysis of variance (ANOVA) was performed to determine the statistical difference of the measured data.

*Resazurin Assay.* In the resazurin assay, N2a neuroblastoma and HDF cells were plated separately at 200,000 cells/mL in a 96-well plate. Following the steps stated above, 20 μL of warm resazurin was added to each well containing cells. The 96-well plate was incubated in a static incubator at 37 °C for 3.5 h (protocol indicates 1–4 h). Absorbance was measured at 570 nm and 600 nm using a microplate reader. In each experiment, data points were represented by an average ($n \geq 7$) ± standard deviation.

*WST-8 Assay.* In the WST-8 assay, N2a neuroblastoma cells were plated at 100,000 cells/mL in a 96-well plate. Following the steps stated above, 10 μL of warm WST-8 solution was added to each well containing cells. The 96-well plate was incubated in a static incubator at 37 °C for 3.5 h (protocol indicates 1–4 h). Absorbance was measured at 450 nm using a microplate reader. In this experiment, data points were represented by an average ($n \geq 9$) ± standard deviation.

*MTT Assay.* In the MTT assay, cells were plated at 100,000 cells/mL in a 96-well plate. Following the steps stated above, 10 μL of warm MTT solution was added to each well containing cells. The 96-well plate was incubated in a static incubator at 37 °C for 3.5 h (protocol indicates 1–4 h). After the incubation period, 75 μL of media was removed from each well, followed by the addition of 50 μL DMSO to each well. The plate was incubated at 37 °C for an additional 10 min. Absorbance was measured at 540 nm using a microplate reader. In each experiment, data points are represented by an average ($n \geq 7$) ± standard deviation.

**4.3.5 Colony Formation**

*Method.* In the colony formation assays, cells were plated at 100,000 cells/mL in a 24-well plate in 1 mL increments. After 24 h, the media was aspirated and replaced with either 1 mL of media (Positive control—PC; ≥4 samples), 1 mL of 1 mM GSNO (Sample—S; ≥4 samples), or 1 mL of 1 mM GSH (Functional control—GSH; ≥4 samples). After an additional 24 h, the media was removed, and the cells were harvested via trypsin administration, centrifugation, and collection. At this point, cells were re-plated at 200 cells/ mL in a 24-well plate in 1 mL increments. Colony formation was qualitatively monitored daily and quantitatively measured weekly for three weeks by bright field microscopy. Colonies were defined as masses of at least 50 cells. In each experiment, data points are represented by an average ± standard deviation of $n \geq 3$.

**4.3.6 Nitric Oxide Analyzer Analysis of 1 mM GSNO in PBS.** NO release over 24 h was measured at 1 min intervals in 1 mM GSNO in PBS. This measurement was performed in PBS instead of complete DMEM because the constant flow of $N_2$ gas necessary for analysis caused foaming in experimental media that prevented the collection of NO release data. This was achieved using a chemiluminescence-based Nitric Oxide Analyzer (NOA 280i, GE Analytical, Boulder, CO, USA). The instrument was calibrated prior to operation by establishing a baseline with a nitrogen gas sweep followed by delivery of NO/nitrogen calibration gas at a flow rate of 200 mL/min. Immediately prior to data collection, 10 mM GSNO was prepared in a scintillation vial with protection from light and added directly into the NOA sample vessel containing PBS to achieve a final concentration of 1 mM GSNO. The bottom half of the sample vessel that contained solution was immediately submerged in a 37 °C water bath to promote NO release. Finally, the cell and water bath combination were covered with foil to eliminate photolytic decomposition. The NO release profile was ultimately used to determine the total NO release (in mol) of 1 mM GSNO in PBS in 24 h.

**4.3.7 UV-Vis Analysis of 1 mM GSNO in complete DMEM.** NO release from 1 mM GSNO in complete DMEM was assessed using a Nicolet Evolution 300 UV-Vis spectrophotometer (Thermo Electron Corporation, Madison, WI, USA). A baseline was established prior to analysis using complete DMEM media. Absorbance data from 250nm-600nm was collected at 1 min intervals for 24 h to observe the absorbance at the $\lambda_{max}$ of GSNO, 336 nm. A decrease in GSNO absorbance at 336 nm corresponds to the decrease in available NO.

**4.3.8 Data Analysis/Statistics.** All the data points are expressed as the average ± standard deviation. Statistical analysis was performed using one-way ANOVA. Statistically significant differences were defined at $p < 0.01$.

## 4.4 RESULTS

**4.4.1 Cell Viability Assays.** Cell viability assays were performed on murine N2a neuroblastoma cell lines to determine their response to 1 mM GSNO. Overall, resazurin, WST-8, MTT, and colony formation studies consistently showed decreased cell viability in N2a cells. Cell death was attributed to NO based-on control experiments run with reduced glutathione (GSH) in place of GSNO. Cells were also treated with GSH as a control experiment to highlight that GSNO—which is synthesized through the substitution of a NO group with the thiol group on GSH—is the only molecule (between the two aforementioned molecules) that impacts the viability of N2a cells (Figure 1). This indicates that NO, which is released spontaneously from GSNO (due to heat at 37 °C) is responsible for the observed decrease. It is not clear which reactions involving NO induce this response. Finally, cell viability of HDFa, analyzed with the resazurin assay, showed no decrease in viability after therapeutic application. These results exhibit the therapeutic potential of NO as an anticancer treatment against neuroblastoma.

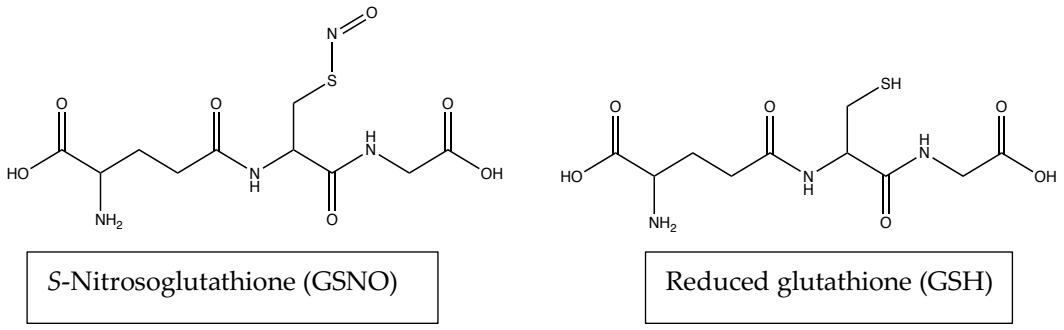


**Figure 4.1** Structures of *S*-Nitrosoglutathione (GSNO) and reduced glutathione (GSH).

*Resazurin Assay Analysis of Cellular Viability.* The resazurin assay was implemented to assess the cellular viability of cells after GSNO-treatment. The results revealed a statistically significant, albeit moderate decrease in the viability, ~21%, of GSNO-exposed cells in comparison to untreated PC and treated-GSH cells (Figure 2). (Note: This data demonstrates an apparent impact on N2a neuroblastoma cells that can be directly correlated to NO release. Specifically, the effect of 1 mM

GSNO on treated cells was determined through direct comparison to the untreated PC which was defined as 100% viable ± standard deviation (±3%). Using this method, cells treated with 1 mM GSNO were found to be 79% ± 4% viable. It is important to reiterate that treated GSH samples were found to be 100% ± 5% viable, indicating that NO was the active therapeutic, not GSNO. Studies done by Kim et al. as well as Suchyta and Schoenfisch on NO-based anticancer therapeutics have shown analogous results, indicating reductions in cellular viability in up to 60% of human SK-N-MC neuroblastoma cells and up to 66% in ovarian cancer cell lines, respectively.[23,26] Although moderate, the effect observed here is particularly promising as it demonstrates the potential of NO-releasing therapeutics to serve as adjuvants to other anticancer therapeutic approaches while decreasing detrimental side effects to the patient.

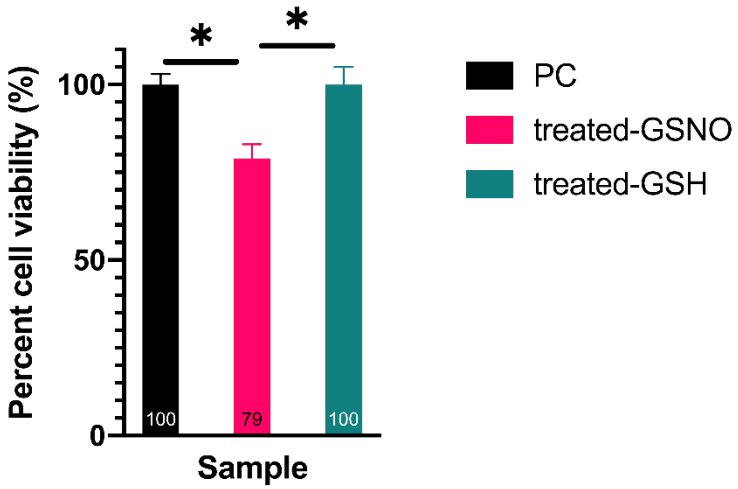


**Figure 4.2** Percent cell viability of N2a neuroblastoma cells when exposed to 1 mM GSNO for 24 h at 37 °C, 5% $CO_2$ assessed by the resazurin assay. Data points represent the mean of n ≥ 32 data points ± standard deviation. Treated-GSNO cells were determined to be statistically different than the positive control (PC) and the treated-GSH samples while the PC and treated-GSH samples were not statistically different at a 99% confidence interval (CI). Statistical significance at the 99% CI was illustrated graphically using * (1 asterisk).

*WST-8 Assay Analysis of Cellular Viability.* Another cell viability assay, the WST-8 assay, was performed to determine the impact of NO on N2a cells. The statistically different results

demonstrated again that GSNO-exposed N2a cells decreased in cellular viability, ~24%, in comparison to untreated PC and treated GSH samples. In an identical fashion as with the resazurin assay, the non-treated PC sample was defined as 100% ± 3% viable. In comparison, cells treated with 1 mM GSNO were found to be 76% ± 1% viable, and treated GSH cells were found to be 108% ± 4% viable (Figure 3). This data further corroborates the previous claims: GSNO-treated cells moderately decrease in cellular viability and the observed decrease is due to NO-release from GSNO. Again, this result was in accordance with similar NO-based anticancer therapeutic studies[23,26] and demonstrates the potential of NO-based anticancer adjuvants.

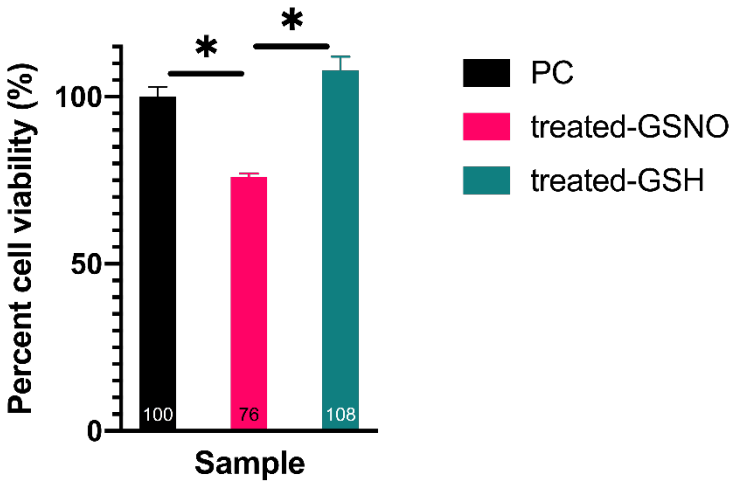


**Figure 4.3** Percent cell viability of N2a neuroblastoma cells when exposed to 1 mM GSNO for 24 h at 37 °C, 5% $CO_2$ assessed by the WST-8 assay. Data points represent the mean of n ≥ 9 data points ± standard deviation. One-way ANOVA results confirmed that treated-GSNO cells exhibited statistically different cellular viability than the PC and treated-GSH cells; the PC and treated-GSH samples were not statistically different at a 99% CI. Graphically, statistical significance at the 99% CI was illustrated using * (1 asterisk).

*MTT Assay – Analysis of Cellular Viability.* Finally, the MTT assay was used to confirm the impact of NO on cellular viability of N2a cells. These results mirrored the previous assays, highlighting a statistically significant decrease in cellular viability of GSNO-treated cells, ~23%, in comparison to untreated PC and treated GSH cells (Figure 4). Once again, the untreated PC sample was defined

as 100% ± 5% viable. Excitingly, cells treated with 1 mM GSNO were found to be 77% ± 2% viable, and treated GSH cells were found to be 98% ± 12% viable. Ultimately, the observed cellular viability of N2a cells treated with GSNO assessed using each assay was remarkably similar, providing important evidence of the antitumor potential of NO in neuroblastoma treatment. The data observed here further corroborated the utility of NO-based anticancer therapeutics that has been presented in various other studies.[23,26] Clearly, the level of reduction identified in this study does not warrant a stand-alone anticancer treatment; however, NO has the potential to be exploited for use as an adjuvant.

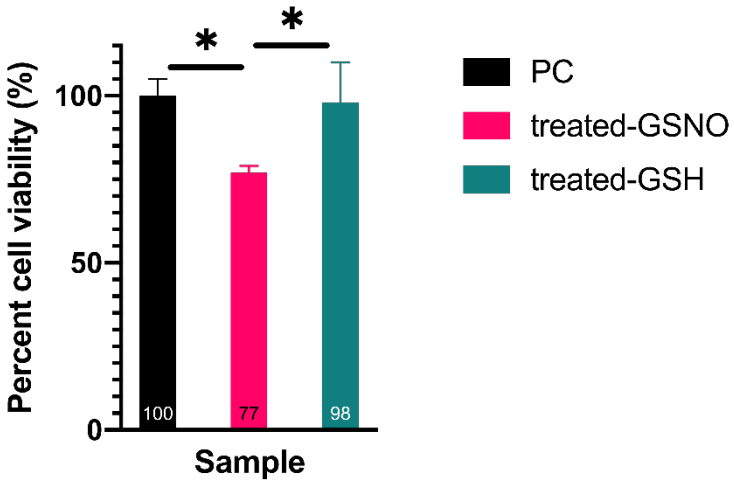


**Figure 4.4** Percent cell viability of N2a neuroblastoma cells when exposed to 1 mM GSNO for 24 h at 37 °C, 5% $CO_2$ assessed by the MTT assay. Data points represent the mean of n ≥ 7 data points ± standard deviation. One-way ANOVA revealed that treated-GSNO cells expressed a statistically different cellular viability than the PC and treated-GSH samples at a 99% CI. Conversely, PC and treated-GSH samples were not statistically different at a 99% CI. Again, statistical significance at the 99% CI was illustrated graphically using * (1 asterisk).

**4.4.2 Colony Formation Assay.** Colony formation assay results showed that untreated PC cells and GSH-treated functional control cells (n ≥ 3) retained colony formation capacity for 3 weeks following the 24 h treatment period. Explicitly, untreated PC cells formed 54 ± 6 colonies and GSH-treated cells formed 67 ± 11 (~16%). Although this number seems much higher than the PC,

they were not statistically different based on one-way ANOVA at a 99% CI. Conversely GSNO-treated sample cells ($n \geq 8$) formed 0 colonies in 3 weeks following the 24 h treatment period, which was statistically different than both the PC and the treated-GSH samples at a 99% CI. Despite some distinct variation in colony formation capacity of treated cells, it is most important to note that GSNO-treated N2a neuroblastoma cells consistently exhibited no colony formation capacity (Figure 5). [It is also important to reiterate that the colonies were defined as masses of at least 50 cells. No colonies larger than 50 cells were detected in the GSNO-treated cells.] Taken together, this information highlights the utility of NO-based anticancer therapeutics, exploiting both anti-proliferative and cytotoxic qualities.

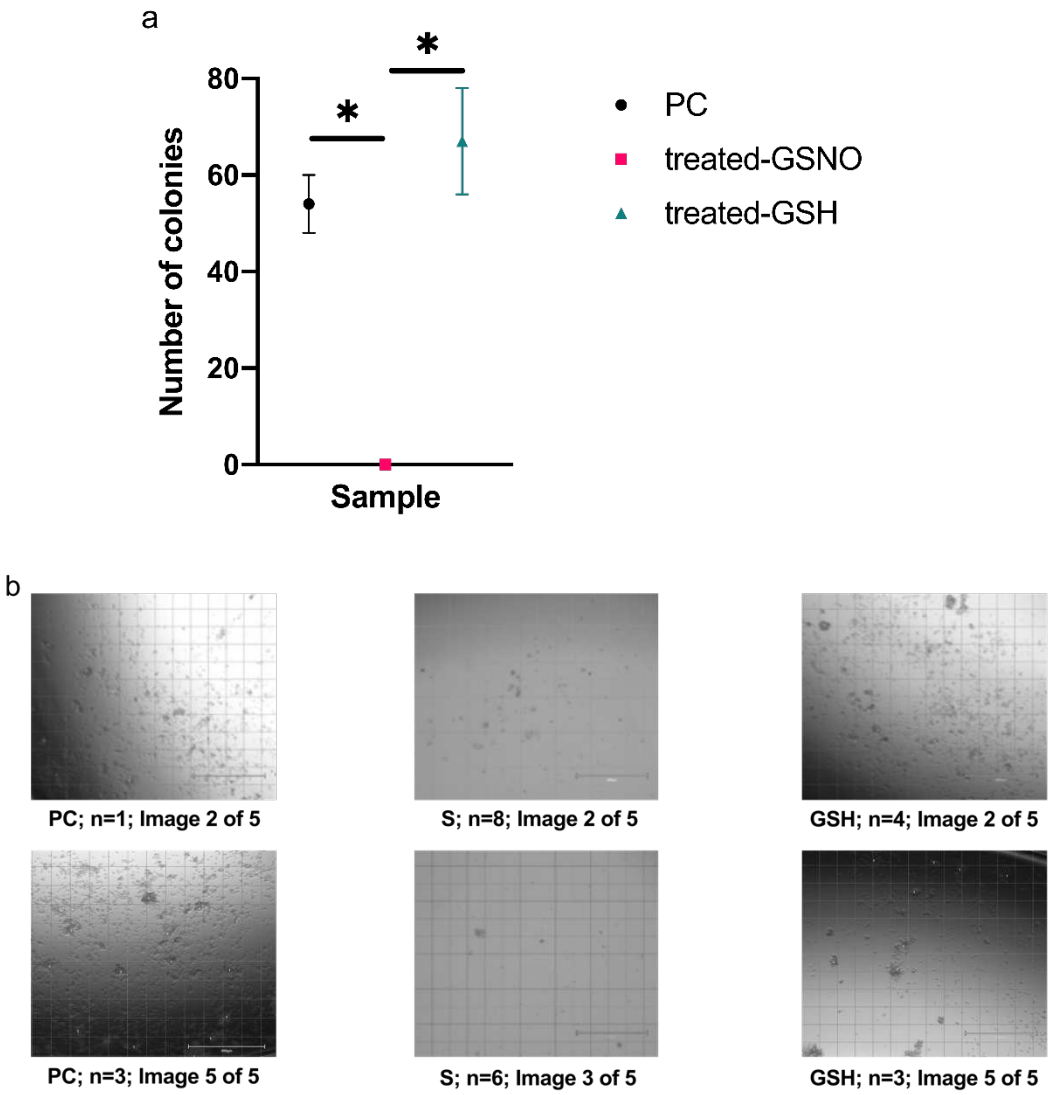


**Figure 4.5** Colony formation capacity of N2a neuroblastoma cells after exposure to 1 mM GSNO for 24 h at 37 °C, 5% $CO_2$. (**a**) Data points represent the mean of n ≥ 3 data points ± standard deviation. One-way ANOVA revealed a statistically significant difference between the treated-GSNO sample (0 colonies detected), the PC (54 ± 6), and treated-GSH (67 ± 11) samples while the PC and treated-GSH samples were not statistically different at a 99% CI. Graphically, statistical significance at the 99% CI was illustrated with * (1 asterisk). (**b**) Representative images of N2a cells after the colony formation period (3 weeks).

**4.4.3 Impact of NO on HDFa Cells—Resazurin Assay.** Human dermal fibroblast cells served as a control to assess effect of NO on healthy cells. After 24 h exposure to 1 mM GSNO, the resazurin assay revealed no observable difference in cell viability of HDFa cells in comparison to nontreated

HDFa cells (Figure 6). Cell viability of untreated PC was defined as 100% ± 5%. In comparison, cell viability of treated-GSNO was found to be 105% ± 5% and treated GSH was found to be 102% ± 4%. According to one-way ANOVA results, there was no statistical difference between any of the three samples tested at a 99% CI. These results provide valuable evidence that the impact of NO is higher on neoplastic cells than healthy cells. This phenomenon is extremely valuable as a potential means of decreasing detrimental side effects to patients, providing surplus justification of the utility of this therapeutic as an anticancer adjuvant.

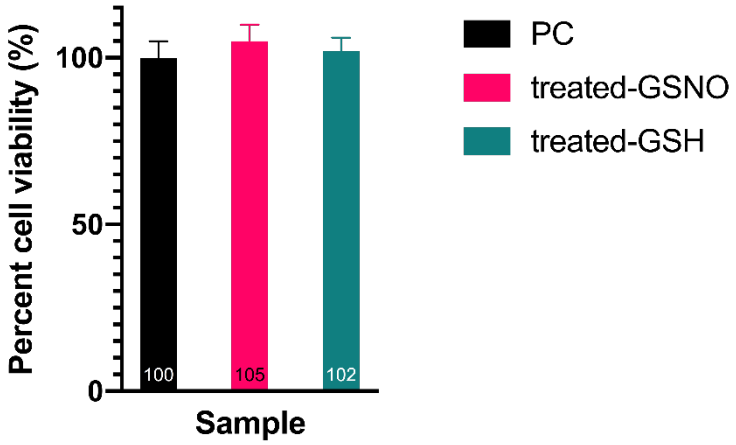


**Figure 4.6** Percent cell viability of Human Dermal Fibroblasts (HDF) cells when exposed to 1 mM GSNO for 24 h at 37 °C, 5% $CO_2$ assessed by the assessed by the CTB assay. Data points represent the mean of n ≥ 7 data points ± standard deviation. One-way ANOVA confirmed that all three sample sets did not statistically differ at a 99% CI.

### 4.4.4 NO-Release from 1 mM GSNO

*NO-Release from 1 mM GSNO in PBS.* The dosage and longevity of NO-release varies based on a variety of factors, such as donor composition, pH, presence of trace metal ions, light, and heat. These factors dictate the resultant biological consequences. In order to convey the amount of NO available to treated cells, NO-release was measured over 24 h in PBS using a Nitric Oxide Analyzer (NOA) (Figure 7). The total NO release in PBS was determined to be 0.54 ± 0.04 μmol

NO over 24 h. This concentration of NO would be expected to induce apoptosis in neuroblastoma cells [29].

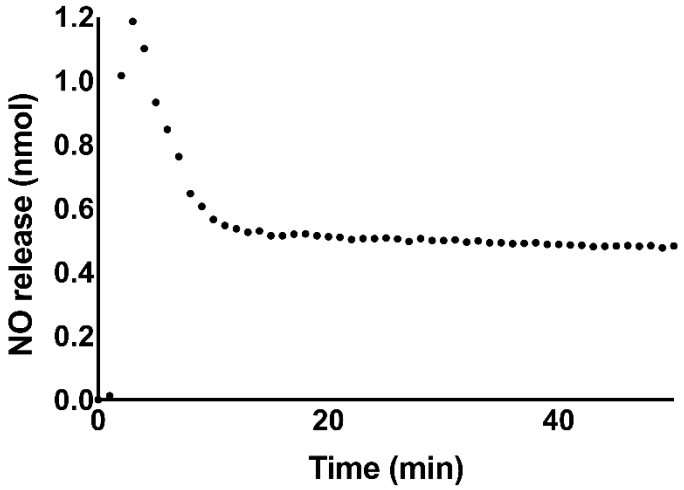


**Figure 4.7** Representative graph of NO-release from 1 mM GSNO in PBS measured using a Nitric Oxide Analyzer (NOA). The total NO-release was measured over 24 h to be 0.54 ± 0.04 μmol NO. The first 50 min of NO-release data collection is shown here to highlight the initial burst of NO release in the first 10 min. After this period, the measured NO content remained nearly stable for the remainder of the 24 h measurement window. Data points represent an average of n = 3 data points.

*Absorbance of GSNO $\lambda_{max}$ via UV/VIS.* To directly demonstrate the NO release profile in experimental media (complete DMEM) (Scheme 1), NO release was monitored via UV/Vis absorbance at 336 nm. In Table 1, it can be seen that the absorbance at the $\lambda_{max}$ of GSNO, 336 nm, decreases over 24 h. This can be attributed directly to the decrease of GSNO over the 24 h period. It can also be seen that the absorbance at 336 nm decreases more rapidly than the chemiluminescent signal from 1 mM GSNO in PBS (Figure 7). This is likely due to a greater uptake and/or scavenging of NO in complete DMEM versus PBS. The data highlights that there is a finite quantity of NO available to cells and that it is mostly depleted in the initial 24 h exposure period.

**Scheme 1.** Hypothesized representation of the spontaneous decomposition of GSNO in complete DMEM to produce a nitric oxide radical (NO) and oxidized glutathione (GSSG).

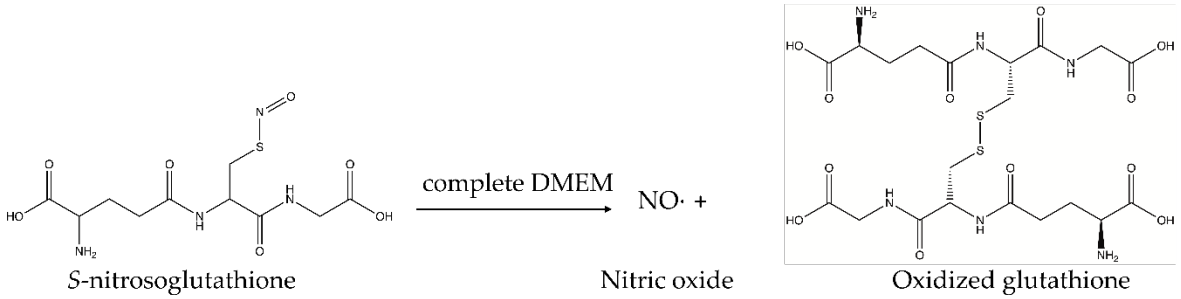


**Table 4.1** Absorbance at 336 nm (GSNO $\lambda_{max}$) of 1 mM GSNO in complete DMEM over 24 h. This data exhibits the decline of GSNO absorbance, particularly in the first 18 h of analysis. Proportionally, the concentration of GSNO and available NO decline over the 24 h period.

| Time (h) | Absorbance at 336 nm (GSNO $\lambda_{max}$) | Concentration of GSNO (mM) | Amount of Available NO (μmol) |
|---|---|---|---|
| 0 h | 0.895 | 0.971 | 0.433 |
| 6 h | 0.598 | 0.649 | 0.290 |
| 12 h | 0.304 | 0.330 | 0.147 |
| 18 h | 0.130 | 0.141 | 0.0630 |
| 24 h | 0.135 | 0.146 | 0.0650 |

## 4.5 DISCUSSION

Nitric oxide (NO) is a small signaling molecule that is endogenously produced in the mammalian body. The various roles and interactions of NO in the body are extremely diverse and frequent, due to its small size and affinity for reactions. As such, its role in anticancer therapy is not straightforward and requires thorough investigation. Some of the important factors to address include the location, concentration, and release kinetics of NO.[24] Additionally, unlike traditional biosignaling molecules which typically influence cells through specific binding events, NO impacts cells via a multitude of potential reactions. The reactions involving NO that do occur depend on the aforementioned factors as well as the intra- and extracellular composition of cells

in close proximity.[1,22-34] These reactions frequently result in the formation of reactive nitrogen species (RNS) such as peroxynitrite and nitrogen dioxide that can further influence cell health and longevity. Thus, effects of NO can be classified in two groups, direct (NO-mediated) and indirect (RNS-mediated).[35-37] Overall, each of these factors impacts the effect of NO and RNS on neoplastic and healthy cells, varying extensively across cell types and strains.

Direct effects of NO can be attributed to rapid reactions between NO and metals, metal-oxygen species, and other radical species inside the cell membrane.[35-37] One pertinent reaction to consider is that of NO with the enzyme guanylate cyclase, which leads to the formation of an Fe(II)-nitrosyl complex. Once this complex is activated, it becomes cyclic guanosine monophosphate (cGMP), a mediator of various intercellular processes (i.e., platelet function, neurotransmission).[36-37] Another important enzymatic reaction of NO results in the inhibition of cytochrome P450, which can lead to both positive (regulatory, protective) and negative (pathophysiological, repress drug metabolism) consequences.[37] Further, the reaction between NO and oxyhemoglobin is understood to play the primary role in regulation of biological movement and concentration of NO.[35,37] Finally, NO scavenging reactions with metal-oxygen species, lipids and other radical species result in tissue protective (NO + metal-oxygen complexes or lipids) and suppression of DNA synthesis and/or DNA-damage (NO + other radical species).[35-37] Indirect effects of NO can be attributed to rapid reactions between NO and its derivatives with oxygen and superoxide to create RNS.[35,37] RNS are directly and indirectly impactful to DNA by creating additional carcinogens (nitrosamines), and influencing existing carcinogens.[35-37] NO further inhibits several DNA-repair enzymes.[37] Ultimately, the biological fate and influence of NO is highly variable.

Due to the vast potential of direct and indirect NO-mediated impacts in physiological and pathological processes, it is not surprising that NO has been shown to induce tumoricidal and tumor-promoting effects.[1,22-34,38-40] Although seemingly contradictory, the evidence produced above provides rationale that these observations are logical. Specifically, current research indicates that one of the three forms of NOS, iNOS or NOS2, is most likely responsible for the tumor promoting and tumoricidal effects of NO.[24,38-41] NO generated via iNOS is involved in various cell processes, such as blood pressure regulation, inflammation, infection, and the onset and progression of malignant diseases.[39] The biological consequences range substantially depending on the occurrence and extent of iNOS expression. High levels of NO generated via iNOS generally exhibit apoptotic effects while low levels appear to be correlated to tumor progression and metastasis.[24,38-40] As such, this phenomenon can benefit researchers via manipulation of three factors according to the desired response: NO concentration, release kinetics, and location.[24] Although NO concentration can be directly manipulated, it is more challenging to control release kinetics and site-specific delivery of NO. To address these challenges various delivery platforms have been explored.[1,25-32]

In anticancer applications the use of NO-based therapeutics is especially intriguing due to the accessibility and cost. Various NO-based therapeutics have been utilized in cancer research, including nitrated fatty acids, NO-loaded nanoparticles, and NO-donors.[1,27-30,33-37,41] NO-donors including diazeniumdiolates and RSNOs have been successfully applied to influence or control NO release kinetics in anticancer research.[1,27-30,33-34,41] Diazeniumdiolates, which consist of two moles of NO per molecule (vs one mole of NO per RSNO molecule), result in higher concentrations of NO-release than RSNOs. However, byproducts of the spontaneous decomposition are highly toxic and limit therapeutic potential. Particularly, RSNOs as NO-donor

therapeutics are desirable since the mammalian body naturally produces and regulates many of these molecules.

Based on this information, cell viability and colony formation assays were used in this research to emphasize the impact of the RSNO, GSNO on N2a neuroblastoma cells. Similar to previous studies,[1,27-30,33-34] direct and indirect effects of NO were analyzed collectively (not distinguished) in this work. These experiments showed that after 24 h of exposure to GSNO, 21–24% of cells were no longer metabolically active and 100% were incapable of colony formation. The ability of high levels of NO to reduce colony formation has been previously observed.[43] Although the underlying molecular mechanisms for this effect are still being elucidated, it is known that excess NO impedes epidermal growth factor receptor/extracellular signal regulated kinase 2 (EGFR/ERK2)-dependent nuclear translocation of pyruvate kinase M2 (PKM2), thereby inhibiting glycolysis and inducing cell death.[42-43] It is also known that various NO-donor treated malignancies and macrophages have shown increased p53 expression, which led to apoptosis.[36-37] However, higher concentrations of NO have been found to decrease p53 expression, yet apoptosis can still be observed.[37] In this case, apoptosis may be influenced more by RNS-mediated DNA-damage and inhibition of DNA-repair.[37]

Despite promising reduction rates in N2a cells and unaffected viability of HDFa cells, it was clear that this concentration of NO expresses the potential of NO as a discriminatory anticancer agent against N2a neuroblastoma cells. However, this current dosage cannot act as a stand-alone treatment against N2a neuroblastoma cells. Additionally, the modest reduction achieved in vitro would likely decrease in vivo. However, this data highlights the applicability and potential of NO as an anticancer agent against neuroblastoma cells and potentially other types of cancer. Practically speaking, there is the greatest potential that NO can be used as an adjuvant to chemotherapy or

another anticancer therapeutic to increase efficacy and efficiency while decreasing detrimental effects to the patient.

Ultimately, supplementary investigation of NO as an anticancer therapeutic is warranted. Several potential avenues can be explored, including increased exposure time to 48 h and/or 72 h and increased therapeutic concentration. Additionally, the effect of NO can be assessed on various forms of neuroblastoma as well as other malignancies. The NO-based therapies can be combined with other cytotoxic or cytostatic therapeutics, such as pre-existing chemotherapeutics and/or alternative therapeutics, to assess synergistic and/or antagonistic effects. In this regard, it is also important to address the concept of NO generation in cancer cells potentially inducing chemoresistance in certain malignancies, (i.e., gliomas and pancreatic carcinomas).[38-39] In the same manner as previously mentioned, development of chemoresistance due to endogenous production of NO has been linked to iNOS expression and production. It is possible that NO indirectly influences this phenomenon as its production upregulates release of an interleukin, such as (IL-1β), that instigates chemoresistance; possible solutions include inhibition of iNOS, which leads to significant reduction of chemoresistance, as well as targeted NO delivery.[38-40] Even with this information, it is still unclear exactly how NO impacts chemoresistance, tumor-promoting, and tumoricidal effects on various cancers. Additionally, it is unclear how the tumor composition and microenvironment influence these same factors. Thus, it is essential to explore the specific impact of NO (and the concentration) on various malignancies and phenotypes.

In this study, there were only tumoricidal effects observed, no tumor-promoting effects detected, and chemoresistance and NO-mediated induction of apoptosis have not yet been explored. It is vitally important to assess these occurrences in N2a neuroblastoma as well as a range of neuroblastoma cell lines through apoptosis assays, RNA-sequence analysis, and

eventually in vivo animal studies. Indeed, these studies show that NO, delivered by GSNO, is a promising adjuvant therapeutic in the treatment of neuroblastoma.

## 4.6 CONCLUSIONS

The majority of original neuroblastoma diagnoses confirm advanced stages, the majority of neuroblastoma patients will relapse after treatment, and the majority of relapsed patients will die from this disease. Obviously, it is essential to develop new methods to prevent, diagnose, and treat this deadly disease. Herein, analysis of NO as an anticancer agent was explored on murine N2a neuroblastoma cells. Ultimately, results from three different cell viability assays, resazurin, WST-8, and MTT, confirm the anticancer activity of NO when delivered through a donor-platform, GSNO. The results consistently revealed a decrease in N2a viability of 20–25% after exposure to 1 mM GSNO for 24 h. Colony formation assays additionally confirmed the lack of colony formation capacity after therapeutic exposure. Overall, NO, delivered via innate bodily compounds such as RSNOs, provides an exciting approach to anticancer therapeutics as it has the potential to increase efficacy of traditional therapeutic approaches while decreasing detrimental effects to patients.

# CHAPTER 4 – REFERENCES


1 M. M. Reynolds, S. D. Witzeling, V. B. Damodaran, T. N. Medeiros, R. D. Knodle, M. A. Edwards, P. P. Lookian and M. A. Brown, *Biochem. Biophys. Res. Commun.*, 2013, **431**, 647–651.

2 M. M. Reynolds, S. D. Witzeling, V. B. Damodaran, D. M. Jarigese, M. A. Edwards, R. D. Knodle, P. P. Lookian and M. A. Brown, *J. Vet. Sci. Med.*

3 G. Cavalli, *Development*, 2006, **133**, 2089–2094.

4 T. Jenuwein and C. D. Allis, *Science (80-. ).*, 2001, **293**, 1074–1080.

5 T. Jenuwein, *FEBS J.*, 2006, **273**, 3121–3135.

6 D. Goyal, S. W. Limesand and R. Goyal, *J. Endocrinol.*, 2019, **242**, T105–T119.

7 M. Esposito and G. L. Sherr, *Front. Neurosci.*, 2019, **13**, 1–12.

8 M. Smith and P. L. Flodman, *Front. Mol. Biosci.*, , DOI:10.3389/fmolb.2018.00101.

9 K. Al-Hasani, P. Mathiyalagan and A. El-Osta, *J. Mol. Cell. Cardiol.*, 2019, **128**, 129–133.

10 M. Ducasse and M. A. Brown, *Mol. Cancer*, 2005, **5**, 1–10.

11 A. Ganesan, P. B. Arimondo, M. G. Rots, C. Jeronimo and M. Berdasco, *Clin. Epigenetics*, 2019, **11**, 174.

12 D. H. Colon, Nadja C.; Chung, *Adv. Pediatr.*, 2012, **23**, 1–7.

13 M. Hayat, *Neuroblastoma*, Springer, 2012.

14 J. Shohet and J. Foster, *Br. Med. J.*, 2017, **357**, j1863;1-8.

15 B. G. M. Brodeur, J. Pritchard, F. Berthold, N. L. T. Carlsen, V. Castel, R. P. Castleberry, B. De Bernardi, A. E. Evans, M. Favrot, F. Hedborg, M. Kaneko, J. Kemshead, F.

Lampert, R. E. J. Lee, A. T. Look, A. D. J. Pearson, T. Philip, B. Roald, T. Sawada, R. C. Seeger, Y. Tsuchida and P. A. Voute, *J. Clin. Oncol.*, 1993, **11**, 1466–1477.

16 C. A. Perez, K. K. Matthay, J. B. Atkinson, R. C. Seeger, H. Shimada, G. M. Haase, D. O. Stram, R. B. Gerbing and J. N. Lukens, *J. Clin. Oncol.*, 2000, **18**, 18–26.

17 J. G. Nuchtem, W. B. London, C. E. Barnewolt, A. Naranjo and P. W. McGrady, *Ann. Surg.*, 2017, **256**, 573–580.

18 D. Pe, C. Le, C. Oscarlambret and H. Dieu, *Br. J. Cancer*, 2003, **89**, 1605–1609.

19 B. H. J. Nickerson, K. K. Matthay, R. C. Seeger, G. M. Brodeur, H. Shimada, C. Perez, J. B. Atkinson, M. Selch, R. B. Gerbing, D. O. Stram and J. Lukens, *J. Clin. Oncol.*, 2000, **18**, 477–486.

20 K. K. Matthay, C. P. Reynolds, R. C. Seeger, H. Shimada, E. S. Adkins, D. Haas-Kogan, R. B. Gerbing, W. B. London and J. G. Villablanca, *J. Clin. Oncol.*, 2009, **27**, 1007–1013.

21 R. Ladenstein, U. Pötschgerulrike.poetschger@ccri.at, D. Valteau-couanet, R. Luksch, V. Castel, S. Ash, G. Laureys, P. Brock, J. M. Michon, C. Owenscormac.owens@olchc.ie, T. Trahair, G. C. F. Chan, E. Ruud, H. Schroeder, M. Beck-popovic, G. Schreier, H. Loibner, P. Ambros, K. Holmes, M. R. Castellani, M. N. Gaze, A. Garaventa, A. D. J. Pearson and H. N. Lode, *Cancers (Basel).*, 2020, **12**, 1–19.

22 K. Oh-hashi, W. Maruyama, H. Yi, T. Takahashi, M. Naoi and K. Isobe, *Biochem. Biophys. Res. Commun.*, 1999, **1999 Sep 2**, 504–509.

23 B.-C. Kim, Y.-S. Kim, J.-W. Lee, J.-H. Seo, E.-S. Ji, H. Lee, Y.-I. Park and C.-J. Kim, *Exp. Neurobiol.*, 2011, **20**, 100.

24 S. Korde Choudhari, M. Chaudhary, S. Bagde, A. R. Gadbail and V. Joshi, *World J. Surg. Oncol.*, 2013, **11**, 1.

25 E. V. Stevens, A. W. Carpenter, J. H. Shin, J. Liu, C. J. Der and M. H. Schoenfisch, *Mol. Pharm.*, 2010, **7**, 775–785.

26 D. J. Suchyta and M. H. Schoenfisch, *RSC Adv.*, 2017, **7**, 53236–53246.

27 E. Kogias, N. Osterberg, B. Baumer, N. Psarras, C. Koentges, A. Papazoglou, J. E. Saavedra, L. K. Keefer and A. Weyerbrock, *Int. J. Cancer*, 2012, **130**, 1184–1194.

28 V. J. Findlay, D. M. Townsend, J. E. Saavedra, G. S. Buzard, M. L. Citro, L. K. Keefer, X. Ji and K. D. Tew, *Mol. Pharmacol.*, 2004, **65**, 1070–1079.

29 Y. Hou, J. Wang, P. R. Andreana, G. Cantauria, S. Tarasia, L. Sharp, P. G. Braunschweiger and P. G. Wang, *Bioorganic Med. Chem. Lett.*, 1999, **9**, 2255–2258.

30 R. Dong, X. Wang, H. Wang, Z. Liu, J. Liu and J. E. Saavedra, *Biomed. Pharmacother.*, 2017, **88**, 367–373.

31 A. Nortcliffe, A. G. Ekstrom, J. R. Black, J. A. Ross, F. K. Habib, N. P. Botting and D. O'Hagan, *Bioorganic Med. Chem.*, 2014, **22**, 756–761.

32 S. Y. Lee, Y. Rim, D. D. McPherson, S. L. Huang and H. Kim, *Biomed. Mater. Eng.*, 2014, **24**, 61–67.

33 J. Fu, J. Han, T. Meng, J. Hu and J. Yin, *Chem. Commun.*, 2019, **55**, 12904–12907.

34 D. J. Suchyta and M. H. Schoenfisch, *Mol. Pharm.*, 2015, **12**, 3569–3574.

35 J. M. Fukuto, *Adv. Pharmacol.*, 1995, **34**, 1–15.

36 A. Kamm, P. Przychodzen, A. Kuban-Jankowska, D. Jacewicz, A. M. Dabrowska, S. Nussberger, M. Wozniak and M. Gorska-Ponikowska, *Nitric Oxide - Biol. Chem.*, 2019, **93**, 102–114.

37 D. A. Wink and J. B. Mitchell, *Free Radic. Biol. Med.*, 1998, **25**, 434–456.

38 D. I. Yang, J. H. Yin, T. C. Ju, L. S. Chen and C. Y. Hsu, *Free Radic. Biol. Med.*, 2004,

**36**, 1317–1328.

39 S. Müerköster, K. Wegehenkel, A. Arlt, M. Witt, B. Sipos, M. L. Kruse, T. Sebens, G. Klöppel, H. Kalthoff, U. R. Fölsch and H. Schäfer, *Cancer Res.*, 2004, **64**, 1331–1337.

40 S. Safdar, C. A. Payne, N. H. Tu and L. J. Taite, *Biotechnol. Bioeng.*, 2013, **110**, 1211–1220.

41 M. Lechner, P. Lirk and J. Rieder, *Semin. Cancer Biol.*, 2005, **15**, 277–289.

42 L. Li, L. Zhu, B. Hao, W. Gao, Q. Wang, K. Li, M. Wang, M. Huang, Z. Liu, Q. Yang, X. Li, Z. Zhong, W. Huang, G. Xiao, Y. Xu, K. Yao and Q. Liu, *Oncotarget*, 2017, **8**, 33047–33063.

43 W. Yang, Y. Zheng, Y. Xia, H. Ji, X. Chen, F. Guo, C. A. Lyssiotis, K. Aldape, L. C. Cantley and Z. Lu, *Nat. Cell Biol.*, 2012, **14**, 1295–1304.

# CHAPTER 5

# ANTICANCER POTENTIAL OF NITRIC OXIDE (NO) IN NEUROBLASTOMA TREATMENT

## 5.1 BACKGROUND

Subsequent to the studies from the previous chapter, additional efforts were allocated to further elucidate the feasibility and significance of nitric oxide (NO) in pediatric neuroblastoma treatment. In this work, neuroblastoma cell lines of various origins (murine - mouse, rat; human) were evaluated via cell viability, colony formation capacity, cytotoxicity, and RNA-sequence analysis after treatment with the NO donor, *S*-Nitrosoglutathione (GSNO). This investigation confirmed the applicability of NO-based anticancer therapeutics across various phenotypes and origins, emphasizing their conceivable application in the clinical management of neuroblastomas. Individuals from Colorado State University (CSU) and the University of Texas at Austin (UT Austin) were involved in the development of these studies and this manuscript. Jenna L Gordon (CSU) and Kristin J Hinsen (CSU) both performed the entirety of the cell-based analyses. Tyler A Smith (UT Austin) and Haley O Tucker (UT Austin) performed the gene ontology analysis of the RNA-sequence data that was acquired and prepared by Marylee Layton at CSU MIP NGS Illumina Core facility. Jenna L Gordon prepared the draft of this manuscript with some contribution from Kristin J Hinsen. Melissa M Reynolds and Mark A Brown acted as advisors and contributed to draft revision. The study was originally published in RSC Advances in 2021 and has been modified with permission. Copyright 2021.[3]

[3] Gordon, J.L.; Hinsen, K.J.; Smith, T.A.; Tucker, H.O.; Reynolds, M.M.; Brown, M.A. Anticancer Potential of Nitric Oxide (NO) in Neuroblastoma Treatment. *RSC Advances* 2021, 11, 9112-9120. doi: 10.1039/D1RA00275A

## 5.2 INTRODUCTION

Pediatric neuroblastoma is characterized by a majority (>60%) of initial diagnoses resulting in high risk categorization and/or recurrence [1,2]. Although low to intermediate risk diagnoses have favorable five-year survival rates, >80% [3–6], high risk diagnoses reveal particularly poor prognosis, only ~40% five-year survival rates [7,8]. Largely, treatment options for high risk neuroblastoma include any variation of successive treatments including surgery, chemotherapy, radiation therapy, immunotherapy and bone marrow transplants[7,8]. Despite the host of potential therapeutic possibilities, high risk and recurrent neuroblastoma continue to perplex doctors and anticancer researchers.

As a result, recent work has focused on the development of various treatment options to combat the aggressive nature of high risk and recurrent neuroblastoma, such as enzyme and angiogenesis inhibition, targeted therapies, cytotoxic agents, and more[1]. Furthermore, current research shows that bursts of elevated concentrations of nitric oxide (NO) effectively induce tumour-specific cytotoxicity in a range of malignancies, including ovarian, breast, prostate, and more[9–15]. However, minimal focus has been placed on the use of NO as a treatment option for neuroblastoma[16,17]. One major challenge in the use of NO as an anticancer therapeutic is the ability to control release kinetics and site-specific delivery. As such, various platforms for NO delivery have been explored, such as liposomes, diazeniumdiolates and *S*-Nitrosothiols (RSNOs)[11–13,18,19]. Two major advantages to RSNOs are their natural occurrence as NO-donors in the human body and the ability to allow prolonged NO release[18–20]. Yet the actual rate of NO release is dependent on the presence of light, metals, heat, and pH. In general, lower pH accelerates the rate of NO release from *S*-Nitrosothiols [21–23]. Theoretically, the decreased pH in tumour

microenvironments will increase the rate of NO release[24], leading to higher concentration of NO near neoplastic cells than healthy cells. NO-delivery via *S*-nitrosothiols presents an impactful adjuvant to current neuroblastoma therapies.

Another perplexing aspect of the use of NO in anticancer treatment is the dual function of NO on malignancies[25–30]. Explicitly, NO has been shown to induce both tumour-promoting, anti-apoptotic effects as well as tumoricidal, apoptotic effects[25–30]. Even though these effects seem to be contradictory, current research indicates that two primary factors influence these results, including concentration and exposure time[27–29]. Generally, high levels of NO (micromolar concentrations) induce DNA-damage and therefore apoptotic effects while low levels of NO are linked to tumour progression and metastasis[28,29]. Exposure time is not as straight forward, as increased exposure time can lead to increased cell death or tumour progression based on the NO concentration[27]. Additional factors that impact the effect of NO on cancer include tumour type, location, microenvironment (including pH and composition), and heterogeneity[25,28].

In a previous foundational study, we showed that micromolar concentrations of NO, delivered from 1 mM GSNO over 24 h, was a moderately effective, discriminatory therapeutic against murine N2a neuroblastoma cells[31]. These studies revealed a consistent decrease in cell viability of N2a cells, ~20-25%, assessed via multiple cellular viability assays as well as a complete cessation of colony formation capacity after therapeutic treatment. Healthy Human Dermal Fibroblast, adult (HDFa) cells were also exposed to 1 mM GNSO for 24 h and showed no decrease in cellular viability or colony formation capacity. Based on these initial results, complementary investigation of NO, delivered by GSNO, as an adjuvant anticancer agent against neuroblastoma was decidedly necessary.

Herein, anticancer applications of NO on murine (rat) and human neuroblastoma cell lines were expanded using *S*-Nitrosoglutathione (GSNO) as a NO-donor. Prominently, various clinically relevant neuroblastoma cell lines, IMR-32 (human), SK-N-SH (human), and B104 (murine, rat), were exposed to 1 mM GSNO for 24 h and analyzed via cellular viability, colony formation, cytotoxicity, and RNA-sequence analysis assays. The goal of this study was to feature NO as a selective agent in the impairment of neuroblastoma cellular viability, colony formation capacity, and initiate the investigation of its role in provocation of cell death and NO-mediated genetic alterations.

## 5.3 EXPERIMENTAL

**5.3.1 Materials.** Hydrochloric acid (HCl) and EPA vials were obtained from Thermo Fisher Scientific (Waltham, MA, USA). Sodium nitrite (99.999% $NaNO_2$) was purchased from Alfa Aesar (Ward Hill, MA, USA). Acetone (≥99.5%) was purchased from Sigma Aldrich (St. Louis, MO, USA). Dulbecco's Modified Eagle's Medium (DMEM), Eagle's Minimum Essential Medium (EMEM), and Penicillin-Streptomycin Solution were purchased from Fisher Scientific (Hampton, NH, USA). EquaFETAL 100% Origin Bovine Serum was purchased from Atlas Biologicals (Fort Collins, CO, USA). Trypsin/EDTA solution was purchased from American Type Culture Collection (Manassas, VA, USA). Reduced glutathione (GSH; High purity), CellTiter-Blue Cell Viability Assay (Resazurin), and 3-(4,5-Dimethylthiazol-2-yl)-2,5-diphyltetrazolium bromide (MTT) were obtained from VWR International (Radnor, PA, USA). Dimethyl sulfoxide (DMSO) was purchased from Sigma-Aldrich. Calcein AM and propidium iodide were purchased from Invitrogen (Eugene, Oregon, USA). The neuroblastoma cell lines used include B104, IMR-32, and SK-N-SH.

**5.3.2 Synthesis of *S*-Nitrosoglutathione (GSNO).** *S*-Nitrosoglutathione (GSNO) was synthesized through a previously developed synthesis. Succinctly, GSNO synthesis involved the addition of sodium nitrite to a solution of reduced glutathione (GSH) in Millipore water and 2 M hydrochloric acid. The GSNO mixture was constantly stirred in an ice bath for 40 min. The solution was then treated with acetone and allowed to continue reacting with constant stirring in an ice bath for 10 min (mixture turned red in colour). The red solution was filtered for 10 min with gravity filtration and then vacuum filtration for 3.5 h to isolate the GSNO precipitate. The final GSNO precipitate was washed successively with ice-water and acetone. The red filtrate solution was discarded as waste and the remaining solid pink powder (GSNO) was kept and analysed by UV-Vis spectrophotometry at 335 nm to confirm >95% purity.

**5.3.3 Cell Culture.** 10% total volume foetal bovine serum and 1% total volume penicillin-streptomycin were added to DMEM/EMEM media to produce complete cell media (complete DMEM/EMEM). 1 mL ($10^6$ cells) were thawed for 1-2 min in a 37$^o$C water bath to prepare the stock culture. The thawed cells were then added to a 15 mL centrifuge tube containing 9 mL of complete media that had been warmed to 37$^o$C. Once centrifuged for 5 minutes at 4$^o$C, 2 000 RPM, the supernatant was removed and discarded while the pellet was resuspended in 5 mL complete media. This was added to a T-25 $cm^2$ flask containing 5 mL of complete media. The cell culture was incubated at 37$^o$C, 5% $CO_2$ for at least 48 h before fresh complete media was appropriately provided every 24-72 h. The cell culture was counted and split based on both macroscopic observation and cell counting via a hemocytometer.

**5.3.4 Cell Viability Assays.** Cells were plated in 96-well plates in 100 µL increments that contained between 100,000-200,000 cells per milliliter (mL). After 24 hours, the media was aspirated and discarded. The positive control samples (PC; ≥ 7 samples) received 100 µL of

complete media, the functional control samples (GSH; ≥ 7 samples) received 100 µL of 1mM GSH, and the other samples received 100 µL of 1mM GSNO (Sample; ≥ 7 samples). After another 24 h of incubation, the media was aspirated and replaced with 100 µl of fresh complete media in each well. The appropriate cell viability assay was then performed.

In the resazurin assay, cells were plated at 200,000 cells per mL in a 96-well plate. Following the procedure above, 20 µL of pre-warmed resazurin stock solution was added to each well. The plate was incubated at 37ºC, 5% $CO_2$ for 3 h before the absorbance was measured at 570 nm and 600 nm via a microplate reader.

In the MTT assay, cells were plated at 100,000 cells per mL in a 96-well plate. Following the procedure above, 10 µL of pre-warmed 12mM MTT stock solution was added to each well before the plate was placed back in the 37ºC, 5% CO2 incubator. After about 3 h of incubation, 50 µL DMSO was added to each well. The plate was again incubated for an additional 10 min before the absorbance was measured at 540 nm via a microplate reader.

A BioTek Synergy 2 Multi-Detection Microplate reader was used to detect absorbance measurements. The absorbance of each measured sample was compared to the calculated average and standard deviation of the PC cells. To determine the statistical difference of the data, ANOVA was performed.

**5.3.5 Colony Formation Assays.** Cells were plated in a 24-well plate in 1 mL increments of 100,000 cells per mL and then placed in a 37ºC, 5% CO2 incubator. After 24 h of incubation, the media was aspirated and discarded. The positive control (PC; ≥ 4 samples) received 1 mL of fresh complete media, the functional control (GSH; ≥ 4 samples) received 1 mL of 1mM GSH, and the remaining samples received 1 mL of 1 mM GSNO (Sample; ≥ 4 samples). After an additional 24 h of incubation, the media from each well was transferred to centrifuge tubes where the cells were

collected via addition of trypsin and centrifugation. The cells were then re-plated in a new 24-well plate in 1 mL increments at 500 cells per mL and placed back into the incubator. The plates were checked every 24-72 h for three weeks using bright field microscopy to assess the formation of colonies – defined as masses of 50 or more cells.

**5.3.6 LIVE/DEAD Assays.** Cells were plated in a 96-well plate in 100 µL increments of 100,000 cells per mL and placed in a 37ºC, 5% CO2 incubator. After 24 h of incubation, the media was aspirated and discarded. The positive control (PC; ≥ 4 samples) received 100 µL of fresh complete media, the functional control (GSH; ≥ 4 samples) received 100 µL of 1 mM GSH, and the remaining samples received 100 µL of 1 mM GSNO (Sample; ≥ 4 samples). The plate was incubated for 24 h before the media was aspirated and discarded. 100 µL of 3 µM Calcein AM stock solution was added to each well before incubating for 30 min. The Calcein AM stock solution was aspirated and replaced with 100 µL of 5 µM PI stock solution and the plate was incubated for an additional 10 min. Fluorescence microscopy was used to capture images for qualitative comparison of the relative number of live versus dead cells in each sample.

**5.3.7 RNA-Sequence Assay.** Cells were plated in 125 $cm^2$ flasks in 25 mL increments of 100,000 cells per mL and placed in a 37ºC, 5% CO2 incubator. After 24 h of incubation, the media was aspirated and discarded. The positive control (PC; ≥ 4 samples) received 25 mL of fresh complete media, the functional control (GSH; ≥ 4 samples) received 25 mL of 1 mM GSH, and the remaining samples received 25 mL of 1 mM GSNO (Sample; ≥ 4 samples). All 12 flasks were incubated for 24 h before the media was aspirated and discarded. Cells were harvested from each flask in 15 mL centrifuge tubes, suspended in frozen 1 mL TriZol reagent, and frozen. The 12 frozen sample tubes were delivered to CSU MIP NGS Illumina Core facility (Microbiology, Pathology and Immunology Next Generation Sequence Facility) for RNA-sequence preparation and analysis.

Libraries were prepared using NEBNext Ultra II Directional RNA kit using half reactions. Sequence analysis was performed on the NextSeq 500 using a High Output 75 cycle kit. Low-quality reads and PCR duplicates were filtered, resulting in ~20 million reads/sample. Hisat2 Indexes were made using the Rattus norvegicus genome downloaded from http://uswest.ensembl.org/Rattus_norvegicus/Info/Index. Background noise was decreased using log fold shrinkage while preserving large differences.[32] Further gene ontology analysis of biological processes was completed on the top 20 up- and downregulated transcripts via Enrichr (https://maayanlab.cloud/Enrichr/).

**5.3.8 Data Analysis and Statistics.**

All statistical analysis was performed using one-way ANOVA with $p<0.01$ to define statistically significant differences. Data points are represented by the mean ± standard deviation (SD).

## 5.4 RESULTS AND DISCUSSION

Based on a previous study, 1 mM GSNO was applied in this work as a NO-donor and 1 mM GSH was used as a functional control[31] (Figure 1 a & b). The results from the aforementioned study as well as analyses performed by other researchers, such as Kim et al. and Suchyta and Schoenfisch[11], informed the hypothesis that the micromolar concentrations of NO (0h – 0.433 μmol to 24h – 0.0650 μmol)[31], delivered by 1 mM GSNO over 24h, would proportionally decrease cellular viability and colony formation capacity while increasing cell death and genetic alterations in the neuroblastoma lines of interest, IMR-32, SK-N-SH, and B104. Excitingly, the results supported this hypothesis with remarkably distinct impacts on the reduction of colony formation capacity across all neuroblastomas analyzed. Further, the results exhibited consistent, moderate reduction of cellular viability and obvious increase in cell death. These results provided impactful

evidence of the potential of NO to act as an adjuvant anticancer therapeutic, increasing therapeutic impact while simultaneously decreasing harmful patient side effects. Markedly, valuable information about the process and occurrence of NO-mediated genetic alterations was acquired via RNA-sequence analysis, leading to a more in-depth understanding of the anticancer role of NO in neuroblastoma. Specifically, all 40 of the most differentially expressed genes are protein coding genes, involved in various molecular processes. After examining the top 20 upregulated transcripts in the GSNO group, it emerged that in neurons, NO is likely to cause ATP depletion, thereby inducing death via apoptosis[33]. Additionally, several of these transcripts were discovered to be involved with oxidative stress and growth inhibition[34–41]. Conclusively, the top 20 downregulated transcripts revealed that cell cycle arrest was a prominent effect of NO on these cells.

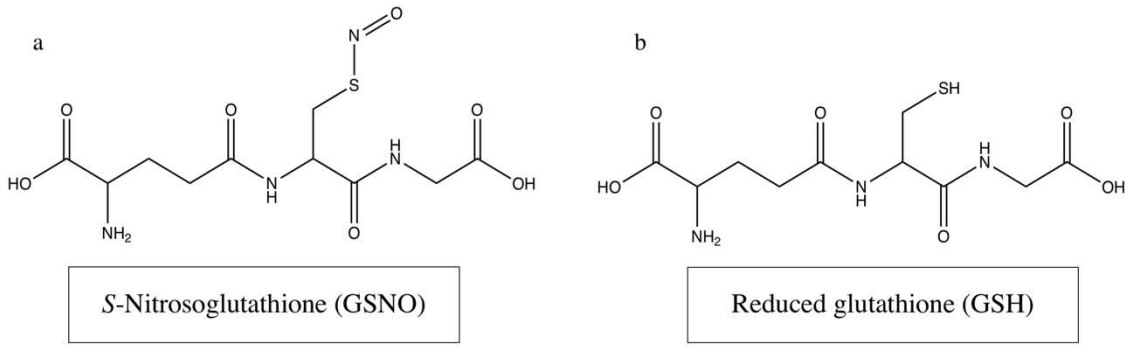


**Figure 5.1** Structures of *S*-Nitrosoglutathione (a) and reduced glutathione (b).

**5.4.1 Cell Viability Assays.** Initial assessment of the anticancer impact of NO on neuroblastomas of murine (rat) and human origin included the cellular viability assays resazurin and MTT. These assays were used synonymously to assess the ability of NO to decrease metabolic activity *in vitro* on three neuroblastoma cell lines, B104, SK-N-SH, and IMR-32. Notably, both of these assays consistently showed a statistically significant reduction of cellular viability, ~13-29% in all three cell lines compared to control (untreated) cells and GSH-treated cells (Figure 2 a & b). Treated IMR-32 cells exhibited 80±8% and 75±3% viability, treated SK-N-SH cells revealed 87±9% and 79±2% viability, treated B104 cells displayed 83±7% and 71±4% viability via resazurin and MTT assays respectively. Control and GSH-treated cells were not statistically different in any case. Also, it is important to note the influential data collected in our previous study highlighting healthy HDFa cells were not impacted by identical NO treatment[31].

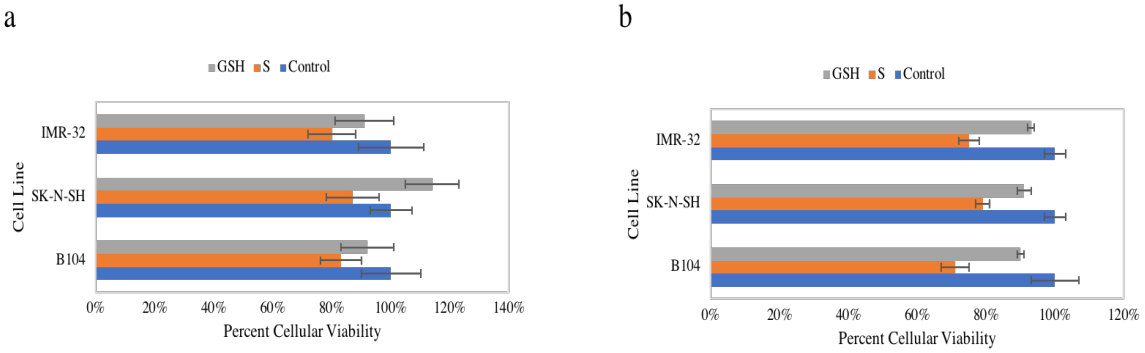


**Figure 5.2** Percent cellular viability of IMR-32, SK-N-SH, and B104 neuroblastoma cells when untreated (blue), exposed to 1 mM GNSO for 24 h (orange), and 1 mM GSH for 24 h (grey), analyzed with the resazurin assay (a) and the MTT assay (b).

**5.4.2 Colony Formation.** Consistent observation of a reduction in cellular viability across the neuroblastomas studied led to an interest in the impact of NO on colony formation. Again, all three cell lines were exposed to 1 mM GSNO and GSH, which were both compared to an untreated control. Strikingly, treatment with NO yielded **drastic**, statistically significant reduction of colony formation capacity across all cell lines (Figure 3). Again, our previous study remarkably showed no impact on clonogenic activity of identically treated healthy HDFa cells[31]. This result is extraordinarily important, indicating a discriminatory effect of NO on neoplastic versus healthy cells.

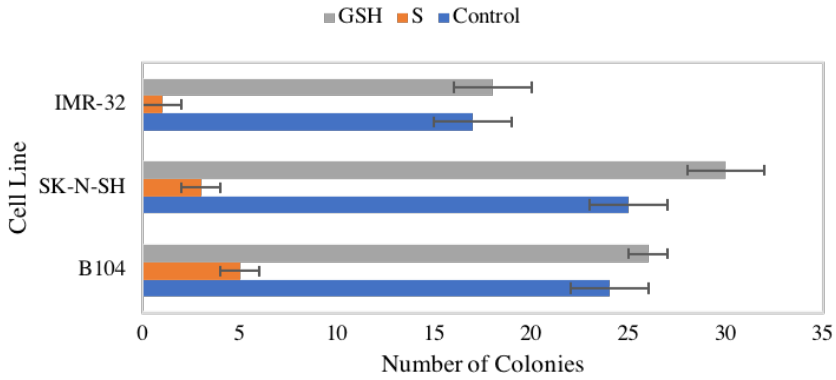


**Figure 5.3** Clonogenic activity of IMR-32, SK-N-SH, and B104 neuroblastoma cells when untreated (blue), exposed to 1 mM GNSO for 24 h (orange), and 1 mM GSH for 24 h (grey), counted via brightfield microscopy.

**5.4.3 LIVE/DEAD Cytotoxicity Assays.** Next, cytotoxicity analysis of NO-treated neuroblastomas was completed to qualitatively investigate the relative quantity of live and dead cells in untreated and treated (1 mM GSNO and GSH for 24 h) cells. Using PI/calcein AM staining and fluorescence microscopy, images of treated (GNSO and GSH) and untreated cells were captured. As shown in Figure 4, it is blatantly clear that the number of live (green) cells is much higher in untreated samples than dead (red) cells. The opposite is true for the treated samples, which show a lower number of cells overall as well as a higher relative number of dead (red) cells

than in their untreated counterparts. [The images of GSH-treated cells have not been included in this image to highlight the differences between the images of untreated and NO-treated cells.] It is important to address the obvious differences between cell lines. Since it was expected that NO would have different impacts on each cell line, it was important to analyze multiple neuroblastoma lines of various species. Explicitly, the B104 cells show an obvious presence of live and dead cells after treatment. This result clearly reflects the results seen via cell viability and clonogenic assays. However, treated SK-N-SH cells appear to show very few (almost indistinguishable) dead cells with a fair number of live cells still present. There are a couple of hypotheses to explain this: NO impacts the metabolic activity and colony formation capacity of SK-N-SH cells much more than the death of these cells (via necrosis or apoptosis) and the size of the conglomerations of live SK-N-SH cells is much larger than the size of the individual dead cells, making it difficult to capture both in the overlay (some of the live cells are overlapping the dead cells – can be seen when zoomed in). Finally, treated IMR-32 cells appear to show a much larger number of dead cells than live cells (while the cell viability is similar to that of the other two cell lines). Opposite to SK-N-SH cells, it is possible that NO causes more cell death (via apoptosis or necrosis) to IMR-32 cells than the other neuroblastoma cell lines investigated. In this case, the apparent lack of live cells can also be explained by size, as the size of the live IMR-32 cells is smaller than the size of the conglomerations of dead cells, making it difficult to capture the cells on the overlay (these cannot be seen as well due to the red color concealing the green color).

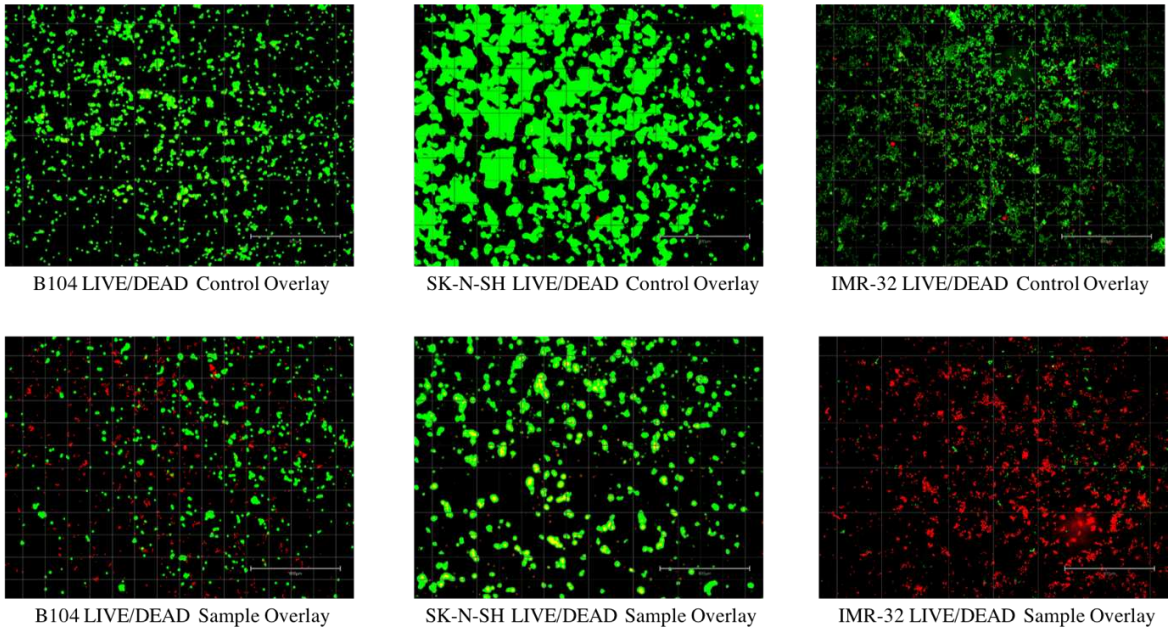


**Figure 5.4** LIVE/DEAD cytotoxicity fluorescence images for all three cell lines, untreated (control) and treated (1 mM GSNO for 24 h). These images serve as qualitative data to highlight the majority presence of live (green) cells in the control (untreated) samples versus the lack of overall cell count as well as presence of dead (red) cells in the treated samples. The white scale bar in each image represents 800 μM.

**5.4.4 RNA-Sequence Analysis Assay.** Ultimately, RNA-Sequence analysis was performed on a single cell line, B104 to determine the differentially expressed genes after exposure to 1 mM GSNO for 24 h. All sample reads (~20 million reads/sample) confirmed the genome to be Rattus norvegicus as expected (~94%). After the initial analysis, successful log fold change (LFC) shrinkage was performed to decrease background noise while preserving large differences (Figure 5 a & b). LFC shrinkage data was used for further analyses. In the comparison of GSH versus control samples, 18% of genes were up-regulated ($0 < LFC < 2$) and 18% were down-regulated ($0 > LFC > -2$) out of 23,078 genes with a nonzero total read count with a p-value<0.1 (Figure 5a). In the comparison of GSNO versus control samples, 26% of genes were up-regulated ($0 < LFC < 2$) and 24% were down-regulated ($0 > LFC > -2$) out of 23,078 genes with a nonzero total read count with a p-value of $< 0.1$ (Figure 5b). This analysis powerfully evidenced that there were

significantly more genes differentially expressed in the GSNO-treated samples compared to the GSH-treated samples. A heatmap showing the 30 most differentially expressed genes was generated to narrow down the results of this experiment and allow for interpretation (Figure 6). Gene ontology (GO) analysis of biological processes was done only on the GSNO-treated samples due to a lack of transcripts available as input to generate reliable gene ontology annotations for the GSH-treated samples. The top 5 gene ontology biological processes for both up- and downregulated transcripts were specified in Figure 7 and explored further to interpret the mechanism of NO-induced impact on B104 neuroblastoma. Imposingly, the biological processes implicated in the upregulated transcripts highlighted previously reported knowledge that NO regulates voltage-gated K+ channels as well as ATP-sensitive K+ channels in sensory neurons in a concentration-dependent manner. In ATP-sensitive K+ channels, NO has the opposite effect in which NO stimulates the channel. NO inhibits cellular respiration in astrocytes and contributes to resistance to NO-mediated cytotoxicity. However, neurons do not appear to utilize the same mechanism and are more likely to succumb to ATP depletion and die via apoptosis[33]. Additionally, investigation of the top 20 upregulated transcripts in the GSNO-treated samples, several interesting transcripts were linked to oxidative stress, apoptosis, and growth inhibition including Fas cell surface death receptor (FAS), oxidative stress induced growth inhibitor 1 (OSGIN1 aka OKL38), heme oxygenase 1 (HMOX1), DNA damage inducible transcript 3 (DDIT3 aka CHOP/GADD153), Ectodysplasin A2 receptor (EDA2R), tribbles pseudokinase 3 (TRIB3), tumour protein 53-induced nuclear protein 1 (TP53INP1), phorbol-12-myristrate-13-acetate-induced protein 1 (PMAIP1 aka NOXA) [34–41]. Specifically, NO and FAS are linked to DNA damage and p53 activation which induces adult motor neuron apoptosis[34]; OSGIN1 was recognized as a cell growth inhibitor in response to oxidative stress as well as a chemotherapeutic

sensor, in which it was upregulated in response to DNA damage and p53 activation and thereby induced apoptosis[35]; neurons that overexpress HMOX1 resist oxidation-induced stress and apoptosis[36]; DDIT3 induces cell cycle arrest and endoplasmic reticulum (ER)-mediated apoptosis in response to ER-related stress[37]; EDAR2 stimulates apoptosis via trans-activation by p53[38]; during ER-stress TRIB3 is involved in CHOP-dependent cell death by downregulating its own activation through repression of CHOP/ATF4 functions[39]; TP53INP1 is a p53-target gene that is expressed in response to stress and is interrelated with anti-proliferative and pro-apoptotic characteristics[40]; PMAIP1 upregulation is linked to downregulation of Usp9x (a deubiquitinase) and reduction of Mcl-1 expression, which fosters ubiquitination and degradation and leads to apoptosis of neoplastic cells[41]. Finally, the biological processes indicated in the downregulated transcripts suggested that cell cycle arrest is a prominent effect of NO on these cells.

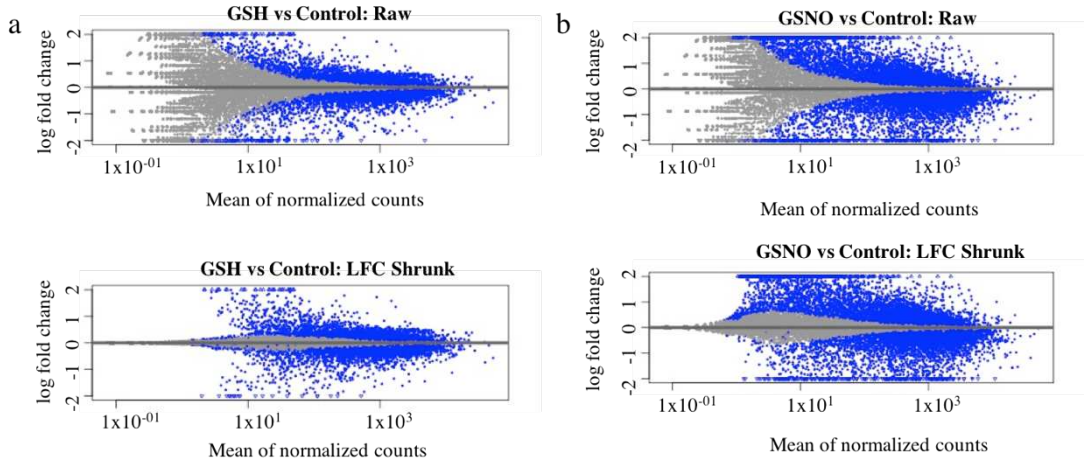


**Figure 5.5** Differentially expressed genes in GSH (a) and GSNO (b)-treated samples versus control. 18% of genes were up-regulated (0 < LFC < 2) and 18% of genes were down-regulated (0 > LFC > -2) out of 23,078 total genes with a non-zero read count, p<0.1. Log fold change (LFC) shrinkage (LFC Shrunk) was performed to minimize noise while preserving large differences.

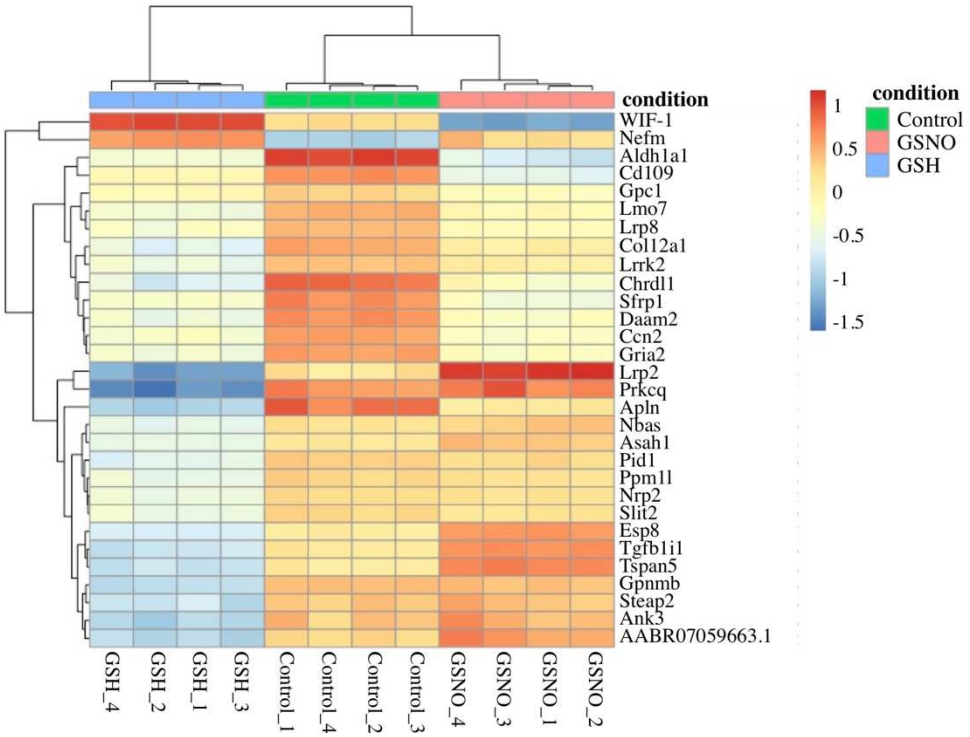


**Figure 5.6** Heat map expressing 30 most differentially expressed genes. This map displays the names of the differentially expressed genes as well as the extent to which each gene was differentially expressed in all samples.

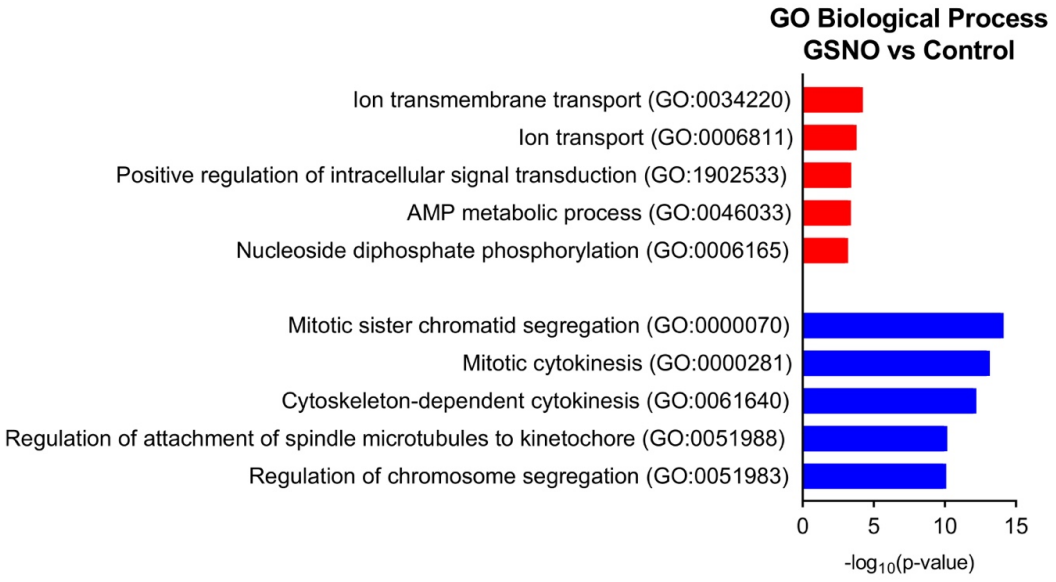


**Figure 5.7** Top 5 gene ontology biological processes for up- (red) and downregulated (blue) transcripts in GSNO-treated samples versus control.

## 5.5 CONCLUSIONS

Nitric oxide-based therapeutics offer exciting potential in anticancer applications due to accessibility, low-cost, and potential for tunability. Particularly, *S*-Nitrosothiols (RSNOs) provide desirable characteristics for anticancer treatment, including endogenous production of many of these molecules and the prospective to influence timing and longevity of NO-release. Herein, analysis of NO, delivered by GSNO, as an anticancer agent was explored on human, murine, and rat neuroblastoma cell lines (IMR-32, SK-N-SH, and B104) via cell viability, colony formation, cytotoxicity, and RNA-sequence analysis assays. Impactful results from two different cell viability assays, resazurin and MTT, consistently portrayed a 13-29% decrease in viability of all three cell lines after 24h of exposure to 1 mM GSNO. Remarkably, colony formation assays displayed a tremendously significant decrease in the ability of all three cell lines to form colonies after 24h of exposure to an identical concentration of GSNO. Further, qualitative cytotoxicity assays performed on each cell line reinforced these findings, exhibiting a blatant decrease in the number of live cells

as well as an increase in the number of dead cells after treatment with 1 mM GSNO. Finally, RNA-sequence analysis on B104 cells showcased a statistically significant increase in the number of up-regulated and down-regulated differentially expressed genes in the GSNO-treated samples as compared to the GSH-treated and control samples. Strikingly, the identity and biological processes of these genes provided valuable insight into the mechanism of action of NO on neuroblastoma cells, indicating its involvement in oxidative stress, apoptosis, growth inhibition, regulation of cell cycle progression, and mitosis. Inclusively, this data presents a convincing rationalization for use of NO, delivered via RSNOs, as anticancer adjuvants in treatment of neuroblastoma and incites further exploration of its conceivable application in other malignancies. Specifically, it would be highly informative to perform apoptosis and cell cycle analysis assays on these cell lines as well as RNA-sequence analysis assays on both SK-N-SH and IMR-32 cells to further elaborate on these results and their clinical translatability.

**Table 5.1** Table of the top 20 upregulated transcripts in GSNO-treated samples, ranked by *p*-value (padj).

| Ensembl ID | Log2FoldChange | padj | Name | Description |
|---|---|---|---|---|
| ENSRNOG00000014117 | 2.642690485 | 0 | Hmox1 | heme oxygenase 1 [Source:RGD Symbol;Acc:2806] |
| ENSRNOG00000018126 | 2.100712674 | 0 | Abca1 | ATP binding cassette subfamily A member 1 [Source:RGD Symbol;Acc:631344] |
| ENSRNOG00000006789 | 2.108566582 | $3.22^{-262}$ | Ddit3 | DNA-damage inducible transcript 3 [Source:RGD Symbol;Acc:62391] |
| ENSRNOG00000013484 | 2.934381196 | $6.59^{-212}$ | Gsta1 | glutathione S-transferase alpha 1 [Source:RGD Symbol;Acc:2753] |
| ENSRNOG00000037621 | 2.566554367 | $4.57^{-165}$ | Spata48 | spermatogenesis associated 48 [Source:RGD Symbol;Acc:1309870] |
| ENSRNOG00000054561 | 2.721372192 | $4.95^{-149}$ | Isg20 | interferon stimulated exonuclease gene 20 [Source:RGD Symbol;Acc:1306407] |
| ENSRNOG00000013018 | 2.455220167 | $5.22^{-139}$ | Eda2r | ectodysplasin A2 receptor [Source:RGD Symbol;Acc:1564025] |
| ENSRNOG00000047697 | 3.675674714 | $2.52^{-123}$ | Ggt1 | gamma-glutamyltransferase 1 [Source:RGD Symbol;Acc:2683] |
| ENSRNOG00000007964 | 2.145360583 | $3.79^{-107}$ | Tp53inp1 | tumour protein p53 inducible nuclear protein 1 [Source:RGD Symbol;Acc:631423] |
| ENSRNOG00000011316 | 3.689711899 | $3.87^{-106}$ | Fam167a | family with sequence similarity 167, member A [Source:RGD Symbol;Acc:1561302] |
| ENSRNOG00000007319 | 2.106674517 | $1.87^{-103}$ | Trib3 | tribbles pseudokinase 3 [Source:RGD Symbol;Acc:708432] |
| ENSRNOG00000027016 | 2.39177707 | $2.13^{-99}$ | Cobll1 | cordon-bleu WH2 repeat protein-like 1 [Source:RGD Symbol;Acc:1308954] |
| ENSRNOG00000018770 | 2.231130335 | $5.18^{-99}$ | Pmaip1 | phorbol-12-myristate-13-acetate-induced protein 1 [Source:RGD Symbol;Acc:1359266] |
| ENSRNOG00000014948 | 3.876937844 | $2.13^{-94}$ | Osgin1 | oxidative stress induced growth inhibitor 1 [Source:RGD Symbol;Acc:620679] |
| ENSRNOG00000003189 | 3.281285701 | $3.35^{-89}$ | Cited1 | Cbp/p300-interacting transactivator with Glu/Asp-rich carboxy-terminal domain 1 [Source:RGD Symbol;Acc:620781] |
| ENSRNOG00000019142 | 2.052936986 | $3.16^{-86}$ | Fas | Fas cell surface death receptor [Source:RGD Symbol;Acc:619831] |
| ENSRNOG00000012892 | 2.807251669 | $4.52^{-85}$ | Abca4 | ATP binding cassette subfamily A member 4 [Source:RGD Symbol;Acc:1309445] |
| ENSRNOG00000036571 | 5.054889497 | $3.39^{-84}$ | Ces2c | carboxylesterase 2C [Source:RGD Symbol;Acc:621510] |
| ENSRNOG00000000245 | 2.020890852 | $1.18^{-69}$ | Slc16a6 | solute carrier family 16, member 6 [Source:RGD Symbol;Acc:735117] |
| ENSRNOG00000001527 | 2.735921532 | $1.52^{-64}$ | Cd80 | Cd80 molecule [Source:RGD Symbol;Acc:2314] |

**Table 5.2** Table of the top 20 downregulated transcripts in GSNO-treated samples, ranked by *p*-value (padj). Most of these transcripts are involved in regulation of cell cycle progression and mitosis.

| Ensembl ID | Log2FoldChange | padj | Name | Description |
|---|---|---|---|---|
| ENSRNOG00000008040 | -3.993065851 | 0 | Pimreg | PICALM interacting mitotic regulator [Source:RGD Symbol;Acc:1308747] |
| ENSRNOG00000032178 | -3.41779947 | 0 | Cenpa | centromere protein A [Source:RGD Symbol;Acc:1563607] |
| ENSRNOG00000037211 | -3.389787634 | 0 | Kif14 | kinesin family member 14 [Source:RGD Symbol;Acc:1310650] |
| ENSRNOG00000018815 | -3.271780618 | 0 | Plk1 | polo-like kinase 1 [Source:RGD Symbol;Acc:3352] |
| ENSRNOG00000027894 | -3.180043549 | 0 | Lqgap3 | IQ motif containing GTPase activating protein 3 [Source:RGD Symbol;Acc:1305951] |
| ENSRNOG00000009946 | -3.114863936 | 0 | Ldlr | low density lipoprotein receptor [Source:RGD Symbol;Acc:2998] |
| ENSRNOG00000007906 | -3.011339242 | 0 | Bub1b | BUB1 mitotic checkpoint serine/threonine kinase B [Source:RGD Symbol;Acc:619791] |
| ENSRNOG00000003388 | -2.946409613 | 0 | Cenpf | centromere protein F [Source:RGD Symbol;Acc:628667] |
| ENSRNOG00000008837 | -2.911178509 | 0 | Ass1 | argininosuccinate synthase 1 [Source:RGD Symbol;Acc:2163] |
| ENSRNOG00000058539 | -2.863922882 | 0 | Ccnb1 | cyclin B1 [Source:RGD Symbol;Acc:2291] |
| ENSRNOG00000028415 | -2.774143201 | 0 | Cdc20 | cell division cycle 20 [Source:RGD Symbol;Acc:620477] |
| ENSRNOG00000019100 | -2.748690893 | 0 | Kif2c | kinesin family member 2C [Source:RGD Symbol;Acc:620239] |
| ENSRNOG00000038035 | -2.742181645 | 0 | Kif4a | kinesin family member 4A [Source:RGD Symbol;Acc:620526] |
| ENSRNOG00000047314 | -2.731455572 | 0 | Tk1 | thymidine kinase 1 [Source:RGD Symbol;Acc:621014] |
| ENSRNOG00000011777 | -2.661567123 | 0 | Spag5 | sperm associated antigen 5 [Source:RGD Symbol;Acc:620152] |
| ENSRNOG00000053047 | -2.638046934 | 0 | Top2a | DNA topoisomerase II alpha [Source:RGD Symbol;Acc:62048] |
| ENSRNOG00000017259 | -2.618329127 | 0 | Tacc3 | transforming, acidic coiled-coil containing protein 3 [Source:RGD Symbol;Acc:1302948] |
| ENSRNOG00000024428 | -2.555145555 | 0 | Kif20a | kinesin family member 20A [Source:RGD Symbol;Acc:1307695] |
| ENSRNOG00000004921 | -2.547345074 | 0 | Nusasp1 | nucleolar and spindle associated protein 1 [Source:RGD Symbol;Acc:1305764] |
| ENSRNOG00000000479 | -2.49309011 | 0 | Kifc1 | kinesin family member C1 [Source:RGD Symbol;Acc:1359118] |

# CHAPTER 5 REFERENCES


1 M. Hayat, *Neuroblastoma*, Springer, 2012.

2 J. Shohet and J. Foster, *Br. Med. J.*, 2017, **357**, j1863;1-8.

3 J. G. Nuchtem, W. B. London, C. E. Barnewolt, A. Naranjo and P. W. McGrady, *Ann. Surg.*, 2017, **256**, 573–580.

4 C. A. Perez, K. K. Matthay, J. B. Atkinson, R. C. Seeger, H. Shimada, G. M. Haase, D. O. Stram, R. B. Gerbing and J. N. Lukens, *J. Clin. Oncol.*, 2000, **18**, 18–26.

5 D. Pe, C. Le, C. Oscarlambret and H. Dieu, *Br. J. Cancer*, 2003, **89**, 1605–1609.

6 B. H. J. Nickerson, K. K. Matthay, R. C. Seeger, G. M. Brodeur, H. Shimada, C. Perez, J. B. Atkinson, M. Selch, R. B. Gerbing, D. O. Stram and J. Lukens, *J. Clin. Oncol.*, 2000, **18**, 477–486.

7 K. K. Matthay, C. P. Reynolds, R. C. Seeger, H. Shimada, E. S. Adkins, D. Haas-Kogan, R. B. Gerbing, W. B. London and J. G. Villablanca, *J. Clin. Oncol.*, 2009, **27**, 1007–1013.

8 R. Ladenstein, U. Pötschgerulrike.poetschger@ccri.at, D. Valteau-couanet, R. Luksch, V. Castel, S. Ash, G. Laureys, P. Brock, J. M. Michon, C. Owenscormac.owens@olchc.ie, T. Trahair, G. C. F. Chan, E. Ruud, H. Schroeder, M. Beck-popovic, G. Schreier, H. Loibner, P. Ambros, K. Holmes, M. R. Castellani, M. N. Gaze, A. Garaventa, A. D. J. Pearson and H. N. Lode, *Cancers (Basel).*, 2020, **12**, 1–19.

9 S. Korde Choudhari, M. Chaudhary, S. Bagde, A. R. Gadbail and V. Joshi, *World J. Surg. Oncol.*, 2013, **11**, 1.

10 E. V. Stevens, A. W. Carpenter, J. H. Shin, J. Liu, C. J. Der and M. H. Schoenfisch, *Mol. Pharm.*, 2010, **7**, 775–785.

11 D. J. Suchyta and M. H. Schoenfisch, *RSC Adv.*, 2017, **7**, 53236–53246.

12 R. Dong, X. Wang, H. Wang, Z. Liu, J. Liu and J. E. Saavedra, *Biomed. Pharmacother.*, 2017, **88**, 367–373.

13 M. M. Reynolds, S. D. Witzeling, V. B. Damodaran, T. N. Medeiros, R. D. Knodle, M. A. Edwards, P. P. Lookian and M. A. Brown, *Biochem. Biophys. Res. Commun.*, 2013, **431**, 647–651.

14 A. Nortcliffe, A. G. Ekstrom, J. R. Black, J. A. Ross, F. K. Habib, N. P. Botting and D. O'Hagan, *Bioorganic Med. Chem.*, 2014, **22**, 756–761.

15 S. Y. Lee, Y. Rim, D. D. McPherson, S. L. Huang and H. Kim, *Biomed. Mater. Eng.*, 2014, **24**, 61–67.

16 K. Oh-hashi, W. Maruyama, H. Yi, T. Takahashi, M. Naoi and K. Isobe, *Biochem. Biophys. Res. Commun.*, 1999, **1999 Sep 2**, 504–509.

17 B.-C. Kim, Y.-S. Kim, J.-W. Lee, J.-H. Seo, E.-S. Ji, H. Lee, Y.-I. Park and C.-J. Kim, *Exp. Neurobiol.*, 2011, **20**, 100.

18 V. J. Findlay, D. M. Townsend, J. E. Saavedra, G. S. Buzard, M. L. Citro, L. K. Keefer, X. Ji and K. D. Tew, *Mol. Pharmacol.*, 2004, **65**, 1070–1079.

19 Y. Hou, J. Wang, P. R. Andreana, G. Cantauria, S. Tarasia, L. Sharp, P. G. Braunschweiger and P. G. Wang, *Bioorganic Med. Chem. Lett.*, 1999, **9**, 2255–2258.

20 E. Kogias, N. Osterberg, B. Baumer, N. Psarras, C. Koentges, A. Papazoglou, J. E. Saavedra, L. K. Keefer and A. Weyerbrock, *Int. J. Cancer*, 2012, **130**, 1184–1194.

21 J. M. Joslin, B. H. Neufeld and M. M. Reynolds, *RSC Adv.*, 2014, **4**, 42039–42043.

22 L. Grossi and P. Carlo, *Chem. Eur. J*, 2002, **8**, 380–387.

23 D. L. H. Williams, *Acc. Chem. Res.*, 1999, **32**, 869–876.

24 Y. Kato, S. Ozawa, C. Miyamoto, Y. Maehata, A. Suzuki, T. Maeda and Y. Baba, *Cancer Cell Int.*, 2013, **13**, 1.

25 D. A. Wink, Y. Vodovotz, J. Laval, F. Laval, M. W. Dewhirst and J. B. Mitchell, *Carcinogenesis*, 1998, **19**, 711–721.

26 B. J. Oleson and J. A. Corbett, *Antioxidants Redox Signal.*, 2018, **29**, 1432–1445.

27 S. Pervin, R. Singh, S. Sen and G. Chaudhuri, *Nitric Oxide (NO) and Cancer*, 2010, 39–57.

28 J. Hickok and D. Thomas, *Curr. Pharm. Des.*, 2010, **16**, 381–391.

29 Z. Huang, J. Fu and Y. Zhang, *J. Med. Chem.*, 2017, **60**, 7617–7635.

30 W. Badn and P. Siesjo, *Curr Pharm Des*, 2010, **16**, 428–30.

31 J. L. Gordon, M. M. Reynolds and M. A. Brown, *Vet. Sci.*, 2020, **7**, 51.

32 A. Zhu, J. G. Ibrahim and M. I. Love, *Bioinformatics*, 2019, **35**, 2084–2092.

33 A. Almeida, S. Moncada and J. P. Bolaños, *Nat. Cell Biol.*, 2004, **6**, 45–51.

34 L. J. Martin, K. Chen and Z. Liu, *J. Neurosci.*, 2005, **25**, 6449–6459.

35 M. Liu, Y. Li, L. Chen, T. H. Man Chan, Y. Song, L. Fu, T. T. Zeng, Y. D. Dai, Y. H. Zhu, J. Chen, Y. F. Yuan and X. Y. Guan, *Gastroenterology*, 2014, **146**, 1084–1096.

36 K. Chen, K. Gunter and M. D. Maines, *J. Neurochem.*, 2000, **75**, 304–313.

37 S. Oyadomari and M. Mori, *Cell Death Differ.*, 2004, **11**, 381–389.

38 R. Brosh, R. Sarig, E. B. Natan, A. Molchadsky, S. Madar, C. Bornstein, Y. Buganim, T. Shapira, N. Goldfinger, R. Paus and V. Rotter, *FEBS Lett.*, 2010, **584**, 2473–2477.

39 N. Ohoka, S. Yoshii, T. Hattori, K. Onozaki and H. Hayashi, *EMBO J.*, 2005, **24**, 1243–1255.

40 J. Shahbazi, R. Lock and T. Liu, *Front. Genet.*, 2013, **4**, 1–7.

41 J. Yan, N. Zhong, G. Liu, K. Chen, X. Liu, L. Su and S. Singha, *Cell Death Dis.*, 2014, **5**, 1–7.

# CHAPTER 6

# ANTICANCER IMPACT OF NITRIC OXIDE (NO) ON ADULT BREAST CANCERS

## 6.1 BACKGROUND

Since the two previous chapters critically expanded the scope of knowledge surrounding NO as an anticancer therapeutic against pediatric neuroblastomas, this chapter was developed to broaden that scope to adult cancers. As such, this study implemented NO, delivered by *S*-Nitrosoglutathione (GSNO), on human adult breast cancers. To evaluate the anticancer potency of each therapeutic, treated cells were analyzed for cell viability, colony formation capacity, cytotoxicity, and apoptosis. Also, normal adult breast cells were identically treated and analyzed to determine the discrimination potential of this treatment. Overall, the results of this study showed the potential of NO, delivered by GSNO, to knockdown MCF7 and MDA-MB-231 breast cancer cell count. Unfortunately, normal MCF10A cell count was also decreased, limiting the conceivable application of NO in breast cancer treatment. However, further experimentaion is necessary. Also, if combined with another therapeutic that does not impact normal breast cells, like SMYD-3 inhibition, NO could still show promise as a potential treatment for breast cancer. Jenna L Gordon and Kristin J Hinsen were both involved in the accrual and analysis of the cell based assays. Jenna L Gordon is preparing the draft for this manuscript with some contribution from Kristin J Hinsen. Melissa M Reynolds and Mark A Brown are contributing to draft revision and acting as advisors for this work. This manuscript is in progress and will consist of these studies as well as the additionaal studies regarding NO + the SMYD-3 inhibitor, Inhibitor-4, on the same cell lines.

## 6.2 INTRODUCTION

Female breast cancer cases in the United States have been continually increasing over the past 20 years.[1] Fortunately, 5-year survival rates remain optimistic.[2] This is possible because of continued advancements in breast cancer detection and treatment options. In modern practice, the course of treatment is dependent upon three subcategories of breast cancer that are defined by the presence or absence of specific molecular markers for estrogen or progesterone receptors and human epidermal growth factor 2 (*ERBB2*; formerly HER2).[3,4] Currently, chemotherapy, endocrine therapy, and *ERBB2*-targeted antibody or small molecule inhibitor therapy combined with chemotherapy are mainstays in breast cancer treatment.[2,5–9] Still, breast cancer far exceeds all other cancers in new cancer diagnoses and has the second highest mortality rate.[1]

Enormous efforts are dedicated to developing new, effective therapeutic options for breast cancer. For example, several studies have highlighted the potential of nitric oxide (NO).[10–14] However, the effect of nitric oxide on breast cancers is dichotomous: augmenting tumor growth and encouraging metastasis at low concentrations (nanomolar)[11,15] while promoting tumor apoptosis and cytostasis at high concentrations (micromolar)[11–14]. Unfortunately, the ability to provoke site-specific delivery and control release kinetics limit its practical application. Thus, various NO-delivery platforms have been investigated, such as NONOates, *N*-diazeniumdiolates, and *S*-Nitrosothiols (RSNOs).[10-21] RSNOs present two major advantages over other delivery platforms, they allow prolonged NO-release and naturally exist in the body.[20–22]

Another therapeutic strategy focuses on SMYD (SET and MYND domain-containing) family proteins as molecular targets in cancer treatment.[23–25] In particular, SMYD3 is

known to regulate cancer cell growth and proliferation. [23,24] Consequently, SMYD3 overexpression has been linked to increased proliferation and transformation and metastasis of various cancers, including breast cancer. [26,27] Multiple studies highlight that when SMYD3 is inhibited, a substantial decrease in proliferative capacity of breast cell lines is observed.[23,28,29]

Herein, the impact of NO, delivered via *S*-Nitrosoglutathione (GSNO), was explored to determine its impact on adult breast cancer cell lines, MCF7 and MDA-MB-231, and normal breast cell line, MCF10A. In previous studies, the RSNO, GSNO, was shown to exhibit tumoricidal characteristics.[30–32] To evaluate the efficacy of NO, cell viability, colony formation capacity, and cytotoxicity were examined. This work only contains the results pertaining to NO, delivered by GSNO.

Yet, the novel combination of SMYD3 inhibition, via Inhibitor-4, plus No, delivered by GSNO, will be investigated for anticancer potential against breast cancers. This combination was selected based on these studies as well as a separate study that indicated the SYMD3 inhibitor, Inhibitor-4, demonstrated potent impacts on two breast cancer lines, MCF7 and MDA-MB-231 (both lines linked to overexpression of SMYD3), without impacting normal MCF10A breast cells.[29] By combining the two therapeutics, GSNO and Inhibitor-4, it is expected that the efficacy of the combination will be more potent than each individual therapeutic on the breast cancer cell lines.

## 6.3 EXPERIMENTAL

**6.3.1 Materials.** Dulbecco's Modified Eagle's Medium (DMEM), Eagle's Minimum Essential Medium (EMEM), F-12 Medium, Gibco Horse Serum (New Zealand origin), Invitrogen Cholera Toxin Subunit B (Recombinant), Alexa Fluor 488 Conjugate, Lonza

Walkersville MEGM Mammary Epithelial Cell Growth Medium SingleQuots Supplements and Growth Factors (Insulin, BPE, Hydrocortisone), Promega Caspase-Glo 3/7 Assay Kit, and Penicillin-Streptomycin Solution were obtained from Fisher Scientific (Hampton, NH, USA). EquaFETAL 100% Bovine Serum was purchased from Atlas Biologicals (Fort Collins, CO, USA). Reduced glutathione (GSH, High Purity), CellTiter-Blue Cell Viability Assay (CTB), and 3-(4,5-Dimethylthiazol-2-yl)-2,5-diphyltetrazolium bromide (MTT) were purchased from VWR International (Randor, PA, USA). Hydrochloric acid (HCl), EPA vials, and Invitrogen ReadyProbes Cell Viability Imaging Kit were obtained from Thermo Fisher Scientific (Waltham, MA, USA). Dimethyl sulfoxide (DMSO) and Acetone (≥99.5%) were purchased from Sigma Aldrich (St. Louis, MO, USA). Sodium nitrate (99.999% NaNO2) was obtained from Alfa Aesar (Ward Hill, MA, USA). Trypsin/EDTA solution was purchased from American Type Culture Collections (Manassas, VA, USA). The breast cancer cell lines MCF7 and MDA-MB-231, as well as the healthy breast epithelial cell line used, MCF10A, were purchased from American Type Culture Collection (ATCC).

**6.3.2 Synthesis of *S*-Nitrosoglutathione (GSNO).** *S*-Nitrosoglutathione (GSNO) was synthesized through a previously developed method. In brief, sodium nitrite ($NaNO_2$) was added to a solution of reduced glutathione (GSH) in Millipore water and 2 M hydrochloric acid (HCl). The mixture was constantly stirred in an ice bath for 40 min. The solution was treated with acetone, followed by an additional 10 min of stirring in the ice bath (mixture turned a red colour). The red solution was filtered for 10 min, first with gravity filtration for 10 min and then vacuum filtration for 3.5 h. After the GSNO precipitate was isolated, it was washed successively with ice-water and acetone. The remaining red filtrate solution

was discarded while the solid pink powder (GSNO) was retained. The precipitate was analysed by UV-Vis spectrophotometry at 335 nm to confirm >95% purity.

**6.3.3 Cell Culture.** Complete cell media (complete DMEM/EMEM) for both breast cancer cell lines consisted of 500 mL of DMEM/EMEM cell media supplemented with 10% total volume fetal bovine serum and 1% total volume penicillin-streptomycin. Complete cell media for healthy breast tissue cells, MCF10A, consisted of 500 mL of a 50/50 mixture of DMEM and F-12 media supplemented with 25 mL horse serum, 5 mL penicillin-streptomycin solution, 0.5 mL insulin, 2 mL BPE, 0.5 mL EGF, 0.5 mL hydrocortisone, and 50 µL of 0.1 mg/mL stock of cholera toxin. Initially, 1 mL containing $10^6$ cells were thawed for 1-2 min in a 37°C water bath, added to a 15 mL centrifuge tube containing 9 mL of pre-warmed complete media, and centrifuged for 5 min at 4°C, 2000 RPM. Then, the supernatant was aspirated, and the remaining pellet was resuspended in 5 mL of complete media. This was added to T-25 $cm^2$ flasks containing 5 mL of complete media. Cultures were incubated at 37°C, 5% CO2 for at least 48 h before fresh complete media was provided every 24-72 h. Macroscopic observation and cell counting via hemocytometer were used to count and split cell cultures.

**6.3.4 Cell Viability Assays**

**6.3.4.1 Setup.** In the samples exposed to GSNO, cells were plated at 100,000 or 200,000 cells/mL (MTT and CTB, respectively) in 100µL increments in 96-well plates and then incubated at 37°C, 5% CO2. The media was aspirated and discarded after 24 h. The following day, on day 2, the positive control samples (PC; ≥ 5 samples) received 100 µL of complete media, the functional control samples (GSH; ≥ 5 samples) received 100 µL of 1mM GSH, and the other samples received 100 µL of 1mM GSNO (Sample; ≥ 5 samples).

After another 24 h of incubation, on day 3, the media was aspirated, and each well was given 100 µL of complete media. The appropriate cell viability assay was then performed.

**6.3.4.2 Procedure.** In all viability assays, absorbance measurements were detected using a BioTek Synergy 2 Multi-Detection Microplate Reader. Data points represent the mean ± standard deviation (SD).

*MTT Assays*. Following the outlined experimental setup, 10 µL of 12 mM MTT stock solution was added to each well. Plates were incubated for 3 h. Then, 50 µL of DMSO was added to each well. Plates were placed back in the incubator for 10 min to solubilize the MTT formazan. Finally, a microplate reader was used to measure absorbance values at 540 nm.

*CTB Assays*. Subsequent to the experimental setup above, 20 µL of CTB stock solution was added to each well. Plates were incubated for 3 h. Finally, a microplate reader was used to measure absorbance values at 570 nm and 600 nm.

**6.3.5 Colony Formation Assays.** Colony formation images were captured with brightfield microscopy using an Invitrogen Cytation 7 Fluorescence Microscope. Data points represent the mean ± standard deviation (SD).

In all colony formation assays, cells were plated at 100,000 cells/mL in 1mL increments in 24-well plates and then incubated at 37°C, 5% $CO_2$ for 24 h in 24-well plates. The media was then aspirated from all wells and discarded. Then, the positive control samples (PC; ≥ 4 samples) received 1 mL of complete media, the other samples received 1 mL of 1mM GSNO (Sample; ≥ 4 samples), and the functional control samples (GSH; ≥ 4 samples) received 1 mL of 1 mM GSH, before the plate was incubated for another 24 h. Cells were harvested, counted, and then re-plated at 500 cells/mL in new 24-well plates. These plates were placed back into the incubator and

observed every 24-72 h for up to three weeks via brightfield microscopy to determine the number of colonies (defined as masses ≥ 50 cells) formed.

**6.3.6 LIVE/DEAD Assays.** LIVE/DEAD images were captured with fluorescence microscopy using an Invitrogen Cytation 7 Fluorescence Microscope. Live cells exhibited blue fluorescence while dead cells exhibited green fluorescence.

In the cytotoxicity assays, cells were plated at 100 μL increments of 100,000 cells/mL in 96-well plates before 24h of incubation at 37°C, 5% $CO_2$. Next, all media was aspirated and discarded before the positive control samples (PC; ≥ 7 samples) received 100 μL of complete media, the treated samples received 100 μL of 1mM GSNO (Sample; ≥ 7 samples), and the functional control samples (GSH; ≥ 7 samples) received 100 μL of 1mM GSH. Following another 24 h of incubation, 10 drops of both the Blue and Green ReadyProbes Cell Viability Imagine Kit stock solutions were added to 5 mL complete media. The media was aspirated from each well and 100 μL of the Blue/Green stock solution was added to each well before it was again incubated for 15 min. Imaging via fluorescent microscopy was used for qualitative comparison of the relative number of live cells versus dead cells in each well.

**6.3.7 Data Analysis and Statistics.** One way-ANOVA was used to perform all statistical analysis and $p < 0.01$ defined statistically significant differences. Data points represent the mean ± standard deviation.

## 6.4 RESULTS AND DISCUSSION

The overall goal of this study was to determine the relative efficacy of NO (delivered by GSNO), on human MCF7 and MDA-MB-231 breast cancer cells. Additionally, healthy MCF10A breast cells were evaluated in an identical manner to probe potential side effects to normal cells if applied in a clinical setting. In all assays, the sample groups consisted of

positive control (PC) cells, sample (S) cells (NO-treated), and functional control (GSH) cells. Various methods were used to determine efficacy, including cell viability assays (MTT and CTB), colony formation assays, and LIVE/DEAD cytotoxicity assays. The study described herein was designed to assess the effect of NO only (via GSNO).

To expand this work, the impact of a combination treatment, NO (delivered by GSNO) and Inhibitor-4, a SMYD-3 inhibitor, will be evaluated. Ideally, the combination treatment will show greater potential than either treatment individually. Inhibitor-4 alone was assessed in a separate study done by collaborators, Alshiraihi, et. al.[29] In this study, Alshiraihi et. al. presented exciting evidence showing that Inhibitor-4 reduced viability and colony formation capacity and induced apoptosis of MCF7 and MDA-MB-231 breast cancer cells, while normal MCF10A cells were not affected.[29]

**6.4.1 Cell Viability Assays.** Initially, the effect of NO (delivered by 1 mM GSNO) was assessed for its impact on viability of MCF7 and MDA-MB-231 breast cancer cells compared to normal MCF10A breast cells. Both MTT and CTB cell viability assays showed a significant decrease in viability after the 24 h treatment period for each treatment group.

**6.4.1.1 MTT Assay.** In the cells treated with NO only (from 1 mM GSNO), the MTT assay revealed a decrease in breast cancer cell viability of ~18-23% in comparison to untreated cells. Explicitly, after the 24 h treatment period, the viability of PC MCF7 cells was 100% ± 2% ($n \geq 7$), the viability of S cells was 82% ± 7% ($n \geq 7$), and the viability of GSH cells was 98% ± 2%($n \geq 7$). After 24 h treatment in MDA-MB-231 cells, PC viability was 100% ± 3%, S viability was 77% ± 4%, and GSH viability was 105% ± 5% (Figure 1). Identically treated MCF10A PC cell viability was 100% ± 7%, S viability was 71% ± 9%, and GSH viability was 110% ± 8%.

Overall, the MTT viability assay revealed a significant decrease in cellular viability of MCF7 and MDA-MB-231 breast cancer cells. Unfortunately, a significant decrease in viability of normal MCF10A breast cells was also observed. Collectively, this data illustrates potential limitations in anticancer applications of NO (delivered by GSNO) on breast cancers. Still, if paired with other methods, like SMYD-3 inhibition, NO still has potential to be an effective treatment.

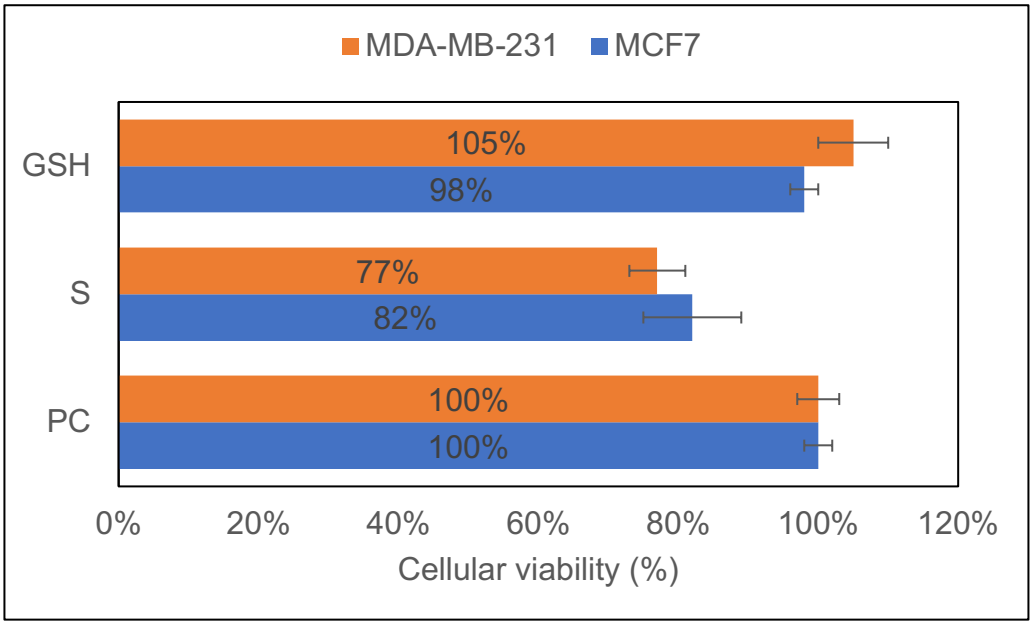


**Figure 6.1** Cellular viability of MCF7 and MDA-MB-231 breast cancer cells as well as normal MCF10A cells after treatment with 1 mM GSNO for 24 h, assessed by the MTT assay. Data points represent the mean ± standard deviation.

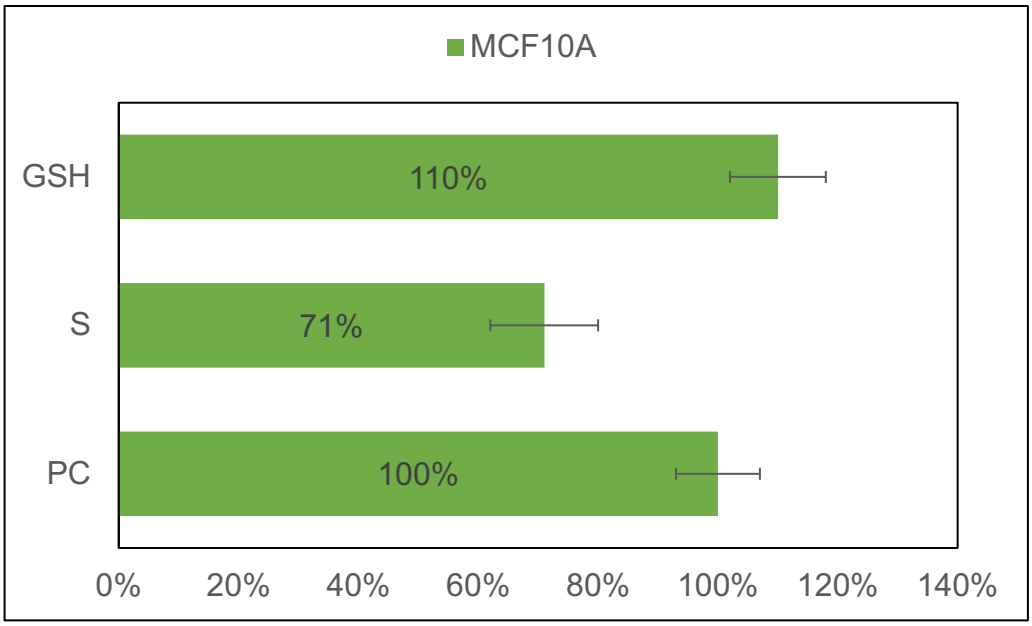


**Figure 6.2** Normal MCF10A cell viability after treatment with 1 mM GSNO for 24 h, assessed with the MTT assay. Data points represent the mean ± standard deviation.

**6.4.1.2 CTB Assay.** Comparable to the MTT assay results, the CTB assay revealed a ~18-24% decrease in breast cancer cells treated with NO only. After the treatment period, the CTB assay showed that MCF7 PC cell viability was 100% ± 8% ($n \geq 7$), S viability was 76% ± 8% ($n \geq 7$), and GSH viability was 98% ± 7% ($n \geq 7$). After 24 h treatment in MDA-MB-231 cells, PC viability was 100% ± 9%, S viability was 82%± 7%, and GSH viability was 100% ± 9%. MCF10A cell viability was 100% ± 8%, S viability was 74% ± 5%, and GSH viability was 111% ± 8% after identical treatment.

Ultimately, the CTB results echoed those of the MTT assay, indicating reduced cell viability in both breast cancer cell lines as well as the normal breast cells. This data indicates that NO (delivered by GSNO) will induce physical side effects and does not appear to be a particularly favorable treatment option for breast cancers. However, further experiments are needed and there is potential for combinations of NO and other therapeutic methods that do not affect normal breast cells, such as SMYD-3 inhibition.

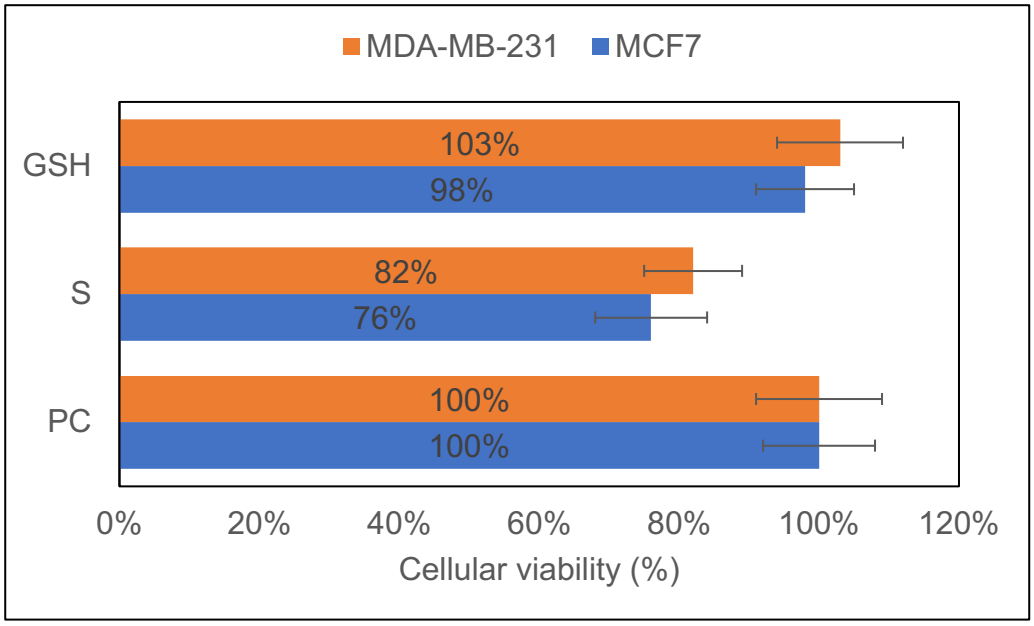


**Figure 6.3** Cellular viability of MCF7 and MDA-MB-231 breast cancer cells after treatment with 1 mM GSNO for 24 h, assessed with the CTB assay. Data points represent the mean ± standard deviation.

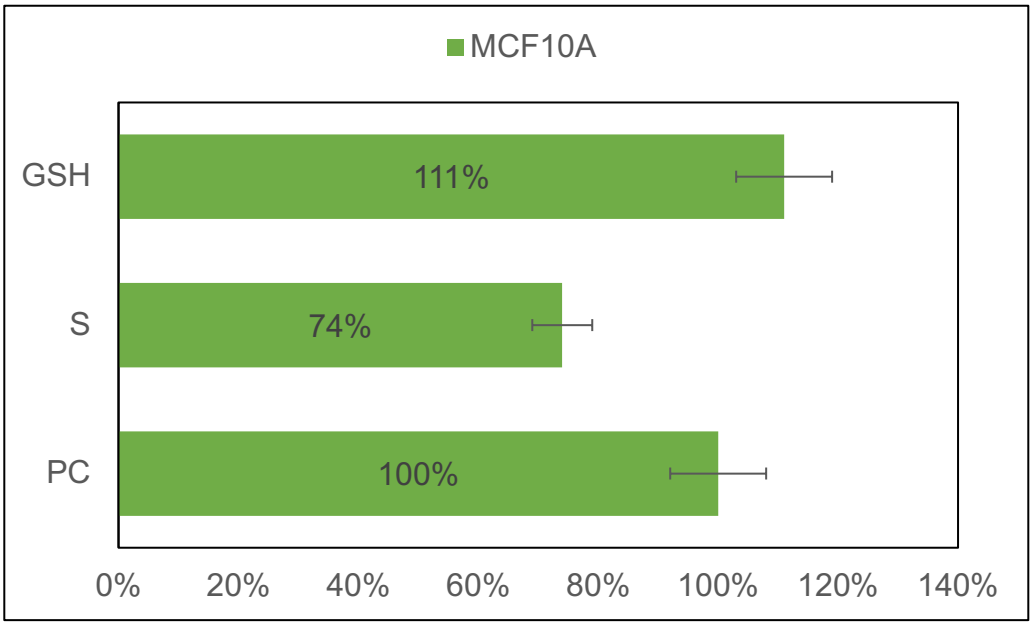


**Figure 6.4** Viability of normal MCF10A cells after treatment with 1 mM GSNO for 24 h, assessed with the CTB assay. Data points represent the mean ± standard deviation.

**6.4.2 Colony Formation Assays.** MCF7 and MDA-MB-231 breast cancer cells were also assessed for clonogenic capacity after a 24 h treatment period with NO (from 1 mM GSNO). Explicitly, treated S cells experienced a reduction of 20 to 3, or 86% ± 9% , for MCF7 cells and 27 to 4, or 87% ± 6%, for MDA-MB-231 cells. This data strikingly illustrates that NO, delivered by GSNO, significantly reduced colony formation of both breast cancer cell lines.

These results suggest that NO is highly efficacious in reduction of clonogenic capacity and holds great potential for clinical application in breast cancers.

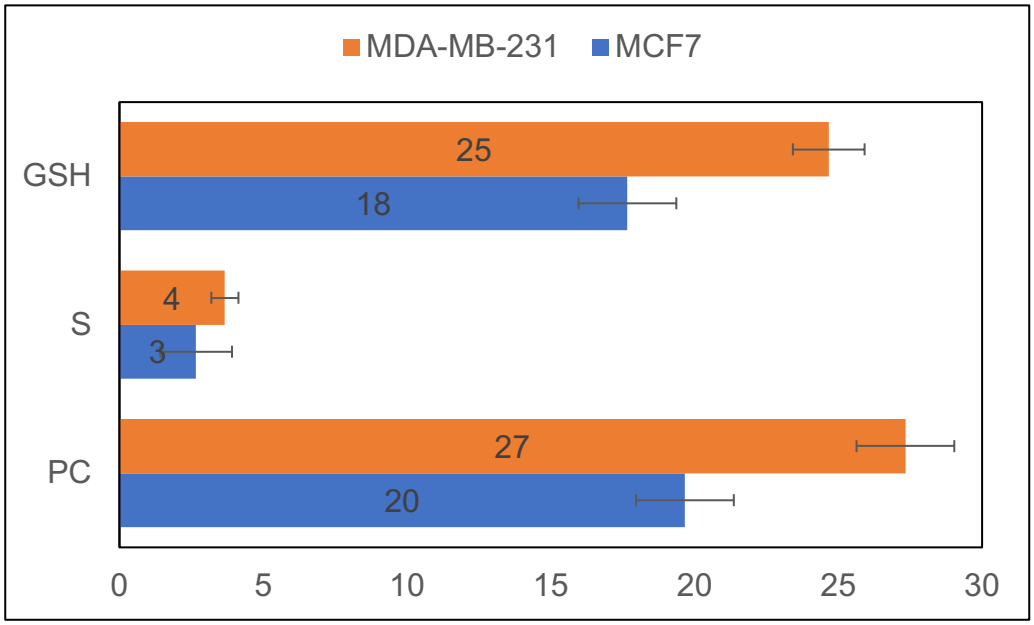


**Figure 6.5** Colony formation capacity of MCF7 and MDA-MB-231 breast cancer cells after treatment with 1 mM GSNO for 24 h, assessed via brightfield microscopy. Data points represent the mean ± standard deviation.

**6.4.3 LIVE/DEAD Assays.** Finally, LIVE/DEAD cytotoxicity assays were applied as a last qualitative verification of NO as anticancer therapeutic against MCF7 and MDA-MB-231 breast cancer cells. These images exhibit much a much greater number of dead (green) cells than live (blue) cells in the GSNO-treated samples in both MCF7 and MDA-MB-231 breast cancer cells. Also, there are visually more dead cells present in the GSNO-treated cells than PC or GSH-treated cells in both cell lines. Further, the number of live and dead

cells in the GSNO-treated MCF10A cells appears to be similar to the number of live and dead cells in the PC and GSH-treated cells. This data supports the previous information, indicating the potential of NO, delivered by GSNO, to be an effective treatment option for breast cancers.

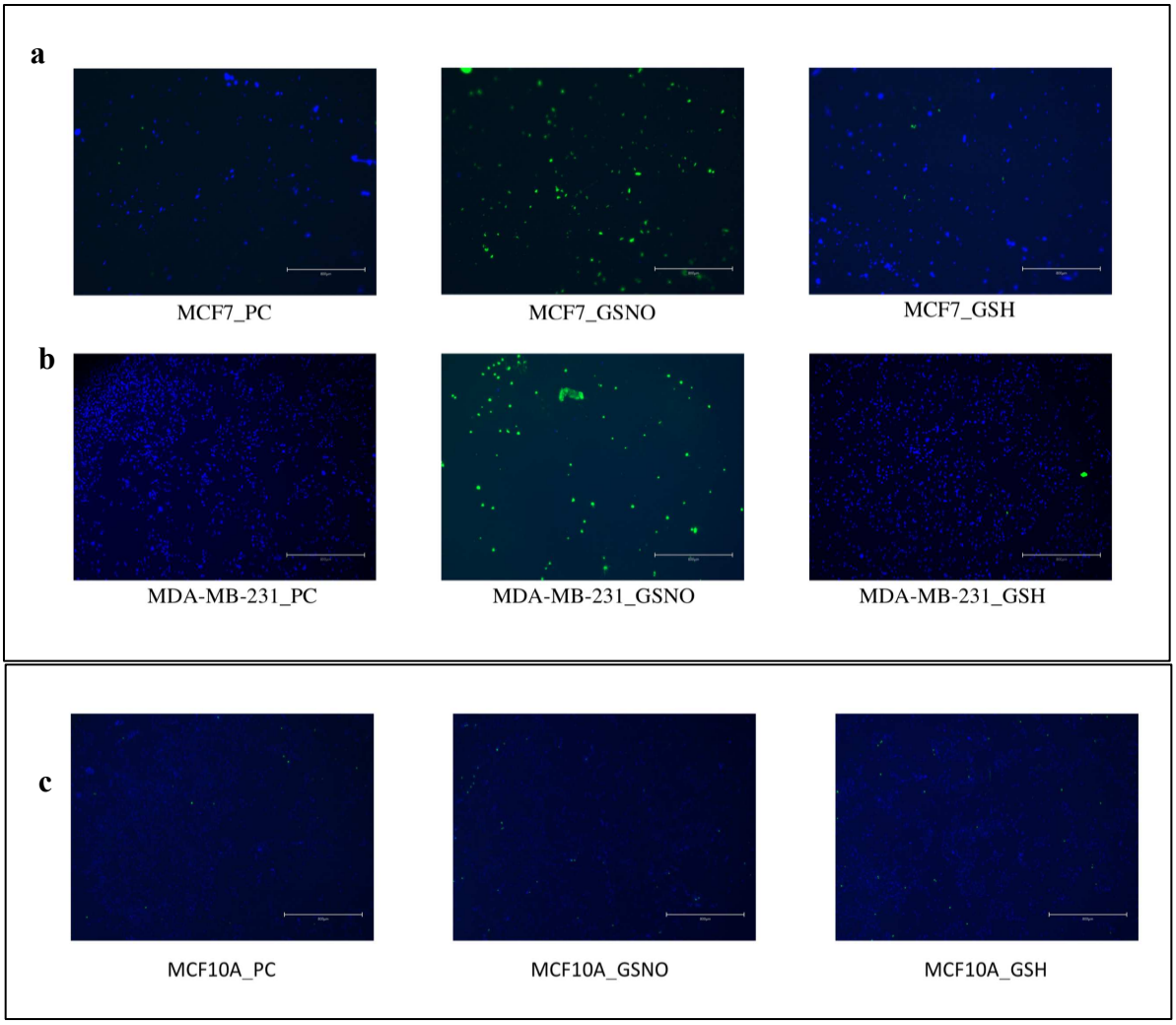


**Figure 6.6** Qualitative representation of live (blue) and dead (green) untreated PC cells, GSNO-treated (S-sample) cells, and GSH-treated functional control (GSH) cells. Images of (a) MCF7 and (b) MDA-MB-23 breast cancer cells as well as (c) normal MCF10A cells were captured via fluorescence microscopy.

## 6.5 CONCLUSIONS

Collectively, this data shows that NO (delivered by GSNO) moderately reduces cellular viability and greatly reduces colony formation of MCF7 and MDA-MB-231 breast cancer cells. However, cellular viability of normal MCF10A is also impacted by NO to a similar degree, limiting its conceivable application in breast cancer treatment. Future implementation of apoptosis assays will help elucidate the overall impact of NO on breast cancers. Ultimately, it is vital to find alternative approaches to the application of NO in breast cancer treatment studies. One with exciting potential is the combination of NO (delivered by GSNO) and the SMYD-3 inhibitor, Inhibitor-4 (investigated by Alshiraihi, et. al.). Since Inhibitor-4 was observed to comparably impact MCF7 and MDA-MB-231 breast cancers while not affecting normal MCF10A cells, it can potentially be a promising adjuvant to NO. As such, future experiments will be focused on the combination of NO and Inhibitor-4. The results from these studies can then be compared to each individual therapeutic.

# CHAPTER 6 REFERENCES


1 U.S. Department of Health and Human Services, Centers for Disease Control and Prevention and National Cancer Institude. U.S. Cancer Statistics Working Group. U.S. Cancer Statistics Data Visulaizations Tool, Based on 2019 Submission Data (1999-2017);

2 A. G. Waks and E. P. Winer, *JAMA - J. Am. Med. Assoc.*, 2019, **321**, 288–300.

3 A. Verma, J. Kaur and K. Mehta, *Asian J. Oncol.*, 2015, **01**, 065–072.

4 M. E. H. Hammond, D. F. Hayes, M. Dowsett, D. C. Allred, K. L. Hagerty, S. Badve, P. L. Fitzgibbons, G. Francis, N. S. Goldstein, M. Hayes, D. G. Hicks, S. Lester, R. Love, P. B. Mangu, L. McShane, K. Miller, C. K. Osborne, S. Paik, J. Perlmutter, A. Rhodes, H. Sasano, J. N. Schwartz, F. C. G. Sweep, S. Taube, E. E. Torlakovic, P. Valenstein, G. Viale, D. Visscher, T. Wheeler, R. B. Williams, J. L. Wittliff and A. C. Wolff, *J. Clin. Oncol.*, 2010, **28**, 2784–2795.

5 I. Smith, M. Procter, R. D. Gelber, S. Guillaume, A. Feyereislova, M. Dowsett, A. Goldhirsch, M. Untch, G. Mariani, J. Baselga, M. Kaufmann, D. Cameron, R. Bell, J. Bergh, R. Coleman, A. Wardley, N. Harbeck, R. I. Lopez, P. Mallmann, K. Gelmon, N. Wilcken, E. Wist, P. Sánchez Rovira and M. J. Piccart-Gebhart, *Lancet*, 2007, **369**, 29–36.

6 L. Gianni, U. Dafni, R. D. Gelber, E. Azambuja, S. Muehlbauer, A. Goldhirsch, M. Untch, I. Smith, J. Baselga, C. Jackisch, D. Cameron, M. Mano, J. L. Pedrini, A. Veronesi, C. Mendiola, A. Pluzanska, V. Semiglazov, E. Vrdoljak, M. J. Eckart, Z. Shen, G. Skiadopoulos, M. Procter, K. I. Pritchard, M. J. Piccart-Gebhart and R. Bell, *Lancet Oncol.*, 2011, **12**, 236–244.

7 C. Denkert, C. Liedtke, A. Tutt and G. von Minckwitz, *Lancet*, 2017, **389**, 2430–2442.

8 J. S. Reis-filho and D. Ph, .

9 N. Howlader, S. F. Altekruse, C. I. Li, V. W. Chen, C. A. Clarke, L. A. G. Ries and K. A. Cronin, *J. Natl. Cancer Inst.*, , DOI:10.1093/jnci/dju055.

10 L. Thomsen, D. Miles, L. Happerfield, L. Bobrow, R. Knowles and S. Monacada, *Br. J. Cancer*, 1995, 41–44.

11 S. Pervin, R. Singh and G. Chaudhuri, *Nitric Oxide - Biol. Chem.*, 2008, **19**, 103–106.

12 S. Pervin, R. Singh and G. Chaudhuri, *Proc. Natl. Acad. Sci. U. S. A.*, 2001, **98**, 3583–3588.

13 S. Pervin, R. Singh, W. A. Freije and G. Chaudhuri, *Cancer Res.*, 2003, **63**, 8853–8860.

14 S. Pervin, R. Singh and G. Chaudhuri, *Cancer Res.*, 2003, **63**, 5470–5479.

15 S. Pervin, R. Singh, E. Hernandez, G. Wu and G. Chaudhuri, *Cancer Res.*, 2007, **67**, 289–299.

16 D. J. Suchyta and M. H. Schoenfisch, *Mol. Pharm.*, 2015, **12**, 3569–3574.

17 D. J. Suchyta and M. H. Schoenfisch, *RSC Adv.*, 2017, **7**, 53236–53246.

18 R. Dong, X. Wang, H. Wang, Z. Liu, J. Liu and J. E. Saavedra, *Biomed. Pharmacother.*, 2017, **88**, 367–373.

19 M. M. Reynolds, S. D. Witzeling, V. B. Damodaran, T. N. Medeiros, R. D. Knodle, M. A. Edwards, P. P. Lookian and M. A. Brown, *Biochem. Biophys. Res. Commun.*, 2013, **431**, 647–651.

20 V. J. Findlay, D. M. Townsend, J. E. Saavedra, G. S. Buzard, M. L. Citro, L. K. Keefer, X. Ji and K. D. Tew, *Mol. Pharmacol.*, 2004, **65**, 1070–1079.

21 Y. Hou, J. Wang, P. R. Andreana, G. Cantauria, S. Tarasia, L. Sharp, P. G. Braunschweiger and P. G. Wang, *Bioorganic Med. Chem. Lett.*, 1999, **9**, 2255–2258.

22 E. Kogias, N. Osterberg, B. Baumer, N. Psarras, C. Koentges, A. Papazoglou, J. E. Saavedra, L. K. Keefer and A. Weyerbrock, *Int. J. Cancer*, 2012, **130**, 1184–1194.

23 R. Hamamoto, Y. Furukawa, M. Morita, Y. Iimura, F. P. Silva, M. Li, R. Yagyu and Y. Nakamura, *Nat. Cell Biol.*, 2004, **6**, 731–740.

24 M. A. Brown, K. Foreman, J. Harriss, C. Das, L. Zhu, M. Edwards, S. Shaaban and H. Tucker, *Oncotarget*, 2015, **6**, 4005–4019.

25 S. Komatsu, I. Imoto, H. Tsuda, K. I. Kozaki, T. Muramatsu, Y. Shimada, S. Aiko, Y. Yoshizumi, D. Ichikawa, E. Otsuji and J. Inazawa, *Carcinogenesis*, 2009, **30**, 1139–1146.

26 A. M. Cock-Rada, S. Medjkane, N. Janski, N. Yousfi, M. Perichon, M. Chaussepied, J. Chluba, G. Langsley and J. B. Weitzman, *Cancer Res.*, 2012, **72**, 810–820.

27 X. G. Luo, C. L. Zhang, W. W. Zhao, Z. P. Liu, L. Liu, A. Mu, S. Guo, N. Wang, H. Zhou and T. C. Zhang, *Cancer Lett.*, 2014, **344**, 129–137.

28 R. Hamamoto, F. P. Silva, M. Tsuge, T. Nishidate, T. Katagiri, Y. Nakamura and Y. Furukawa, *Cancer Sci.*, 2006, **97**, 113–118.

29 I. M. Alshiraihi, D. K. Jarrell, Z. Arhouma, K. N. Hassell, J. Montgomery, A. Padilla, H. M. Ibrahim, D. C. Crans, T. A. Kato and M. A. Brown, *Int. J. Mol. Sci.*, 2020, **21**, 1–15.

30 J. L. Gordon, M. M. Reynolds and M. A. Brown, *Vet. Sci.*, 2020, **7**, 51.

31 J. L. Gordon, K. J. Hinsen, M. M. Reynolds, T. A. Smith, H. O. Tucker and M. A. Brown, *RSC Adv.*, 2021, **11**, 9112–9120.

32 Y. Zhang, C. Sun, G. Xiao, H. Shan, L. Tang, Y. Yi, W. Yu and Y. Gu, *Cell Death Dis.*, , DOI:10.1038/s41419-019-1561-x.

# CHAPTER 7

# CONCLUSIONS AND FUTURE DIRECTIONS

## 7.1 CONCLUSIONS

The contributions detailed in this dissertation significantly impact the field of anticancer research in several areas: 1) a comprehensive compilation investigation of indicators of anticancer therapeutic efficacy, 2) an investigation of protocol development and potential interferences in cellular viability assays, and 3) multiple investigations into the impact of NO on malignancies of pediatric and adult origin. Chapter 2's review of the indicators of therapeutic efficacy was the first thorough examination of the numerous methods in current use in anticancer research and when it is useful to implement them. Additionally, careful examination of potential interferences and assay properties in the protocol development process presented in Chapter 3 provides invaluable information regarding the standardization of cellular viability assay protocols. Further, the exciting evidence of the potency of NO as an anticancer therapeutic on various pediatric neuroblastomas and adult breast cancers gleaned in Chapters 4-6 critically expanded the existing, underdeveloped investigation. These analyses highlighted the promising effects that NO exhibits on cellular viability, cellular death, and clonogenic capacity of pediatric neuroblastomas and adult breast cancers while simultaneously displaying discriminatory characteristics toward neoplastic cells (retained normal cell health). Additionally, the data gathered about the mechanism of action of NO on pediatric neuroblastomas critically advanced the understanding of its potential use as an adjuvant therapeutic in cancer management. Finally, the in-progress innovative study exploring the application of NO in combination with a SMYD-3 inhibitor, Inhibitor-4, on adult breast cancers will catapult the previously nonexistent investigation. Overall, this dissertation positively advances the application of anticancer therapeutics, particularly NO-based therapeutics.

## 7.2 FUTURE DIRECTIONS

*Yielding accurate and reproducible measurements in tumor-derived cell line research.* Despite over a century of cancer research, the field lacks a comprehensive guide to the multitude of assessments implemented in the determination of efficacy of candidate anticancer therapeutics. As a result, researchers implement a diverse assortment of analyses, which can make the comparisons between two or more therapeutics very challenging. To that end, the second and third chapter of this dissertation (Chapter 2: *Diseases* **2018,** 6(4), 85.) explored two underdeveloped areas of anticancer therapeutic efficacy testing using tumor-derived cell lines: a compilation of the indicators of therapeutic efficacy on tumor-derived cell lines and a discussion of the protocol development and potential interferences in cellular viability assays. However, work in this area remains unfinished. There is vast potential to create and develop standardized classifications of the methods applied in in tumor-derived cell lines, animal models, and clinical trials and their appropriate and accurate use. Further, the accurate and appropriate application of the aforementioned methods could be further investigated and documented. The amassing of this information would improve researcher's and clinician's ability to evaluate and compare two or more anticancer therapeutics.

*NO as an adjuvant anticancer therapeutic.* The potential of NO as an anticancer therapeutic is not thoroughly understood. Numerous studies have shown an anticancer effect of NO delivered in various forms. However, questions still remain about various aspects of NO on cancer, such as the ideal form, concentration, and delivery method. Additionally, the mechanism of action of NO on cancers is not well characterized or understood. Chapters 4-6 sought to expand upon this knowledge when the *S*-Nitrosothiol, *S*-Nitrosoglutathione (GSNO), was exposed to pediatric neuroblastomas (*Vet Sci* **2020,** 7(2), 51. and *RSC Advances* **2021,** 11, 9112-9120.) and adult breast

cancers (*manuscript in progress*). These studies produced exciting evidence about the prospective of NO as an adjuvant therapeutic in clinical cancer management as well as the mechanism of action of NO as an anticancer therapeutic. Still, this investigation deserves further exploration.

*NO combinations in anticancer applications.* Application of NO-based therapeutics in combination with other non-traditional therapeutic methods has been vastly understudied. The goal of Chapter 6 of this dissertation was to expand that inquiry through innovating analyses of NO in combination with a SMYD-3 inhibitor (*manuscript in progress*). This study aims to probe the anticancer potency of the combination of NO and Inhibitor-4 with a direct comparison to each individual therapeutic. Overall, the possibilities of NO combination therapeutics are immense, having the potential to be particularly valuable in increasing attainability and affordability of treatment while greatly reducing patient side effects. Conceivable research in NO combination therapeutics is boundless and would propel advancements in NO and cancer research.